



Title	Preparation and characterization of calcium phosphate ceramics and polymer composites as potential bone substitutes
Author(s)	Manchinasetty, Naga Vijaya Lakshmi
Citation	北海道大学. 博士(工学) 甲第13085号
Issue Date	2018-03-22
DOI	10.14943/doctoral.k13085
Doc URL	http://hdl.handle.net/2115/70539
Type	theses (doctoral)
File Information	Naga_Vijaya_Lakshmi_Manchinasett.pdf



[Instructions for use](#)

**PREPARATION AND CHARACTERIZATION OF
CALCIUM PHOSPHATE CERAMICS AND
POLYMER COMPOSITES AS POTENTIAL
BONE SUBSTITUTES**

NAGA VIJAYA LAKSHMI MANCHINASETTY

**DIVISION OF BIOENGINEERING AND
BIOINFORMATICS**

**GRADUATE SCHOOL OF INFORMATION
SCIENCE AND TECHNOLOGY**

HOKKAIDO UNIVERSITY

2018

Table of Contents

Abstract	iii
Chapter 1	1
Introduction	
1.1 Basics of bone	1
1.2 Bone grafts and current treatment.....	3
1.3 Synthetic bone substitutes.....	4
1.4 Marine organisms derived CaPs for bone repair and regeneration.....	9
1.5 Overview of thesis.....	12
1.6 References.....	14
Chapter 2	22
Conversion of sea urchin tests to calcium phosphate	
2.1 Introduction	22
2.2 Materials and Methods.....	23
2.3 Results and Discussion	25
2.4 Conclusion	32
2.5 References	33
Chapter 3	36
Preparation of flexible scaffolds utilizing test of sea urchin with collagen or gelatin as binder	
3.1 Introduction	36
3.2 Materials and Methods.....	37
3.3 Results.....	40
3.4 Discussion.....	44
3.5 Conclusion.....	46
3.6 References.....	46
Chapter 4	49
Evaluation of biocompatibility of scaffolds under static cell culture conditions	
4.1 Introduction	49
4.2 Materials and Methods.....	50
4.3 Results.....	53

4.4 Discussion.....	58
4.5 Conclusion.....	60
4.6 References.....	61
Chapter 5	64
Evaluation of biocompatibility of scaffolds under pressure/perfusion cell culture conditions	
5.1 Introduction	64
5.2 Materials and Methods.....	66
5.3 Results.....	71
5.4 Discussion.....	74
5.5 Conclusion.....	78
5.6 References.....	79
Chapter 6	82
Combined supplementation of calcium citrate and calcium carbonate on injectable and anti-washout hydroxyapatite/collagen paste utilizing sodium alginate	
6.1 Introduction	82
6.2 Materials and Methods.....	84
6.3 Results.....	87
6.4 Discussion.....	90
6.5 Conclusion.....	92
6.6 References.....	93
Chapter 7 Summary	95
Publications and Research record	99
Acknowledgement	101

Abstract

Hydroxyapatite (HAp), β -tricalcium phosphate (β -TCP) and their composites with natural polymers are widely used as filler materials for their biocompatibility and osteoconductivity. A three dimensional interconnection of both macro- and micro-pores (bimodal pores) is important for a porous scaffold, because macropores allow cell, blood vessel and tissue ingrowths and micropores serve as an effective pathway for exchange of fluid in which nutrition and wastes are dissolved. Marine derived biomaterials from corals, cuttlebones, sea urchin spines etc., have shown good potential as bone substitutes due to their interconnected porous structure and ease of conversion to calcium phosphate without any change in their original porous structure. However, corals are considered as reservoir of carbonate gas to decrease greenhouse effect and not recommended to collect from sea, cuttlebones consist of only macropores and sea urchin spines consist of only micropores. Contrarily, gonads of sea urchins are consumed as food in Japan and their skeletons are discarded as waste. Their skeletons consist of bimodal pores and hence utilization of sea urchin skeletons would reduce the waste, encourage Japanese fishery. In this study, calcium phosphate granules were prepared by hydrothermal phosphatization of sea urchin tests in an aqueous phosphate solution. The obtained calcium phosphate (CP1/CP2) was found to be biphasic in nature with 82 % Mg containing β -TCP and 18 % non-stoichiometric carbonate containing HAp (biphasic calcium phosphate, BCP) retaining their their original porous structure.

Scaffolds, CP1Col/CP2Col (collagen as binder) and CP1Gel_GA/CP2Gel_GA (gelatin as binder) were prepared by mixing the obtained BCP granules with collagen or gelatin solution. The scaffolds obtained exhibited open porous structure and had sufficient strength for good operability during surgery. The *in vitro* evaluation of scaffolds using human osteoblast-like cell line, MG63 cells under static conditions showed negligible toxicity,

higher distribution, proliferation and osteogenic activity in comparison to control collagen or gelatin sponges. From *in vitro* evaluation of scaffolds under pressure/perfusion cell culture condition, which mimics the biological conditions of bone, significant increase in proliferation (from total DNA analysis) and osteogenic activity from (gene expression analysis) was observed in scaffolds compared to control. The homogeneous, bimodal porous structure enhanced the cell distribution and the Mg^{2+} containing BCP granules promoted effective osteogenic activity in the scaffolds in both static and dynamic cell culture conditions. The scaffolds prepared by sea urchin-derived calcium phosphates with collagen or gelatin as binder could be a potential candidate for artificial bone filler in non-load bearing defects.

The supplementation of calcium carbonate and calcium citrate to an injectable hydroxyapatite/collagen (HAp/Col) paste prepared with sodium alginate increased its anti-washout property and pH controllability. This is due to coordinate effects of initial washout inhibition by weak but rapid formation of long-range network by citric acid followed by long term anti-washout inhibition by strong but slow network formation by Ca^{2+} ions. The paste also showed good cytocompatibility, MG63 cells proliferated with the culture time without any significant difference with the HAp/Col dense bodies. The HAp/Col paste is expected to be utilized in minimally invasive surgery of bone defect to fit irregular bone defects.

The calcium phosphate and natural polymers composites investigated in this study are expected to be utilised as filler materials for replacement and reconstruction of bone defects.

Chapter 1

Introduction

1.1 Basics of bone

Bone performs various functions such as provide support, protect internal organs, help in movement, store minerals and produce red and white blood cells. Bone is usually characterized by its solidity and flexibility. This remarkable living tissue which is very dynamic, mineralized and considered to be highly vascular also has the ability to heal, repair and even remodel itself. A bone is composed of multi-phase materials comprising cells embedded in a matrix of organic and inorganic elements. While lipids, proteins, peptides, collagen fibres, polysaccharides, glycoproteins and citrates constitute the organic elements, carbonates, sodium, calcium phosphates, magnesium and fluoride salts constitute inorganic elements of the matrix [1,2].

1.1.1 Bone structure

Based on its structure, the bone is classified into two types which are cortical, also known as the compact bone or cancellous which is also known as the spongy bone. The outer layer of the bone is made up of the cortical bone is known to be in outer layers of the bone, while the cancellous bone fills the interior. Cancellous bone remodels more often and has a higher metabolic activity in comparison to the cortical bone. The other type of classification of bone, classifies it into non-lamellar bone which occurs only in the foetus, young children and fractures in their healing stage, and into lamellar bone which is called the mature bone [3,4]. A bone's structure comprises of these major components: bone matrix, bone cells, bone marrow and a vascular network. The mechanical strength in the bone is provided by the matrix, while also acting as the body's mineral warehouse. Bone cells take care of the

maintenance and regulation of oxygen and nutrient supply, where they manage storage and release of minerals as needed by the body. The vascular network along with the bone marrow acts as a source of stem cells while also taking care of communication and interaction within the body [5].

1.1.2 Bone matrix

Collagen fibres and inorganic bone mineral crystals, which are basically two main components of the bone matrix, together make up ~95 % of the dry weight of bone. The rest of the bone is made up of various organic molecules and some poorly crystalline inorganic salts. Varying from a highly organized system of helical bundles or parallel-fibred sheets to a nearly random network of coarse bundles, collagen accounts 70-90% of the non-mineralized component of the bone matrix. Of the different types, type-I collagen accounts for 90% of the body's total collagen content [2,6] .

Within the bone, biological apatite also known as hydroxyapatite is the main inorganic crystal phase. It is characterized by calcium (Ca), phosphate (P) and hydroxyl (HAp, reported Ca:P ratio range 1.37–1.87) also containing significant traces of elements such as sodium (Na^+), magnesium (Mg^{2+}), fluorine (F⁻), chlorine (Cl^-) and carbonate (CO_3^{2-}). Bone apatite, although not a direct equivalent of HAp, it is more closely related to an A–B type carbonate-substituted apatite. Type A is a CO_3^{2-} for -OH substitution, and type B is CO_3^{2-} for - PO_4 substitution[2,7–12].

1.1.3 Bone cells

Bone constantly repairs itself through a process called remodelling. Coupled cells within the bone network work to remove old bone and replace it with new bone. A number

of different types of cells are present in bone namely: osteoblasts, osteoblasts, osteoclasts and osteoprogenitor cells.

Osteoblasts are bone forming cells which produce the proteins and organic components that make up osteoid, the un-mineralised form of bone tissue. Once osteoblasts are fully surrounded by extra cellular matrix, they become osteocytes. Osteocytes are networked with each other and maintain the bone matrix. Osteoclasts are responsible for bone resorption. They use secreted acids and enzymes to dissolve bone matrix. Osteoprogenitor cells are semi-differentiated stem cells within the bone marrow that can differentiate into osteoblasts.

When a bone defect or a fracture occurs, a blood clot forms, osteoprogenitor cells divide into osteoblasts, then they move to defect area. A callus forms around the fracture to temporarily stabilize the fracture. This callus is then replaced and reshaped by new bone formation through osteoclast and osteoblast activity. After a certain period, the whole bone around the defect area is remodelled. Unlike cartilage, bone is capable of repairing itself. However, fracture healing occurs only in defects below a critical size which depends on the fracture. If the defect creates a gap in the bone that is too large, it cannot be bridged and the fracture will not heal by itself. This is termed a non-union fracture or defect and a bone graft has to be used to enable full healing [13–17].

1.2 Bone grafts and current treatment

Bone grafts are required to aid bone defect and non-union healing, to restore function in the damaged area. The most commonly used treatment in bone replacement is autograft. An autograft is bone tissue harvested from and implanted into the same individual. This process is expensive and the size of the graft that can be obtained is limited. Other problems would be donor site morbidity, chronic pain and infection.

Allografts, the most common alternative to autografts, are bone grafts obtained from a organ donor. Xenogeneic bone grafts are bone from species other than human being. However, these products have limited success due to their rejection and foreign body response [18–21]. So other synthetic substitutes are desired by surgeons.

1.3 Synthetic bone substitutes

Artificial materials, which are believed to be safe and easily available are desired by surgeons to treat both load and non-load bearing defects. For this treatment, vast research has been conducted in the biomaterial research and development. Available and widely chosen synthetic bone grafts by surgeons can be characterized into Calcium phosphates (CaPs), and their composites [4]

1.3.1 Calcium phosphates (CaPs)

Like mentioned above, CaPs have been widely studied and used for bone substitution, reinforcement and regeneration. CaPs can be either natural or synthetic which can be prepared by various methods. They can also be fabricated into various forms like dense, microporous and/or macroporous: particles or blocks as desired. The mineral or the inorganic component in bone is composed of calcium phosphate materials. There has been wide research in various calcium phosphate compounds. Among them, HAp, β -tricalcium phosphate (β -TCP) and combination (mixture) of HAP and β -TCP called biphasic calcium phosphate (BCP) are widely used in orthopaedic and dental applications. HAp, β -TCP and BCP are known to be biocompatible and bioactive [22–25].

HAp is the most studied calcium phosphate for bone graft or bone tissue engineering applications due to its similarity in composition and structure to the inorganic element of bone. Its Ca:P ratio is known to be 1.67; however this can vary depending on the application

of synthetic method. Although HAp is chemically similar to bone, important differences remain. Like discussed above in section 1.1.2, natural bone's inorganic matrix is known to have trace elements such as Mg^{2+} , Na^+ , Cl^- , F^- and CO_3^{2-} . So, to mimic and enhance the activity, different substituted variants have been researched [26–28].

β -TCP exists in forms namely, α -TCP and β -TCP. Their difference is only the temperature at which they form. β -TCP can be detected from a minimum temperature of $700^\circ C$ and α -TCP at temperature greater than $1100^\circ C$. β -TCP cannot be directly prepared through aqueous methods such as precipitation due to its instability in water, so in order to obtain β -TCP, the procedure should contain a heat treatment above $700^\circ C$. β -TCP is highly known for its resorbability and degradability than HAp. This property is very essential for bone grafts, because the degradability can be tailored to match the rate of formation of bone at the defect site [4,29,30].

Even with the advantages of HAp and β -TCP, they are known to have poor resorbability and faster resorption rate respectively. So, effective control in degradation rate must be obtained to achieve proper bone formation. BCP, which consist of HAp and β -TCP combined, have been investigated to control the resorption rate. The resorption rate of BCP depends on the molar ratio of β -TCP/HAp in the mixture and the higher the ratio, the faster the resorption. BCP can be prepared by several methods like mechanical mixing of HAp and β -TCP, precipitation, solid-state reaction or microwave processing [4,31,32].

1.3.2 Commercially available bone grafts

Several commercially available bone graft substitutes claim promising results in bone repair; an overview of some bone graft substitutes from a pool of vast research are discussed in the following **Table 1.1**.

Taken together, most of the commercial available bone grafts have some advantages and disadvantages. Despite, numerous attempts, a synthetic bone substitute has yet to be produced that incorporates all the properties required for a bone graft.

Table 1.1 Commercial bone grafts

Commercial name	Composition	Form	Advantages
APACERAM® [33,34]	Hydroxyapatite	Blocks, granules and spacers	<ul style="list-style-type: none"> • High porosity • Integration to bone tissue • Early bone formation
ProOsteon® [35,36]	Coralline derived hydroxyapatite/Calcium carbonate composite	Granular or block	<ul style="list-style-type: none"> • Osteoconduction • Bioresorbable
Collapat® [37,38]	Collagen matrix with hydroxyapatite granules	Fleece like, when wet forms a paste	<ul style="list-style-type: none"> • Osteoconductive • Biodegradable • Bioresorbable
MasterGraft® [39]	BCP (15 % HAP/ 85 % β -TCP)	Granules	<ul style="list-style-type: none"> • Osteoconduction • Bioresorbable
ReFit® [40]	HAp and collagen composite	Sponge	<ul style="list-style-type: none"> • Flexibility in operation • Absorption and replacement in vivo • High porosity
SUPERPORE® [41]	β -TCP	Granules, blocks, cylinders	<ul style="list-style-type: none"> • High porosity • Balanced absorption and replacement
Bioset® [42]	Demineralised bone matrix combined with gelatin carrier	Injectable paste, putty, strips, blocks	<ul style="list-style-type: none"> • Osteoconduction • Bioresorbable • Osteoinduction
Healos® [43]	Mineralized collagen matrix	Sponge like strips	<ul style="list-style-type: none"> • Osteoconduction • Creeping substitution • Osteoinduction

1.3.3 Composites with polymers

Bioactive ceramics such as CaPs, in combination with polymers, have two fold purposes. The combination enhances the osteoconductive properties of the polymers and, serves to improve the composite's mechanical properties. It is evident from these two properties that a combination of the both materials draws on the advantages of each to build a superior composite biomaterial in comparison to the individual materials [44,45].

Tissue engineering has been investigating many polymers over the years for use in its applications. Of these, the FDA approved polylactide acid, polyglycolic acid and their combination, poly-lactic-go-glycolic acid are the most widely used polymers. Manufacturing of synthetic polymers provides us the advantage of infusing in them a tailored range of mechanical properties and architectures. But the fundamental problem in synthetic polymers is associated with their degradation by-products, alcohol content and acidity. Their acidity has been particularly implicated in speeding up the degradation of the scaffolds and producing a significant inflammatory response in the site surrounding the tissue. This further leads to an inhibition of tissue formation [46,47].

Collagen, chitosan, gelatin silk etc. are examples of natural polymers which exhibit excellent biocompatibility and their degradation produces non-toxic by-products. Collagen, a fibrous animal protein, is a major structural component of ECM of human body. It constitutes 30% of human body's proteins. It comprises triple helical fibrils, which have a role in maintaining the structural and mechanical integrity of the connective tissues. Important biological processes such as cell adhesion, wound healing, platelet activation and angiogenesis have collagen's high bioactivity playing a key role in them. This high bioactivity is a result of the presence of RGD peptides, which are known to be the best cell recognition signalling sequences. Human body has several types of collagen found in the ECM of connective tissues. Of these type I, II, III and IV are the most common. Of these four

collagen varieties, type I exhibits impressive mechanical and bioactivity properties. Therefore it is the most commonly used collagen in preparation of biomimetic scaffolds. Contamination of these materials is directly dependent upon the purity of the collagen used. Collagen is also known for its low antigenicity. The G-X-Y amino acid sequence which constitutes the collagen molecule differs among the animal species. Its low antigenicity is assumed to be the result of the presence of terminal telopeptides which lack the G-X-Y sequence. Commercial Type I Collagen is available in different purity grades. In its purest form it is available as Atelocollagen, which is synthesized from the terminal telopeptides sequence of collagen triple helices by their protease digestion. Lack of terminal telopeptides in atelocollagen lowers its antigenic character in comparison to natural collagen [48–51].

Partial hydrolysis and denaturation of collagen gives Gelatin. There are two basic processes involved in producing Gelatin from collagen. 1. Heat treatment around 40 °C in presence of water which lead to destruction of both hydrogen bond and the electrostatic interactions. 2. Presence of water facilitates the hydrolytic degradation of covalent linkages either in acidic or alkaline conditions. The acidic degradation leads to formation of type A and alkaline degradation lead to formation of type B gelatin. Type B gelatin is considered as purest form of gelatin. It has been used in many tissue engineering and drug delivery applications [51–54] .

The advances that have been made in utilizing natural polymers and ceramics to develop bone graft substitutes have not yet resulted in any single successful approach. Although natural polymers have excellent biological performance, they fare poorly in their mechanical properties. On the other hand, ceramics exhibit good mechanical properties but, they also exhibit brittle behaviour. Therefore recent studies have focused their investigations on composites that use natural polymers reinforced with CaPs such as HAp, β -TCP or BCP [55–60].

Two dimensional (2D) and three dimensional (3D) mineralized collagen scaffolds have shown significantly better results in comparison to collagen-only scaffolds in their osteogenic differentiation of bone marrow stem cells [61]. Collagen-HAp has proven to be an ideal material in preparing scaffolds due to their characteristics ideal for bone. Also, scaffolds made from combination of CaPs and natural polymers have shown improved cell response to osteoblasts, in comparison to polymer-only scaffolds. Similarly, compared to gelatin-only scaffolds, Gelatin-HA[62,63] and Gelatin- β -TCP [64,65] composites have shown increased osteogenic response of osteoblasts. Mineralised polymers differ from pure polymers in their respective physical and mechanical properties and also have better biocompatibility.

The efforts put in development of composite scaffolds by combining bioceramic materials and natural polymers have been promising so far in their results which combine the benefits of the both materials. Despite these efforts, there are still issues which need to be addressed along the way towards the development of an ideal scaffold for bone tissue engineering.

1.4 Marine organisms derived CaPs for bone repair and regeneration

Marine derived and inspired bioceramics have great potential in producing the materials of required physiochemical characteristics, suitable for bone repair. Marine organism minerals are usually either silica based minerals or calcium carbonate in its aragonite form or calcite form. CaPs present in the bone or skeletons of certain marine organisms could be a useful resource in preparation of scaffolds. These scaffolds could be directly used for bone growth either *ex vivo* or *in situ* tissue engineering [66].

Also, the porous nature of these structures available in marine organisms lends themselves to be useful in bone repair. As discussed in prior sections, despite being closest to the mineral phase of the bone, early synthetic bone substitutes such as solid particles of CaP,

usually hydroxyapatite (HAp), they remain visible in situ much longer after implantation due to the body's difficulty in absorbing them. In order to overcome this slow absorption problem, Hulbert *et al.*, have suggested the use of porous structures and this suggestion has dichotomized the problem into mechanical strength and percentage porosity, while at the same time ensuing a debate over the most optimum features of pores which include pores size, connectivity of pores (i.e., interconnected or closed), their tortuosity (the difficulty of the route through the material) and the overall porosity (some materials have >90% porosity with very little actual ceramic providing a much larger surface area) [67,68]. Even after years of discussion or debates where the optimum pore size varied from 100 μm to as large as 500 μm diameter, there still is no consensus over the best optimum size of a pore either for bone ingrowth or resorption. More recently, there has been an observed enhancement in bone repair upon the addition of microporosity (<10 μm) which is doing so by possibly improving fluid flow and promoting neovascularisation [69–71].

When it comes to porous materials, marine organisms have always been a readily available resource. These organisms' exhibit pores whose size varies from submicron to millimetre diameters. This wide variety of pore sizes allows for creation of materials suitable for pore-size dependent applications such as neovascularisation, bone ingrowth and material resorption based on their individual medical specifications [72]. Some of the marine organisms used in the derivation of biomaterials for bone tissue engineering are discussed in **Table 1.2.**

Two marine derived products have been commercialised in the 1970s after years of studies on corals. These are Pro-Osteon (Biomet, USA) and Biocoral. They have been derived from differing genera of stony corals, which exhibit a skeletal morphology similar to human cancellous bone. Although these products have been available for many years, their use in the clinic remains low, due to their low resorbability[73,74]. Third commercially

available product is derived from species of mineralising red algae, known as Algipore® is a HAp bone graft; its internal microporous (5 – 10 µm) and interconnected morphology makes it interesting from other commercial products available in market. It obtained FDA approval in 2003, however, that high temperature and pressure synthesis processes employed by the manufacturer produce a crystalline by-product and rise the similar concerns about bioresorbability like found with coral-based products[66,75] .

Table 1.2 Marine organisms derived Calcium phosphates (CaPs)

Common name	Skeletal mineral	Conversion procedure	Final product
Red Algae [76]	CaCO ₃ /Calcite	Hydrothermal treatment	Non-stoichiometric HAP retaining the porous structure
Corals [77]	CaCO ₃ /Aragonite	Hydrothermal treatment	HAP retaining the porous structure
Snails [78,79]	CaCO ₃ /Aragonite	Ultrasonic and hot plate treatment	Powder form consisting of monetite and β-TCP
Sea shells [80]	CaCO ₃ /Aragonite	Hydrothermal treatment	Dense HAP
Cuttlefish [81]	CaCO ₃ /Aragonite	Hydrothermal treatment	HAP retaining porous structure
Starfish [82]	CaCO ₃ /Calcite	Hydrothermal treatment	β- Mg TCP retaining porous structure
Sea urchin spines [83]	CaCO ₃ /Calcite	Hydrothermal treatment	β- Mg TCP retaining porous structure
Sea urchin skeletons [84,85]	CaCO ₃ /Calcite	a) Ultrasonic and hot plate treatment b) Hydrothermal treatment	a) Powder form containing monetite and β-TCP b) Mg- β TCP and HAp

1.5 Overview of thesis

The general purpose of the studies in this thesis was to develop functional biomaterials with calcium phosphates and their composites with biocompatible polymers to be used as a potential substitute for artificial bone fillers. The potential substitutes discussed in this study are in the form of shape controllable three dimensional scaffolds, injectable past for non-load bearing and irregular bone defects respectively.

In **chapter 2**, conversion of tests of sea urchin, the widely available food waste due to the consumption of sea urchin, namely *strongylocentrotus nudus* and *strongylocentrotus intermediu*, to calcium phosphate using hydrothermal treatment was described. The obtained calcium phosphate and unconverted sea urchin tests were characterized. The differences in the microstructure, composition were discussed.

In **chapter 3**, the preparation of flexible and shape controllable three dimensional (3D) scaffolds utilizing the porous granules of calcium phosphate obtained sea urchin test and biocompatible polymers collagen or gelatin was described. The focus was the on the microstructure, open porosity and mechanical properties of the obtained scaffolds.

In **chapter 4**, the biocompatibility evaluation of the scaffolds prepared with collagen or gelatin as binder is discussed. The scaffolds were subjected to cell culture with osteoblast-like cell line MG-63 cells and evaluated for viability/cytotoxicity, cell adherence, distribution and proliferation under two dimensional (2D)/ static cell culture conditions.

In **Chapter 5**, the biocompatibility evaluation of the scaffolds performed under three dimensional (3D)/ dynamic cell culture conditions was discussed. The scaffolds were evaluated using MG-63 cell line for cell proliferation, distribution and gene expression. The

results for scaffolds prepared with collagen and gelatin as binder were outlined and their potential to be used as artificial bone fillers for non-load bearing defects was proposed.

Chapter 6, records the improvement of the washout property of the injectable bone paste prepared with bone like nanocomposite hydroxyapatite/collagen (HAp/Col) and sodium alginate by the combined supplementation of calcium carbonate and calcium citrate. The changes in the viscosity, washout property and the cytocompatibility of the paste with the combined supplementation of calcium carbonate and calcium citrate were examined. The potential of this improved paste as injectable bone filler was proposed.

In **Chapter 7**, the contents of each chapter were briefly summarized to discuss the preparation and evaluation of materials to obtain functional composites in the form of 3D scaffolds and injectable paste for bone defects, along with recommendation for future investigations.

1.6 References

1. RR C. The biochemistry and physiology of bone, vol 1: Structure. JAMA. 1972;222:367.
2. Kelly S. Fabrication of polymer composites as potential bone replacement materials. 2012;258.
3. Jacobs C. Skeletal Tissue Mechanics R. Bruce Martin, David B. Burr and Neil A. Sharkey (Eds.); Springer, New York, 1998, 392 pages, ISBN: 0-387-98474-7. J. Biomech. Elsevier; 2017;33:1339.
4. Zhang X. Preparation and characterization of calcium phosphate ceramics and composites as bone substitutes. University of California; 2013.
5. BOURNE GH. Preface to First Edition BT - The Biology and Physiology of Bone (Second Edition). Academic Press; 1972. p. xiii–xiv.
6. Ferreira AM, Gentile P, Chiono V, Ciardelli G. Collagen for bone tissue regeneration. Acta Biomater. 2012;8:3191–200.
7. Zapanta LeGeros R. Apatites in biological systems. Prog. Cryst. Growth Charact. 1981;4:1–45.
8. Posner AS. Crystal chemistry of bone mineral. Physiol. Rev. United States; 1969;49:760–92.
9. Suchanek W, Yoshimura M. Processing and properties of hydroxyapatite-based biomaterials for use as hard tissue replacement implants. J. Mater. Res. 2011/01/01. Cambridge University Press; 1998;13:94–117.
10. Hughes JM. Structure and Chemistry of the Apatites and Other Calcium Orthophosphates By J. C. Elliot (The London Hospital Medical College). Elsevier: Amsterdam. 1994. xii + 389 pp. ISBN 0-444-81582-1. J. Am. Chem. Soc. American Chemical Society; 1996;118:3072.
11. LeGeros RZ, LeGeros JP. DENSE HYDROXYAPATITE. An Introd. to Bioceram. WORLD SCIENTIFIC; 1993. p. 139–80.
12. BOURNE GH. PREFACE BT - The Biochemistry and Physiology of Bone. Academic

Press; 1956. p. v–vi.

13. Florencio-Silva R, Sasso GR da S, Sasso-Cerri E, Simões MJ, Cerri PS. Biology of Bone Tissue: Structure, Function, and Factors That Influence Bone Cells. *Biomed Res. Int.* Hindawi Publishing Corporation; 2015;2015:421746.
14. Ozawa H, Amizuka N. [Structure and function of bone cells]. *Nihon Rinsho.* Japan; 1994;52:2246–54.
15. Mohamed AM. An Overview of Bone Cells and their Regulating Factors of Differentiation. *Malays. J. Med. Sci.* Penerbit Universiti Sains Malaysia; 2008;15:4–12.
16. Crockett JC, Rogers MJ, Coxon FP, Hocking LJ, Helfrich MH. Bone remodelling at a glance. *J. Cell Sci.* The Company of Biologists Ltd; 2011;124:991–8.
17. Raggatt LJ, Partridge NC. Cellular and Molecular Mechanisms of Bone Remodeling. *J. Biol. Chem.* . 2010;285:25103–8.
18. Campana V, Milano G, Pagano E, Barba M, Cicione C, Salonna G, et al. Bone substitutes in orthopaedic surgery: from basic science to clinical practice. *J. Mater. Sci. Mater. Med.* Boston: Springer US; 2014;25:2445–61.
19. Kumar P, Vinitha B, Fathima G. Bone grafts in dentistry. *J. Pharm. Bioallied Sci. India:* Medknow Publications & Media Pvt Ltd; 2013;5:S125–7.
20. Shibuya N, Jupiter DC. Bone graft substitute: allograft and xenograft. *Clin. Podiatr. Med. Surg.* United States; 2015;32:21–34.
21. Chiarello E, Cadossi M, Tedesco G, Capra P, Calamelli C, Shehu A, et al. Autograft, allograft and bone substitutes in reconstructive orthopedic surgery. *Aging Clin. Exp. Res.* Germany; 2013;25 Suppl 1:S101-3.
22. Saikia KC, Bhattacharya TD, Bhuyan SK, Talukdar DJ, Saikia SP, Jitesh P. Calcium phosphate ceramics as bone graft substitutes in filling bone tumor defects. *Indian J. Orthop.* India: Medknow Publications; 2008;42:169–72.
23. Habraken W, Habibovic P, Epple M, Böhner M. Calcium phosphates in biomedical applications: materials for the future? *Mater. Today.* 2016;19:69–87.
24. Böhner M, Galea L, Doebelin N. Calcium phosphate bone graft substitutes: Failures and

hopes. *J. Eur. Ceram. Soc.* 2012;32:2663–71.

25. Burger EL, Patel V. Calcium phosphates as bone graft extenders. *Orthopedics*. United States; 2007;30:939–42.

26. Lin K, Chang J. 1 - Structure and properties of hydroxyapatite for biomedical applications
A2 - Mucalo, Michael BT - Hydroxyapatite (Hap) for Biomedical Applications. Woodhead Publ. Ser. Biomater. Woodhead Publishing; 2015. p. 3–19.

27. Szcześ A, Hołysz L, Chibowski E. Synthesis of hydroxyapatite for biomedical applications. *Adv. Colloid Interface Sci.* 2017;

28. Haider A, Haider S, Han SS, Kang I-K. Recent advances in the synthesis{,} functionalization and biomedical applications of hydroxyapatite: a review. *RSC Adv. The Royal Society of Chemistry*; 2017;7:7442–58.

29. Bucholz RW, Carlton A, Holmes RE. Hydroxyapatite and tricalcium phosphate bone graft substitutes. *Orthop. Clin. North Am. United States*; 1987;18:323–34.

30. Horowitz RA, Mazor Z, Foitzik C, Prasad H, Rohrer M, Palti A. β -tricalcium phosphate as bone substitute material: properties and clinical applications. *J. Osseointegration*; Vol 2 No 2. 2010;

31. Lobo SE, Livingston Arinzeh T. Biphase Calcium Phosphate Ceramics for Bone Regeneration and Tissue Engineering Applications. *Mater.* . 2010.

32. LeGeros RZ, Lin S, Rohanizadeh R, Mijares D, LeGeros JP. Biphase calcium phosphate bioceramics: preparation, properties and applications. *J. Mater. Sci. Mater. Med. United States*; 2003;14:201–9.

33. Tran YH, Ohsaki K, Ii K, Ye Q, Yokozeki M, Moriyama K. Histological reaction of auditory bulla bone to synthetic auditory ossicle (Apaceram) in rats. *J. Med. Invest. Japan*; 2000;47:56–60.

34. Fukuta Y, Saito Y, Segawa K, Kudo K, Fujioka Y. Clinical evaluation of hydroxylapatite particles, (Apaceram G[®]) into the bony defect following extirpation of jaw cysts. *Dent. J. Iwate Med. Univ.* 1988;13:123–8.

35. Songer M, Baskin D, Kabins M, Reynolds A, Zak P. 3:50 Prospective randomized

comparison of ProOsteon 200 Coralline Hydroxyapatite bone graft substitute versus iliac crest autograft in anterior cervical fusions. *Spine J.* 2002;2:64.

36. Leupold JA, Barfield WR, An YH, Hartsock LA. A comparison of ProOsteon, DBX, and collagraft in a rabbit model. *J. Biomed. Mater. Res. B. Appl. Biomater.* United States; 2006;79:292–7.

37. Katthagen BD, Mittelmeier H. [New implants for the regeneration of bone (Collapat and Pyost)]. *Rev. Chir. Orthop. Reparatrice Appar. Mot.* France; 1986;72 Suppl 2:81–3.

38. Mittelmeier H, Grabowski MT. [Healing of bone defects after using the preparation “collapat”]. *Chir. Narzadow Ruchu Ortop. Pol.* Poland; 1983;48:483–8.

39. Smucker JD, Petersen EB, Nepola J V, Fredericks DC. Assessment of Mastergraft(®) Strip with Bone Marrow Aspirate as a Graft Extender in a Rabbit Posterolateral Fusion Model. *Iowa Orthop. J.* The University of Iowa; 2012;32:61–8.

40. Sotome S, Ae K, Okawa A, Ishizuki M, Morioka H, Matsumoto S, et al. Efficacy and safety of porous hydroxyapatite/type 1 collagen composite implantation for bone regeneration: A randomized controlled study. *J. Orthop. Sci.* The Authors; 2016;21:373–80.

41. Seto S, Muramatsu K, Hashimoto T, Tominaga Y, Taguchi T. A new beta-tricalcium phosphate with uniform triple superporous structure as a filling material after curettage of bone tumor. *Anticancer Res.* Greece; 2013;33:5075–81.

42. Zhukauskas R, Dodds RA, Hartill C, Arola T, Cobb RR, Fox C. Histological and radiographic evaluations of demineralized bone matrix and coralline hydroxyapatite in the rabbit tibia. *J. Biomater. Appl.* England; 2010;24:639–56.

43. Kunakornsawat S, Kirinpanu A, Piyaskulkaew C, Sathira-Angkura V. A comparative study of radiographic results using HEALOS collagen-hydroxyapatite sponge with bone marrow aspiration versus local bone graft in the same patients undergoing posterolateral lumbar fusion. *J. Med. Assoc. Thai.* Thailand; 2013;96:929–35.

44. Baino F, Novajra G, Vitale-Brovarone C. Bioceramics and Scaffolds: A Winning Combination for Tissue Engineering. *Front. Bioeng. Biotechnol.* Frontiers Media S.A.; 2015;3:202.

45. Mohamad Yunos D, Bretcanu O, Boccaccini AR. Polymer-bioceramic composites for

tissue engineering scaffolds. *J. Mater. Sci.* 2008;43:4433.

46. Hollinger JO, Battistone GC. Biodegradable bone repair materials. Synthetic polymers and ceramics. *Clin. Orthop. Relat. Res. United States*; 1986;290–305.

47. Goonoo N, Bhaw-Luximon A, Bowlin GL, Jhurry D. An assessment of biopolymer- and synthetic polymer-based scaffolds for bone and vascular tissue engineering. *Polym. Int.* John Wiley & Sons, Ltd; 2013;62:523–33.

48. Lu H, Ko Y-G, Kawazoe N, Chen G. Cartilage tissue engineering using funnel-like collagen sponges prepared with embossing ice particulate templates. *Biomaterials.* Netherlands; 2010;31:5825–35.

49. Zhang Q, Lu H, Kawazoe N, Chen G. Preparation of collagen porous scaffolds with a gradient pore size structure using ice particulates. *Mater. Lett.* 2013;107:280–3.

50. Yamaoka H, Tanaka Y, Nishizawa S, Asawa Y, Takato T, Hoshi K. The application of atelocollagen gel in combination with porous scaffolds for cartilage tissue engineering and its suitable conditions. *J. Biomed. Mater. Res. A. United States*; 2010;93:123–32.

51. Gómez-Guillén MC, Giménez B, López-Caballero ME, Montero MP. Functional and bioactive properties of collagen and gelatin from alternative sources: A review. *Food Hydrocoll.* 2011;25:1813–27.

52. Chen S, Zhang Q, Nakamoto T, Kawazoe N, Chen G. Gelatin Scaffolds with Controlled Pore Structure and Mechanical Property for Cartilage Tissue Engineering. *Tissue Eng. Part C. Methods.* United States; 2016;22:189–98.

53. Lou X, Chirila T V. Swelling behavior and mechanical properties of chemically cross-linked gelatin gels for biomedical use. *J. Biomater. Appl.* England; 1999;14:184–91.

54. Gámez Sazo RE, Maenaka K, Gu W, Wood PM, Bunge MB. Fabrication of growth factor- and extracellular matrix-loaded, gelatin-based scaffolds and their biocompatibility with Schwann cells and dorsal root ganglia. *Biomaterials.* 2012;33:8529–39.

55. Shue L, Yufeng Z, Mony U. Biomaterials for periodontal regeneration: a review of ceramics and polymers. *Biomatter.* United States; 2012;2:271–7.

56. Lee J-M, Choi BBR, Choi J-H, Kim G-C, Hwang D-S, Chang MC, et al. Osteoblastic

response to the hydroxyapatite/gelatin nanocomposite and bio-calcium phosphate cement. *Tissue Eng. Regen. Med.* 2013;10:47–52.

57. Neumann M, Epple M. Composites of Calcium Phosphate and Polymers as Bone Substitution Materials. *Eur. J. Trauma.* 2006;32:125–31.

58. Antoniac IV, Albu MG, Antoniac A, Rusu LC, Ghica MV. Collagen--Bioceramic Smart Composites. In: Antoniac IV, editor. *Handb. Bioceram. Biocomposites.* Cham: Springer International Publishing; 2016. p. 301–24.

59. Zhang D, Wu X, Chen J, Lin K. The development of collagen based composite scaffolds for bone regeneration. *Bioact. Mater.* 2017;

60. Liu X, Smith LA, Hu J, Ma PX. Biomimetic Nanofibrous Gelatin/Apatite Composite Scaffolds for Bone Tissue Engineering. *Biomaterials.* 2009;30:2252–8.

61. Sikavitsas VI, Bancroft GN, Holtorf HL, Jansen JA, Mikos AG. Mineralized matrix deposition by marrow stromal osteoblasts in 3D perfusion culture increases with increasing fluid shear forces. *Proc. Natl. Acad. Sci. U. S. A. National Academy of Sciences;* 2003;100:14683–8.

62. Kim H-W, Knowles JC, Kim H-E. Porous scaffolds of gelatin-hydroxyapatite nanocomposites obtained by biomimetic approach: characterization and antibiotic drug release. *J. Biomed. Mater. Res. B. Appl. Biomater. United States;* 2005;74:686–98.

63. Azami M, Tavakol S, Samadikuchaksaraei A, Hashjin MS, Baheiraei N, Kamali M, et al. A Porous Hydroxyapatite/Gelatin Nanocomposite Scaffold for Bone Tissue Repair: In Vitro and In Vivo Evaluation. *J. Biomater. Sci. Polym. Ed. England;* 2012;23:2353–68.

64. Furusawa T, Minatoya T, Okudera T, Sakai Y, Sato T, Matsushima Y, et al. Enhancement of mechanical strength and in vivo cytocompatibility of porous beta-tricalcium phosphate ceramics by gelatin coating. *Int. J. Implant Dent. Germany;* 2016;2:4.

65. Kim S-M, Yi S-A, Choi S-H, Kim K-M, Lee Y-K. Gelatin-layered and multi-sized porous β -tricalcium phosphate for tissue engineering scaffold. *Nanoscale Res. Lett. Springer;* 2012;7:78.

66. CLARKE SA, WALSH P. Marine organisms for bone repair and regeneration. Mallick K, editor. *Bone Substit. Biomater. Woodhead Publishing Limited;* 2014.

67. Hulbert SF, Cooke FW, Klawitter JJ, Leonard RB, Sauer BW, Moyle DD, et al. Attachment of prostheses to the musculoskeletal system by tissue ingrowth and mechanical interlocking. *J. Biomed. Mater. Res. United States*; 1973;7:1–23.
68. Hulbert SF, Young FA, Mathews RS, Klawitter JJ, Talbert CD, Stelling FH. Potential of ceramic materials as permanently implantable skeletal prostheses. *J. Biomed. Mater. Res. Interscience Publishers, a division of John Wiley & Sons, Inc.*; 1970;4:433–56.
69. Bohner M, Loosli Y, Baroud G, Lacroix D. Commentary: Deciphering the link between architecture and biological response of a bone graft substitute. *Acta Biomater.* 2011;7:478–84.
70. Karageorgiou V, Kaplan D. Porosity of 3D biomaterial scaffolds and osteogenesis. *Biomaterials.* 2005;26:5474–91.
71. Hing KA, Annaz B, Saeed S, Revell PA, Buckland T. Microporosity enhances bioactivity of synthetic bone graft substitutes. *J. Mater. Sci. Mater. Med. United States*; 2005;16:467–75.
72. Ben-Nissan B. 1 - Discovery and development of marine biomaterials A2 - Kim, Se-Kwon BT - Functional Marine Biomaterials. Woodhead Publ. Ser. Biomater. Woodhead Publishing; 2015. p. 3–32.
73. Holmes RE, Bucholz RW, Mooney V. Porous hydroxyapatite as a bone-graft substitute in metaphyseal defects. A histometric study. *J. Bone Joint Surg. Am. United States*; 1986;68:904–11.
74. Vuola J, Taurio R, Goransson H, Asko-Seljavaara S. Compressive strength of calcium carbonate and hydroxyapatite implants after bone-marrow-induced osteogenesis. *Biomaterials. Netherlands*; 1998;19:223–7.
75. Ewers R. Maxilla sinus grafting with marine algae derived bone forming material: a clinical report of long-term results. *J. Oral Maxillofac. Surg. United States*; 2005;63:1712–23.
76. Felício-Fernandes G, Laranjeira MCM. Calcium phosphate biomaterials from marine algae. Hydrothermal synthesis and characterisation. *Química Nova. scielo*; 2000;23:441–6.
77. ROY DM, LINNEHAN SK. Hydroxyapatite formed from Coral Skeletal Carbonate by Hydrothermal Exchange. *Nature.* 1974;247:220–2.
78. Kel D, Gökçe H, Bilgiç D, Ağaoğulları D, Duman I, Öveçoğlu ML, et al. Production of

Natural Bioceramic from Land Snails. *Key Eng. Mater. Trans Tech Publications*; 2012;493–494:287–92.

79. Ozyegin LS, Sima F, Ristoscu C, Kiyici IA, Mihailescu IN, Meydanoglu O, et al. Sea Snail: An Alternative Source for Nano-Bioceramic Production. *Key Eng. Mater.* 2011;493–494:781–6.

80. Vecchio KS, Zhang X, Massie JB, Wang M, Kim CW. Conversion of bulk seashells to biocompatible hydroxyapatite for bone implants. *Acta Biomater. England*; 2007;3:910–8.

81. Ivankovic H, Gallego Ferrer G, Tkalcec E, Orlic S, Ivankovic M. Preparation of highly porous hydroxyapatite from cuttlefish bone. *J. Mater. Sci. Mater. Med.* 2009;20:1039–46.

82. Takeuchi A, Tsuge T, Kikuchi M. Preparation of porous β -tricalcium phosphate using starfish-derived calcium carbonate as a precursor. *Ceram. Int.* 2016;42:15376–82.

83. Vecchio KS, Zhang X, Massie JB, Wang M, Kim CW. Conversion of sea urchin spines to Mg-substituted tricalcium phosphate for bone implants. *Acta Biomater. England*; 2007;3:785–93.

84. Ağaoğullari D, Kel D, Gökçe H, Duman I, Öveçoğlu ML, Akarsubaşı AT, et al. Bioceramic production from sea urchins. *Acta Phys. Pol. A.* 2012.

85. Manchinasetty NVL, Oshima S, Kikuchi M. Preparation of flexible bone tissue scaffold utilizing sea urchin test and collagen. *J. Mater. Sci. Mater. Med.* 2017;28:184.

Chapter 2

Conversion of sea urchin tests to calcium phosphate

2.1 Introduction

The applications and research to obtain biomaterials from marine organisms started since 1970's[1]. Corals[2], sponges[3], cuttlebone[4], and sea urchin spines[5] (also discussed in Section 1.4) show good potential as bone substitutes by preclinical experiments. The two significant reasons as to why biomaterials from marine organisms are being studied into application for bone fillers, one is that they are generally composed of calcium carbonate in the form of aragonite or calcite which is easily converted to calcium phosphates by hydrothermal conversion and the other is that they have unique porous structures which are useful for cell migration and liquid penetration[6].

Marine organisms are also a rich source of ions like carbonate (CO_3^{2-}), magnesium (Mg^{2+}) and silicate (SiO_4^{4-}) which can be incorporated into a biomaterial when converting the base mineral to calcium phosphate. Magnesium has been reported to enhance osteoblast adhesion, angiogenesis in porous structures [7] and increase bioresorption[8], carbonate and silicon substituted calcium phosphates have been shown to enhance the bone formation *in vivo*[9,10]. So, just by simply choosing the biogenic source of calcite or aragonite, a range of ion substitutions is possible, obtained by simple process compared to the some complex processes required to produce ion-substituted ceramics[11]. Works on the use of marine organisms as a bone substitute resulted in commercialization of two well-known products namely, Pro-osteonTM and Biocoral[®], derived from stony corals. Although these products have been available for many years, their use in the clinic remains low due to their poor bioresorption[12,13].

The big problems on usage of stony corals are coming from ecological point of views. Stony corals play important roles in marine and global eco-systems. Corals form coral reefs provide living and breeding place for large number of marine organisms such as fish, shrimp, and sea slugs and so on, and accumulate carbonate gas, a typical greenhouse effect gas, as a calcium carbonate to decrease greenhouse effect. Accordingly, their collection from the sea is strongly restricted worldwide[14]. Whereas, sea urchins are widely consumed as food in Japan and some countries, and their shells (tests) are discarded as wastes of food processing. The total amount of sea urchin food processing waste in Hokkaido area of Japan was estimated to be approximately 4,000 metric tons in 2013[15]. The costs of disposal are mainly borne by the fisherman, thus utilization of sea urchin tests would reduce the waste as well as encourage Japanese fishery. So, this chapter describes the conversion and characterization of sea urchin tests to calcium phosphate.

2.2 Materials and Methods

2.2.1 Materials

Chemicals used in this research were purchased from Wako Pure Chemical Ltd., Japan if that without further notice. Tests of sea urchins, *strongylocentrotus nudus* and *strongylocentrotus intermedius* were kindly provided from the Shakotan-cho, Hokkaido prefecture, Japan. Skeletons of the sea urchin tests were obtained by removal of their organic substances by soaking in commercial bleach solution (Kitchen power bleach, Lion Hygiene Corporation) at 10 % in volume, several-time washing with distilled water, soaked in warm water overnight to remove excess chlorine, washed with distilled water again and dried in an oven at 60 °C. The skeleton obtained from *strongylocentrotus intermedius* is denoted as SU1 and that from *strongylocentrotus nudus* is denoted as SU2.

2.2.2 Hydrothermal phosphatization

The skeletons, SU1 or SU2, were crushed by hand and hydrothermally treated in Teflon[®] lined stainless steel autoclave (300 mL of internal volume, Taiatsu Techno[®] Corporation) at 180 °C for 6 days with 200 mL of 750 mM (NH₄)₂PO₄ and 25 mL of 300 mM KH₂PO₄ *i.e.*, filling ratio of 75 % in volume. After 6 days of treatment, the autoclave was quenched with tap water. The solid phase was collected by filtration, cleaned in distilled water by an ultrasonication (Ultrasonic multi cleaner, W-113, Honda, Japan) for 5 min and dried in an oven overnight at 60 °C. The skeletons phosphatized from SU1 and SU2 are denoted as CP1 and CP2, respectively.

2.2.3 Characterization of sea urchin skeletons

Microstructures and pore morphologies of them were observed by the scanning electron microscopy (SEM, S4800, Hitachi, Japan) with a Pt coating. The diameter of macropores and micropores were calculated according the method mentioned in ISO 13175-3. Qualitative chemical analyses of them were qualitatively identified by the energy dispersive X-ray spectroscopy (EDS, E-maxEvolution, Horiba Ltd., Japan) equipped with the SEM.

The CP1 and CP2 were calcined to be the respective CPC1 and CPC2 at 1000 °C for 30 min with a furnace (Nabertherm[®], N150/14, Lillenthal, Germany) to examine the stability of crystal phases. Crystal phases of the SUs, CPs and CPCs were identified by the powder X-ray diffractometry (XRD, RINT-Ultima III, Rigaku Corporation, Japan) using CuK α from 10 to 60 ° for 2θ at a scanning rate of 2 °/min. Ratios of calcium phosphate phases formed in the CP1 and CP2 was calculated from one selected XRD peak of calcium phosphate phases using a standard curve. The standard curve was calculated using the same peaks from XRD patterns of serial mixtures of pure calcium phosphates, contained in the obtained CPs. The Ca/P

atomic ratio was calculated by using relative intensity of 3 0 0 diffraction line of HAp (32.90°) and 0 2 10 diffraction line of TCP (31.03°).

Transmission infrared spectra of the SUs, CPs and CPCs were measured by the KBr (Sigma Aldrich, USA) pellet method with a Fourier-transformed infrared spectrometer (FT-IR, Nicolet 4700, Thermo Electron Corporation, Japan). Quantities of calcium, magnesium and phosphorus for SUs, CPs and CPCs were measured by the inductively coupled plasma atomic emission spectroscopy (ICP-AES, SPS7800, SII, NanoTechnology, Japan). The samples of 50 mg were dissolved in 5 mL of aqueous solution of HNO₃ 1 % in mass, and the sample solutions were subsequently diluted at 1:200 with the same HNO₃ solution for the ICP-AES analysis.

2.3 Results and Discussion

The results of characterization mentioned above were almost the same except for the ICP-AES and quantitative XRD analyses; hence, the CP2 and CPC2 results on physicochemical analyses are mainly used for further discussion in this chapter. Figure 2.1 shows naked-eye observations of sea urchin skeletons before and after hydrothermal phosphatization. The macroscopic shape was retained and its color was removed after treatment.

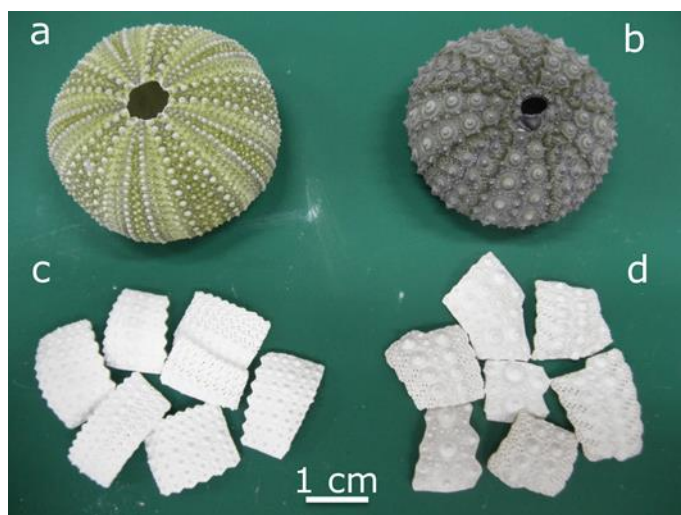


Figure 2.1 Naked eye view of (a) SU1 (b) SU2, (c) CP1 and (d) CP2.

Figure 2.2 shows the XRD results of the SU2, CP2 and CPC2. The SU2 was identified as calcite (JCPDS 5-586) single phase; thus, the SU2 was Mg-containing calcite as stated in previous reports. The CP2 was composed of two phases, β -tricalcium phosphate (β -TCP, JCPDS 9-619) and hydroxyapatite (HAp, JCPDS 9-432). After the hydrothermal phosphatization, the SU2 transformed to a biphasic calcium phosphate (BCP) consisting of Mg-containing β - tricalcium phosphate and a small amount of hydroxyapatite. From the XRD pattern of CPC2, HAp phase was disappeared and became a β -TCP single phase. The SU1, CP1 and CPC1 demonstrated the similar results in the XRD data to the SU2, CP2 and CPC2, respectively. The amount of β -TCP and HAp formed in CP1 and CP2 calculated from XRD pattern is shown in Table 2.1

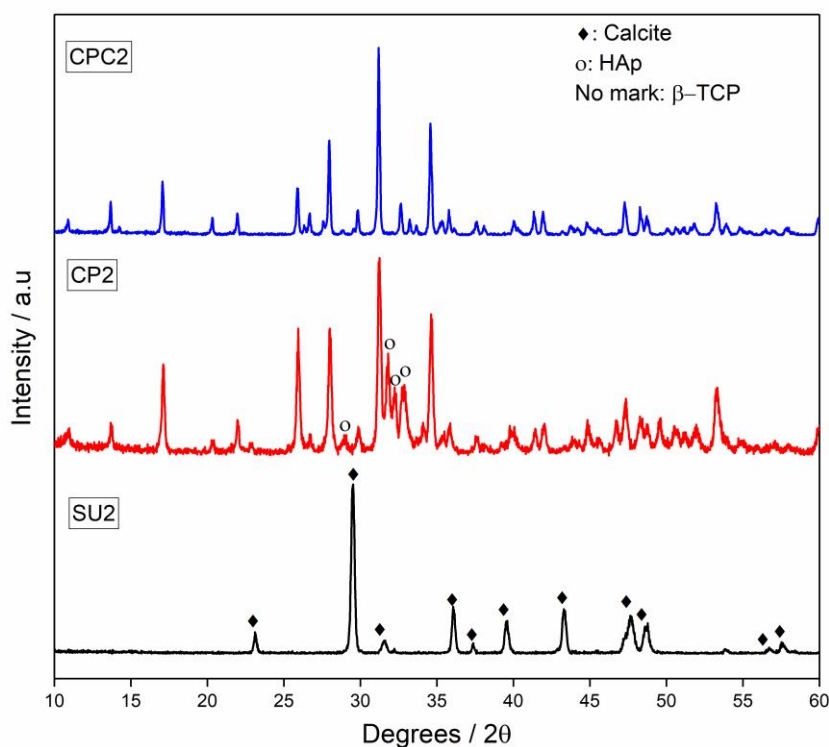


Figure 2.2 XRD pattern of SU2, CP2 and CPC2.

Table 2.1 Quantitative analysis from XRD

Sample	β -TCP (%)	HAp (%)	Ca/P
CP1	82.5	17.5	1.53
CP2	82.0	18.0	1.53

The FT-IR results of the SU2, CP2 and CPC2 are shown in Fig. 2.3 Internal modes of carbonate in calcite at 713, 878 cm^{-1} and broad absorption band around 1450 cm^{-1} was detected in the SU2. The CP2 spectrum showed absorption bands for PO_4^{3-} bending mode at 608 and 561 cm^{-1} ; stretching mode at 962 and 1025 cm^{-1} ; absorption bands for CO_3^{2-} anti-symmetric stretching mode at 1425 cm^{-1} and OH^- stretching mode at 3571 cm^{-1} , but no absorption bands from organic substances were detected. The spectrum of the CPC2 showed no differences with that of the CP2 except for an absence of the CO_3^{2-} and OH^- absorption band. Overall assignments are given in Table 2.2 [16]. As the same as the XRD results, the

FT-IR data for the SU1, CP1 and CPC1 showed the similar results to SU2, CP2 and CPC2, respectively.

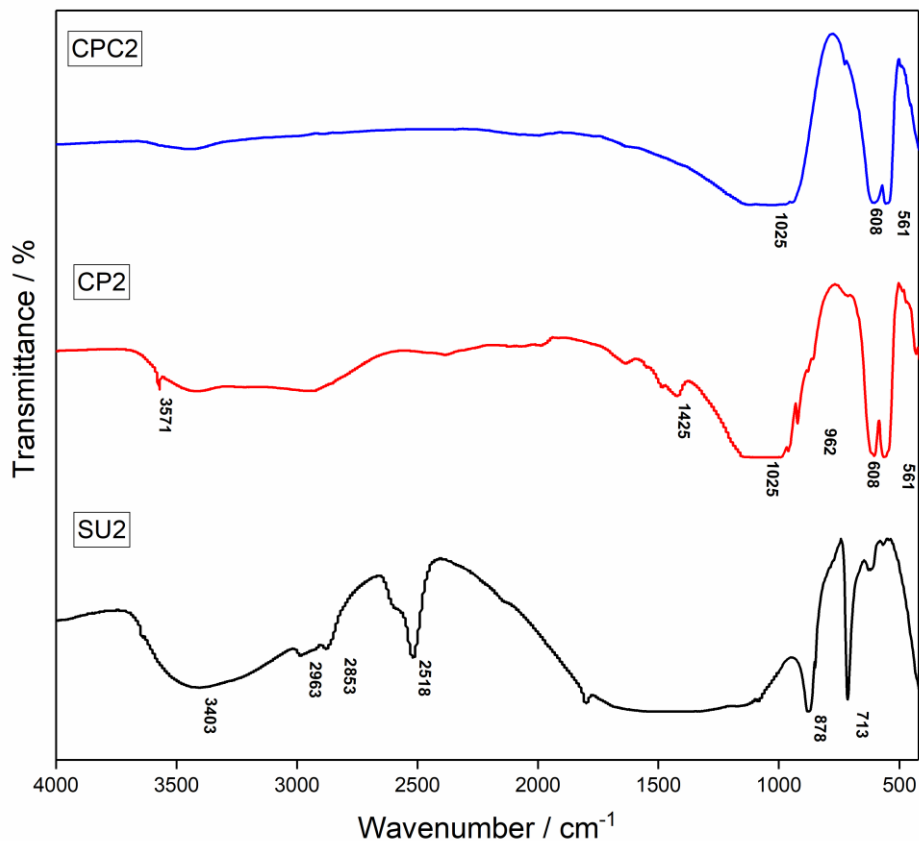


Figure 2.3 FT-IR pattern of SU2, CP2 and CPC2.

Table 2.2 Band assignments of FTIR spectrum given in **Figure 2.2**

Wavenumber, cm^{-1}	Assignment/s
3571	O-H stretching from hydroxyapatite
2963, 2853, 2518	Organic constituents (bio-polymer)
1425	CO_3^{3-} anti-symmetric stretching
1025	P-O in HPO_4 and PO_4 groups (stretching mode)
962	P-O in PO_4 group
878	CO_3^{3-} out of plane bending
713	CO_3^{3-} anti-symmetric bending
608,561	P-O in PO_4 groups (bending mode)

Scanning electron microscopic images of the SU2, shown in Figs. 2.4a&b, revealed that the skeleton had a highly porous and interconnected microstructure composed of macropores in the range of 200-300 μm and micropores in the range of 20-50 μm . Magnesium was detected in the SU2 by the EDS is shown in Fig. 2.4c. Those of the SU1 showed the similar results.

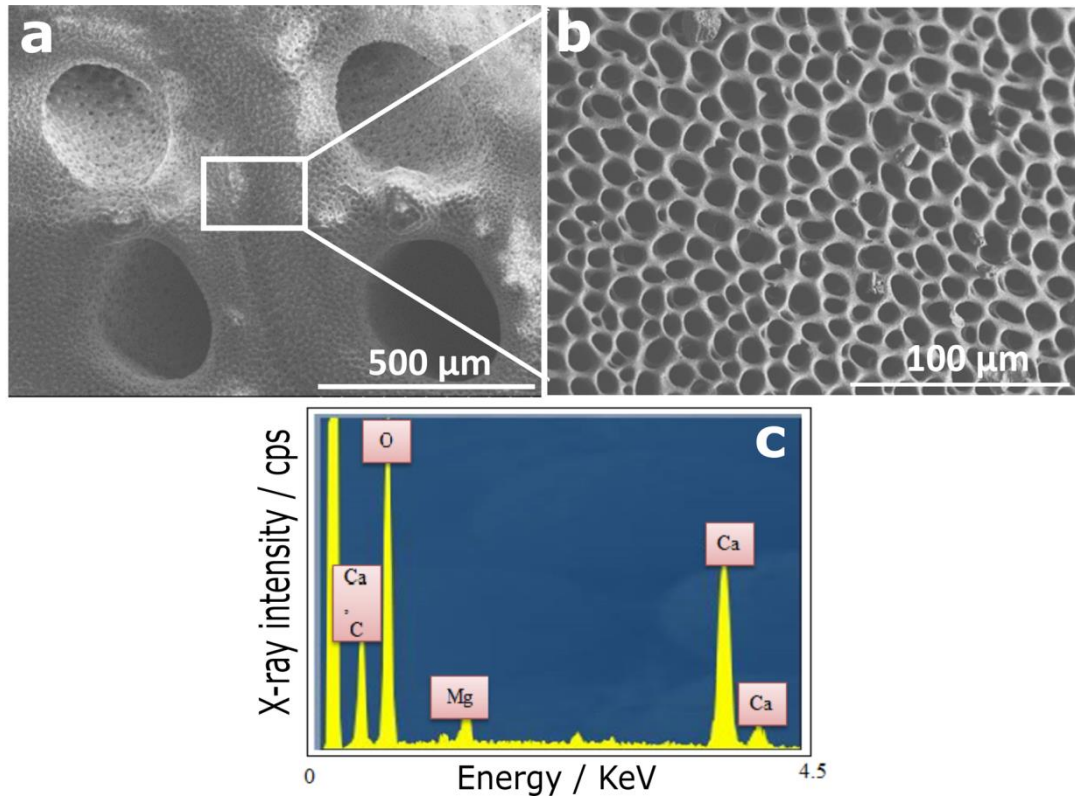


Figure 2.4 SEM images of SU2 (a-b) and (c) shows the EDS pattern of sample surface.

Scanning electron microscope images of the CP2 and related EDS spectrum are shown in Fig. 2.5. Figures 2.5a and 2.5b show SEM image of low and high magnification image of the CP2, where the diameter of the pores ranged from 200 to 250 μm and 20 to 40 μm , respectively. These images demonstrated that the CP2 still retains the porous microstructure of the original skeleton. The EDS spectrum (Fig. 2.5c) indicates the characteristic peaks of calcium, magnesium, phosphorous and oxygen, which demonstrates

that Mg was retained after hydrothermal phosphatization. The similar results were obtained for the CP1 observations.

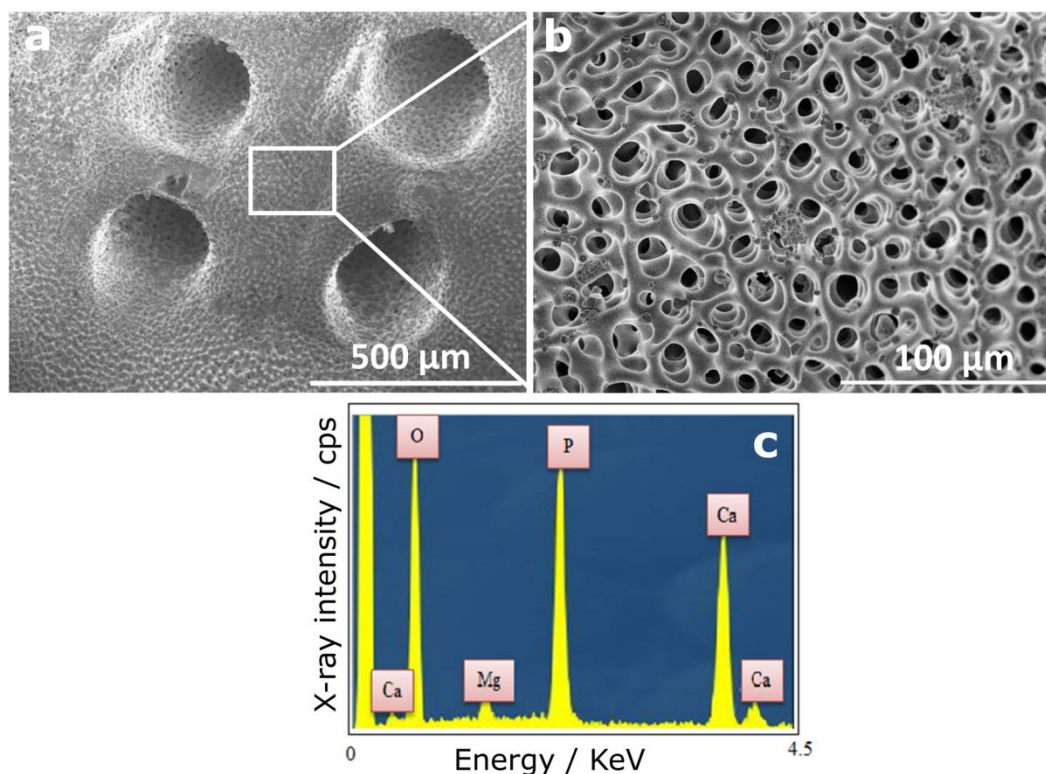


Figure 2.5 SEM images of CP2 (a-b) and (c) shows the EDS pattern of sample surface.

Quantitative chemical analyses and (Ca+Mg)/P atomic ratios from the ICP-AES data, as shown in Table 2.3, revealed no significant differences in the (Ca+Mg)/P ratio between CP1 and CPC1; and CP2 and CPC2.

Table 2.3 Quantitative analysis from ICP-AES

Sample	Mg/Ca	(Ca+Mg)/P
SU1	0.1179 ± 0.0006	-
CP1	0.1196 ± 0.0002	1.5207 ± 0.0223
CPC1	-	1.5050 ± 0.0211
SU2	0.1205 ± 0.0001	-
CP2	0.1226 ± 0.0006	1.5217 ± 0.0153
CPC2	-	1.5097 ± 0.0090

The sea urchin skeletons used in this study are waste products of sea urchin food processing industry in Japan. From SEM imaging, it is revealed that the skeletons are made up of highly interconnected porous structure with both macropores and micropores. X-ray diffraction analysis revealed that the composition of skeletons is Mg-calcite and EDS analysis showed no contamination from heavy metal ions. The SEM analysis of CP1/CP2 showed that the converted skeletons retained their original porous structure.

From XRD and FTIR analysis, hydrothermal phosphatization of sea urchin skeleton converted Mg-calcite to BCP consisting mainly of Mg-containing β -TCP (82 %) and a small amount of HAp (18 %). Hydrothermal conversion of other marine CaCO_3 skeletons, such as coral, cuttlebone and sea shells, has been reported to produce HAp, while sea urchin spines produced β -TCMP[17]. The phosphatization reaction could be a dissolution-re-precipitation[18] process of Mg-calcite and calcium phosphate; where, all re-precipitation process of calcium phosphate occurred on the surface of Mg-calcite and progressed towards the Mg-calcite side, with the dissolution of Mg-calcite. In addition, from the viewpoint of density, TCP and HAp crystals have densities of 3.14 and 3.16, respectively; thus, cavity formed by dissolution of Mg-calcite, density could be less than that of calcite, 2.71, this would provide enough space for TCP and/or HAp formation towards Mg-calcite instead of outside of sea urchin skeleton.

Generally, calcite phosphatization at high-temperature results formation of calcium-deficient and carbonate-containing hydroxyapatite crystals[1]. The formation of β -TCP instead of HAp in the present study is explained by the presence of Mg^{2+} ions, well-known as an inhibitor of HAp formation and stabilizer of the β -TCP structure[19]. In addition, Mg^{2+} ions in calcite structure may additionally be unstable than Ca^{2+} ions, because Mg^{2+} ions do not supersede calcite crystals more than 10 % in the atomic ratio for Ca^{2+} even if the solution consists of high Mg^{2+} concentration[20], and may preferably release from Mg-calcite in

comparison to Ca^{2+} ions. Therefore, the Mg/Ca atomic ratio in the solution at an early stage of phosphatization could be higher than that in sea urchin skeletons and these Mg^{2+} ions stabilize as well as incorporate into β -TCP. In the later stage, Mg^{2+} ion concentration could decrease to allow the formation of Ca-deficient HAp; thus, a small amount of HAp existed in the CP1 and CP2.

Further, the presence of large amounts of carbonate ions results in the formation of carbonate containing HAp, as shown in FT-IR spectrum of CP2 (Fig. 2.3), also supported in the literature[1]. In addition, the carbonate-containing HAp obtained from the phosphatization was a Ca-deficient HAp as reported, because it gets easily decomposed to β -TCP at high temperature[21] which is confirmed by the XRD pattern (Fig. 2.2) and the FT-IR (Fig. 2.3) spectrum of the CPC2, respectively. Slightly high values of the theoretical Ca/P atomic ratios (Table 2.1) in comparison to the observed ratios (Table 2.3) also supported Ca deficiency of the HAp. No significant differences in observed atomic ratios of Ca, Mg and P between CPs and CPCs, which is very reasonable because they do not get vaporized at 1000 °C.

2.4 Conclusion

Raw Sea urchin tests were successfully converted to BCP consisting of magnesium containing tricalcium phosphate (Mg-TCP) with small amount of hydroxyapatite (HAp). Presence of Mg promoted Mg-TCP, instead of HAp by stabilization of β -TCP structure by Mg. The skeleton of the converted tests retained their original porous structure. The converted tests could be a possible candidate for artificial bone filler.

Acknowledgement

This **Chapter 2**, in part, was a reprint of the publication **Manchinasetty NVL, Oshima S, Kikuchi M.** Preparation of flexible bone tissue scaffolds utilizing sea urchin test and collagen. *Journal of Materials Science: Materials in Medicine* 2017; 28(11):184-1- 184-12 with permission.

2.5 References

1. ROY DM, LINNEHAN SK. Hydroxyapatite formed from Coral Skeletal Carbonate by Hydrothermal Exchange. *Nature*. 1974;247:220–2.
2. Ben-Nissan B. Natural bioceramics: from coral to bone and beyond. *Curr. Opin. Solid State Mater. Sci.* 2003;7:283–8.
3. Barros AA, Aroso IM, Silva TH, Mano JF, Duarte AR, Reis RL. In vitro bioactivity studies of ceramic structures isolated from marine sponges. *Biomed Mater.* 2016;11:45004.
4. Ivankovic H, Gallego Ferrer G, Tkalcec E, Orlic S, Ivankovic M. Preparation of highly porous hydroxyapatite from cuttlefish bone. *J. Mater. Sci. Mater. Med.* 2009;20:1039–46.
5. Vecchio KS, Zhang X, Massie JB, Wang M, Kim CW. Conversion of sea urchin spines to Mg-substituted tricalcium phosphate for bone implants. *Acta Biomater.* England; 2007;3:785–93.
6. CLARKE SA, WALSH P. Marine organisms for bone repair and regeneration. Mallick K, editor. *Bone Substit. Biomater.* Woodhead Publishing Limited; 2014.
7. Holzapfel BM, Reichert JC, Schantz J-T, Gbureck U, Rackwitz L, Nöth U, et al. How smart do biomaterials need to be? A translational science and clinical point of view. *Adv. Drug Deliv. Rev.* 2013;65:581–603.

8. Fella BH, Gauthier O, Weiss P, Chappard D, Layrolle P. Osteogenicity of biphasic calcium phosphate ceramics and bone autograft in a goat model. *Biomaterials*. Netherlands; 2008;29:1177–88.
9. Bohner M. Silicon-substituted calcium phosphates - a critical view. *Biomaterials*. Netherlands; 2009;30:6403–6.
10. Habibovic P, Barralet JE. Bioinorganics and biomaterials: bone repair. *Acta Biomater*. England; 2011;7:3013–26.
11. Kannan S, Rocha JHG, Agathopoulos S, Ferreira JMF. Fluorine-substituted hydroxyapatite scaffolds hydrothermally grown from aragonitic cuttlefish bones. *Acta Biomater*. 2007;3:243–9.
12. Holmes RE, Bucholz RW, Mooney V. Porous hydroxyapatite as a bone-graft substitute in metaphyseal defects. A histometric study. *J. Bone Joint Surg. Am.* United States; 1986;68:904–11.
13. Vuola J, Taurio R, Goransson H, Asko-Seljavaara S. Compressive strength of calcium carbonate and hydroxyapatite implants after bone-marrow-induced osteogenesis. *Biomaterials*. Netherlands; 1998;19:223–7.
14. Das S, Mangwani N. Ocean acidification and marine microorganisms: responses and consequences. *Oceanologia*. 2015;57:349–61.
15. Akino M, Aso S, Kimura M. Effectiveness of biological filter media derived from sea urchin skeletons. *Fish. Sci.* 2015;81:923–7.
16. Nyquist RA, Kagel RO. *INFRARED SPECTRA OF INORGANIC COMPOUNDS BT - Handbook of Infrared and Raman Spectra of Inorganic Compounds and Organic Salts*. San Diego: Academic Press; 1971. p. 1–18.
17. Zhang X, Vecchio KS. Conversion of natural marine skeletons as scaffolds for bone tissue engineering. *Front. Mater. Sci.* 2013;7:103–17.

18. Ishikawa K. Bone substitute fabrication based on dissolution-precipitation reactions. *Materials (Basel)*. 2010;3:1138–55.
19. Kannan S, Ventura JM, Ferreira JMF. Aqueous precipitation method for the formation of Mg-stabilized β -tricalcium phosphate: An X-ray diffraction study. *Ceram. Int.* 2007;33:637–41.
20. Reddy MM, Nancollas GH. The crystallization of calcium carbonate. *J. Cryst. Growth*. 1976;35:33–8.
21. Safronova T V, Putlyaev VI, Avramenko OA, Shekhirev MA, Veresov AG. Ca-deficient hydroxyapatite powder for producing tricalcium phosphate based ceramics. *Glas. Ceram.* 2011;68:28–32.

Chapter 3

Preparation of flexible scaffolds utilizing test of sea urchin with collagen or gelatin as binder

3.1 Introduction

The field of bone tissue engineering (BTE) was introduced three decades ago and focuses on alternate treatment options that will ideally eliminate previously described issues of current clinical treatments and also aims to induce new functional bone regeneration via the synergistic combination therapy of biomaterials, cells and biochemical factors [1,2]. Several approaches have been made in the field of BTE to mimic the bone composition and structure in the form of scaffolds. A three-dimensional interconnection (3D) of both macropores ($>100\ \mu\text{m}$) and micropores ($<50\ \mu\text{m}$) are important for a porous scaffold because macropores allow cell and tissue invasion and micropores allow efficient exchange of nutrients and wastes[3]. Essential properties of a scaffold are biocompatibility, porosity, pore interconnectivity, osteoconductivity, osteoinductivity, adequate mechanical strength, and biodegradability[4,5].

Owing to the attributes discussed above with the bimodality in pores, there have been several commercial products available in market as bone graft substitutes. APACERAM (HOYA Technological corporation, Tokyo Japan), which consists of synthetic HAp has proven to be having excellent biocompatibility and biological safety. The product consist both macropores and micropores with wide range of porosity. Another product from same company called SUPERPORE with bimodal pores was developed with β -TCP. Both the products in clinical studies have shown excellent bone regeneration, where new bone formation was observed all over the implanted site with active new bone in the pores, 4

weeks after implantation [6–8]. An another scaffold developed by Morisue et al., a highly porous apatite fiber scaffold (AFS) pwith hydroxyapatite fibers showed excellent bimodal porosity, proven to be efficient in bone formation both *in vitro* and *in vivo* [9].

Like discussed in **Chapter 1, Section 1.3.3**, composites with ceramics and natural polymers were also widely studied for fabrication of BTE scaffolds. Natural polymers, such collagen, gelatin and chitosan; and synthetic polymers, such as poly(glycolic acid) and poly(L-lactic acid), have been previously used as binders because of their favourable biocompatibility [10]. In chapter 2, the author discussed the preparation of porous calcium phosphate (CP1/CP2) granules from phopshatization of sea urchin skeletons. They seem suitable for fabrication of 3D scaffold if the test granules were bound with the help of biocompatible polymers, such as collagen, gelatin or other synthetic polymers. This chapter describes the preparation and characterization of flexible 3D scaffolds utilizing CP1/CP2 granules and collagen or gelatin as binders.

3.2 Materials and Methods

3.2.1 Materials

Chemicals used in this research were purchased from Wako Pure Chemical Ltd., Japan if that without further notice. Calcium phosphate CP1 and CP2 obtained from phosphatization of SU1 and SU2 respectively (chapter 2) were used. The CP1 or CP2 was crushed and classified into granules of 1-2 mm in size by the sieving and used in the fabrication of scaffolds.

3.2.2 Fabrication of scaffolds

3.2.2.1 Collagen as binder

Collagen solution of 1 % in mass was prepared by dissolving freeze-dried porcine dermal type-I atelocollagen (Nitta Gelatin, Japan) sponges in 0.1 M acetic acid solution (pH 3.0). Prior to fabrication, the collagen solution was neutralized with 1 N NaOH and adjusted its ionic strength to the physiological condition with 10X phosphate buffered saline (PBS, Sigma Aldrich, USA). Scaffolds were fabricated by mixing the granules with the collagen solution at a ratio of 1:2 (mass/volume), transferred into an acrylic mold with 10 mm in inner diameter and 15 mm in height and kept in an incubator at 37 °C for 2 h for collagen gelation. After the gelation, the mold was transferred to a -20 °C freezer for 24 h and freeze-dried (VirTis, Advantage, Maruto, Japan) at -20 °C overnight. The scaffolds were removed from the mold after freeze drying and dehydrothermally crosslinked at 140 °C for 12 h under vacuum (Eyela, VOS- 2015D, Tokyo Rikakikai co., Ltd, Japan). The scaffold fabricated with the CP1 granules is denoted as CP1Col and that with the CP2 granules is denoted as CP2Col.

3.2.2.2 Gelatin as binder

Scaffolds were fabricated by mixing CP1 or CP2 granules with 10 % gelatin (type B) solution in mass ratio of 1:1 (mass/volume), transferred into acrylic mould with 10 mm in inner diameter and 10 mm in height and kept at 4 °C for gelation for 4 hours. After gelation, the mould was transferred to a -20 °C freezer for 24 hours and freeze-dried (VirTis, Advantage, Maruto, Japan) at -20 °C overnight. The scaffolds were removed from the mould after freeze drying and dehydrothermally crosslinked at 140 °C for 12 h under vacuum (Eyela, VOS- 2015D, Tokyo Rikakikai co., Ltd, Japan). The scaffold fabricated with the CP1 granules is denoted as CP1Gel and that with the CP2 granules is denoted as CP2Gel.

The freeze dried scaffolds were also crosslinked with 50 mM glutaraldehyde (in 90 % (v/v) ethanol) for 8 h. The scaffolds were washed with distilled water three times, 1mM lysine remove residue of any uncrosslinked GA, washed again with ultrapure water three times and freeze-dried. The scaffold fabricated with CP1 granules is denoted as CP1Gel_GA and the scaffold fabricated with CP2 granules is denoted as CP2Gel_GA.

3.2.3 Characterization of scaffolds

The morphology of the horizontal cross section of the scaffolds was examined using the SEM. The open porosity of the scaffolds was measured by the liquid displacement method [11] using absolute ethanol as the displacement liquid to prevent the scaffolds from swelling or shrinking. Briefly, the scaffold was immersed in the absolute ethanol for 30 min. The scaffolds were weighed before (W_d), during (W_1) and after immersing (W_w). The porosity of the scaffolds was calculated using the formula (1) given below. The experiment was carried out in triplicates.

$$Porosity (\%) = \frac{W_w - W_d}{W_w - W_1} \times 100 \dots\dots\dots(1)$$

The stability of the scaffolds in physiological conditions was confirmed by a soaking in Phosphate buffered saline (PBS) at 37 °C for 7 days with a naked-eye observation. The bending strengths of the scaffolds were measured with a universal testing machine equipped with a 1 kN load cell (AGS-H 1kN, Shimadzu, Japan). The scaffolds were fabricated in the dimension of 40 mm in length, 8 mm in width and 6 mm in height. For wet condition analysis, the scaffolds were soaked in PBS at room temperature and 37 °C, 24 hours prior to measurement. Each five specimens were measured at a crosshead speed of 0.5 mm/min, and three-point bending strength was calculated.

3.2.4 Statistical analysis

All data were expressed as mean \pm standard deviation (SD). Student t-test was performed to reveal significant differences. The difference was considered significant when the *p*-value was less than 0.05.

3.3 Results

3.3.1 Collagen as binder

The open porosities and bending strengths at dry condition of the scaffolds are shown in Table 3.1. Most of the pores were still accessible and contributed to the total open porosity. The bending strengths of the scaffolds under wet condition could not be measured because the scaffolds became too soft for measurement. Even the scaffolds became soft; they can be easily handled by hand and forceps.

Table 3.1 Open porosity and bending strength of scaffolds with collagen as binder

Scaffold	Open porosity (%)	Bending strength (dry state, KPa)
CP1Col	81.94 \pm 1.34	159.89 \pm 31.39
CP2Col	83.84 \pm 2.38	149.71 \pm 27.35

From stability analysis, where the scaffolds were soaked in PBS, 37 °C showed that they were able to maintain their shapes. The collagen used as a binder in the present study, was not decomposed to gelatin at 37 °C and maintained the integrity of the scaffold.

The naked eye observation of the scaffolds, CP1Col and CP2Col, is shown in Fig. 3.1a. The scaffolds can be fabricated into any shape and hence they are shape controllable.

The microstructures of the horizontal cross sections of the scaffolds are shown in Figs. 3.1b-f. The scaffolds had an open pore microstructure with both macropores and micropores along with a high degree of interconnectivity. The intrinsic microstructure of the CP1/CP2 granules was also well maintained.

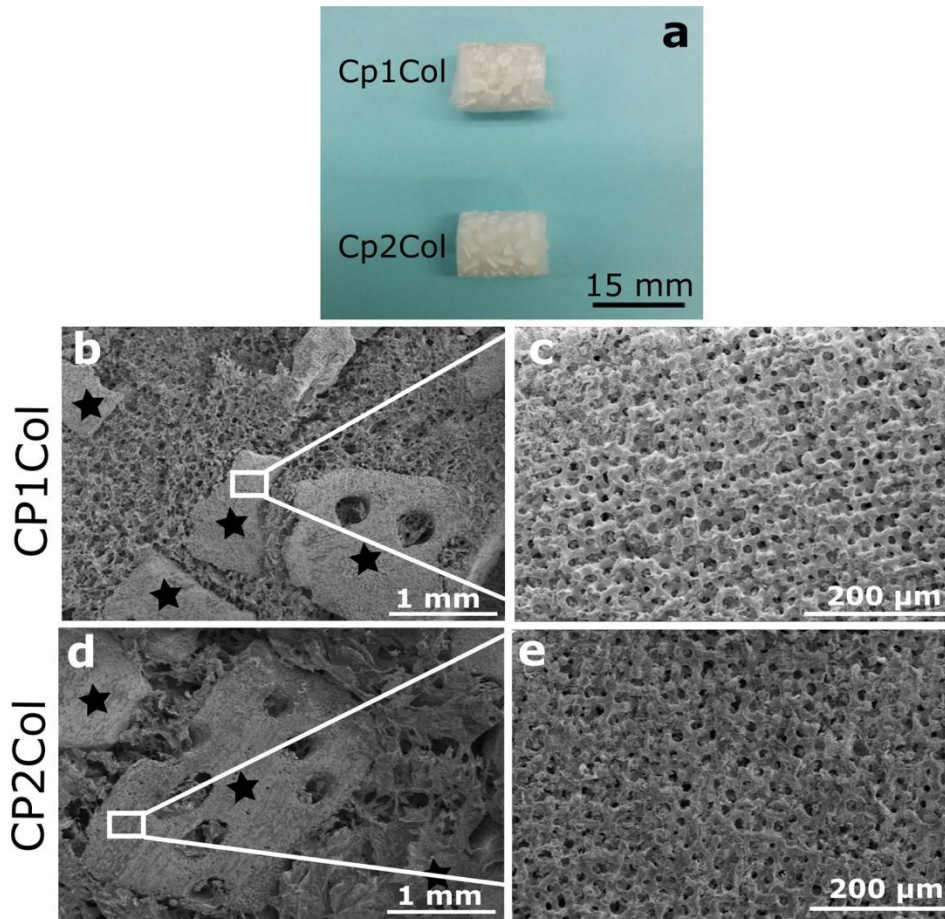


Figure 3.1 (a) Naked eye view of the scaffolds CP1Col and CP2Col. SEM images of horizontal cross section of CP1Col (b-c) and CP2Col (d-e) scaffolds. Closed stars in image b,d indicates CP1 and CP2 granules respectively.

3.3.2 Gelatin as binder

The naked eye observation of the scaffolds, CP1Gel/CP2Gel and CP1Gel_GA/CP2Gel_GA is shown in Fig. 3.2a and b respectively. Scaffolds crosslinked

with GA turned brown in colour after 8 h of crosslinking. The scaffolds can be fabricated into any shape and hence they are shape controllable.

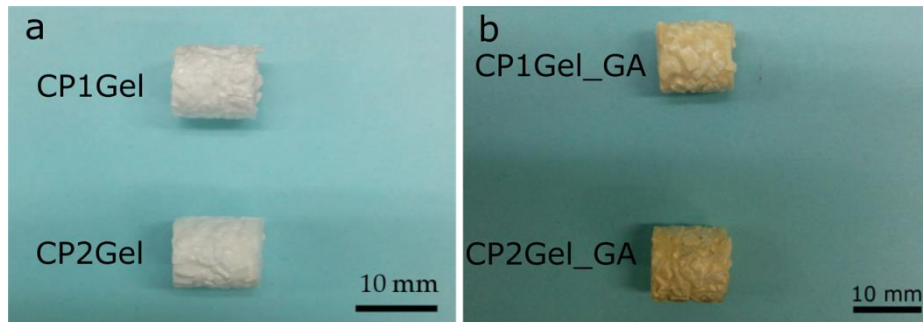


Figure 3.2 Naked eye observation of scaffolds (a) CP1Gel and CP2Gel.
(b) CP2Gel_GA and CP2Gel_GA

The microstructures of the horizontal cross sections of the scaffolds, CP1Gel/CP2Gel and CP1Gel_GA/CP2Gel_GA are shown in Figs. 3.3 and 3.4 respectively. The scaffolds had an open pore microstructure with a high degree of interconnectivity and the microstructure of the CP1/CP2 granules was well maintained.

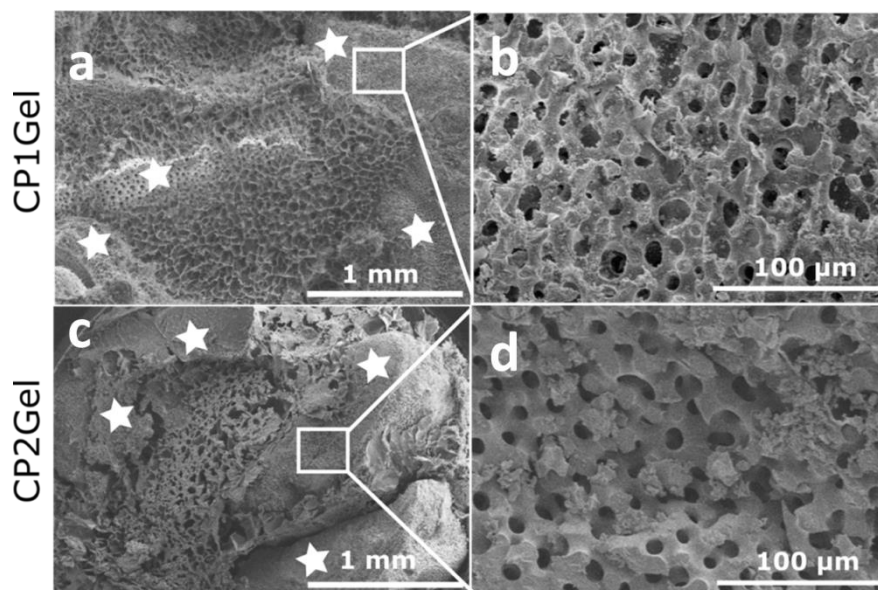


Figure 3.3 SEM images of horizontal cross section of CP1Gel and CP2Gel. Closed stars in images a,c indicates CP1 and CP2 granules respectively.

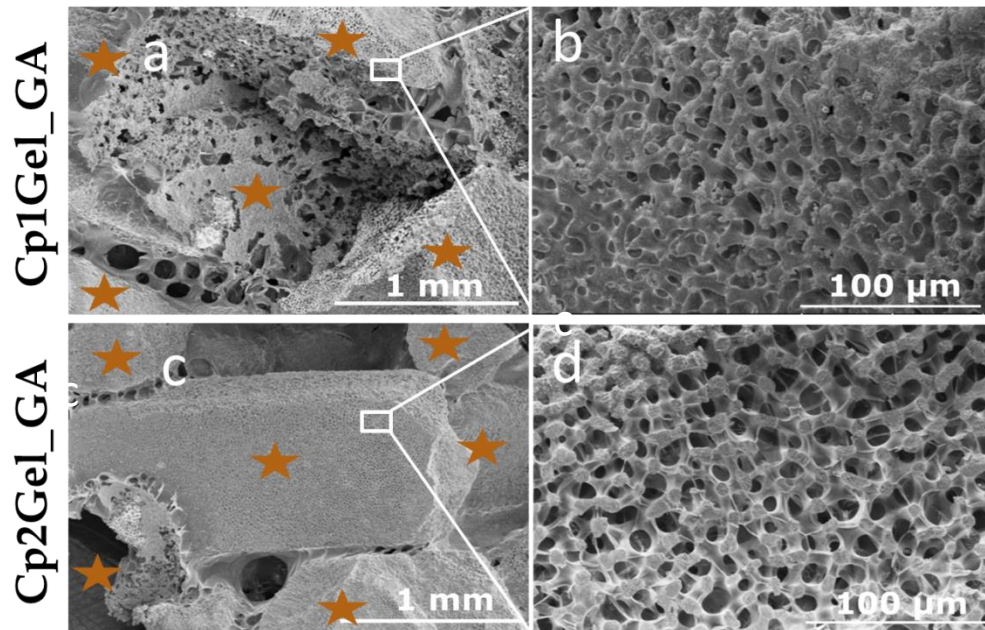


Figure 3.4 SEM images of horizontal cross section of CP1Gel_GA and CP2Gel_GA. Closed stars in images a,c indicates CP1 and CP2 granules respectively.

The open porosities, stability and bending strengths at dry and wet condition of the scaffolds are shown in Table 3.2. Most of the pores were still accessible and contributed to the total open porosity. The open porosity of the GA crosslinked scaffolds was lower than the dehydrothermal crosslinked scaffolds. Bending strength of GA crosslinked scaffolds under wet condition was significantly higher than dehydrothermal crosslinked scaffolds.

From stability analysis, where the scaffolds were soaked in PBS, 37 °C showed that only GA crosslinked scaffolds were able to maintain their shape. The dehydrothermal crosslink was not sufficient to hold the integrity of the scaffolds CP1Gel and CP2Gel.

Table 3.2 Bending strength of scaffolds with gelatin as binder

Property	Dehydrothermal crosslink			GA crosslink		
	Scaffold	Dry (MPa)	Wet (KPa)	Scaffold	Dry (MPa)	Wet (KPa)
Bending strength	CP1Gel	3.29 ± 0.27	116.84 ± 29.63	CP1Gel_GA	3.47 ± 0.21	173.85 ± 19.72*
	CP2Gel	3.18 ± 0.62	111.57 ± 14.27	CP2Gel_GA	3.35 ± 0.19	164.59 ± 10.51*
Open porosity		66.66 ± 2.3 %			52 ± 1.8 %	
Stability at 37 °C in PBS		Not stable			Stable	

3.4 Discussion

The scaffolds fabricated with collagen or gelatin and the CP1/CP2 granules showed good open porosity with both macropores and micropores, even after some pores were covered with the collagen or gelatin fibers. This highly porous structure can be appropriate for the bone tissue engineering applications to allow cell migration, vascularization and nutrient supplementation [12]. Scaffolds fabricated with gelatin as binder and crosslinked with GA showed a decrease in the open porosity due to the increased stiffness [13]. The scaffolds were highly elastic in wet condition and could be molded into any shape to fit irregular bone defects.

Scaffolds fabricated with collagen as a binder maintained the integrity of the scaffold due to the stability of collagen gel at 37 °C in the physiological ion conditions. Whereas scaffolds fabricated with gelatin as binder were stable only under GA crosslink conditions.

Gelatin got denatured at 37 °C under dehydrothermal crosslink due to its hydrophilic nature [14]. Overall, collagen or gelatin (under GA crosslink) acted as a binder and maintained the integrity of the scaffold at 37 °C in the physiological ion conditions, while highly porous CP1/CP2 granules reserved the space for bone formation.

Like discussed in introduction, it is essential that the scaffolds or bone grafts contain bimodal pores. APACERAM, SUPERPORE contain the essential porosity with macropores and micropores, but is made up of only single inorganic phase HAp and β -TCP respectively. HAp is known to be non-bioresorbable and β -TCP is known to be degraded at faster rates [15]. And the AFS scaffold also is a single phase with HAp fibers, where the porosity was introduced by carbon beads[16] . In this study, the author developed similar type of scaffolds but with much closer resemblance to original bone structure (both organic and inorganic) with BCP granules and biocompatible binders, where the bimodal porosity was achieved by simple mixing and freeze drying.

Generally, bone tissue scaffolds fabricated from ceramics and/or polymers do not have sufficient mechanical strength for load bearing; however, the scaffolds have high capability to introduce bone tissues by appropriate time period, they would be useful for bone defect repair. For instance, hydroxyapatite/collagen (HAp/Col) bone like nanocomposite sponge developed by Kikuchi *et al.*, [17] demonstrated good clinical trial results [18]because of their sponge-like elasticity to fit any shape of bone defect, where no gaps remain between the host bone and scaffold. Gaps between the host bone and scaffold would generally delay the bone ingrowth process significantly. Similarly, the CP1Col/CP2Col and CP1Gel_GA/CP2Gel_GA composites possess adequate mechanical strength under wet conditions and shape controllability along with bimodal porosity to be used a bone substitute.

3.5 Conclusion

The scaffolds fabricated with CP1/CP2 granules with collagen or gelatin as binders showed good open porosity for cell migration and fluid infiltration, and adequate mechanical strength for handling operations. Overall, the binder collagen or gelatin helped in maintaining the shape and integrity of the scaffolds, whereas the granules reserved the space for bone formation. The scaffolds could be a potential candidate for nonload -bearing defects.

Acknowledgement

This **Chapter 3**, in part, was a reprint of the publication

1. Manchinasetty NVL, Oshima S, Kikuchi M. Preparation of flexible bone tissue scaffolds utilizing sea urchin test and collagen. *Journal of Materials Science: Materials in Medicine* 2017; 28(11):184-1- 184-12 with permission.

2. Manchinasetty NVL, Kikuchi M. Fabrication and characterization of porous scaffold utilizing the test of sea urchin and gelatin (manuscript under preparation).

3.6 References

1. Amini AR, Laurencin CT, Nukavarapu SP. Bone tissue engineering: recent advances and challenges. *Crit. Rev. Biomed. Eng.* 2012;40:2.
2. Laurencin CT, Ambrosio AMA, Borden MD, Cooper JA. Tissue Engineering: Orthopedic Applications. *Annu. Rev. Biomed. Eng. Annual Reviews*; 1999;1:19–46.
3. Laurencin C, Khan Y, El-Amin SF. Bone graft substitutes. *Expert Rev. Med. Devices.* England; 2006;3:49–57.
4. Finkemeier CG. Bone-grafting and bone-graft substitutes. *J. Bone Joint Surg. Am.* The American Orthopedic Association; 2002;84–A:454–64.
5. Place ES, Evans ND, Stevens MM. Complexity in biomaterials for tissue engineering. *Nat Mater.* Nature Publishing Group; 2009;8:457–70.

6. Tanaka Y. Development of titanium fixation screw for hydroxyapatite osteosynthesis (APACERAM). *Surg. Neurol. United States*; 2008;70:545–9; discussion 549.
7. Ono I, Tateshita T, Satou M, Sasaki T, Matsumoto M, Kodama N. Treatment of large complex cranial bone defects by using hydroxyapatite ceramic implants. *Plast. Reconstr. Surg. United States*; 1999;104:339–49.
8. Sakamoto A. Joint preserved reconstruction after curettage in giant cell tumor of bone arising in the distal radius: Case report. *Int. J. Surg. Case Rep.* 2015. p. 181–3.
9. Suzuki K, Nagata K, Yokota T, Honda M, Aizawa M. Histological evaluations of apatite-fiber scaffold cultured with mesenchymal stem cells by implantation at rat subcutaneous tissue. *Biomed. Mater. Eng. Netherlands*; 2017;28:57–64.
10. Dhandayuthapani B, Yoshida Y, Maekawa T, Kumar DS. Polymeric scaffolds in tissue engineering application: A review. *Int. J. Polym. Sci.* 2011;2011.
11. Chang SJ, Huang Y-T, Yang S-C, Kuo S-M, Lee M-W. In vitro properties of gellan gum sponge as the dental filling to maintain alveolar space. *Carbohydr. Polym.* 2012;88:684–9.
12. Loh QL, Choong C. Three-Dimensional Scaffolds for Tissue Engineering Applications: Role of Porosity and Pore Size. *Tissue Eng. Part B. Rev.* 140 Huguenot Street, 3rd Floor New Rochelle, NY 10801 USA: Mary Ann Liebert, Inc.; 2013;19:485–502.
13. Lou X, Chirila T V. Swelling behavior and mechanical properties of chemically cross-linked gelatin gels for biomedical use. *J. Biomater. Appl. England*; 1999;14:184–91.
14. Davidenko N, Schuster CF, Bax D V, Raynal N, Farndale RW, Best SM, et al. Control of crosslinking for tailoring collagen-based scaffolds stability and mechanics. *Acta Biomater.* 2015;25:131–42.
15. Xu S, Liu J, Zhang L, Yang F, Tang P, Wu D. Effects of HAp and TCP in constructing tissue engineering scaffolds for bone repair. *J. Mater. Chem. B. The Royal Society of Chemistry*; 2017;5:6110–8.
16. Morisue H, Matsumoto M, Chiba K, Matsumoto H, Toyama Y, Aizawa M, et al. Novel apatite fiber scaffolds can promote three-dimensional proliferation of osteoblasts in rodent bone regeneration models. *J. Biomed. Mater. Res. Part A. Wiley Subscription Services, Inc., A Wiley Company*; 2009;90A:811–8.

17. Kikuchi M, Koyama Y, Edamura K, Irie A. Synthesis of Hydroxyapatite/Collagen Bone-Like Nanocomposite and Its Biological Reactions. *Adv. Nanocomposites - Synth. Charact. Ind. Appl.* 2007;2:181–94.
18. Sotome S, Ae K, Okawa A, Ishizuki M, Morioka H, Matsumoto S, et al. Efficacy and safety of porous hydroxyapatite/type 1 collagen composite implantation for bone regeneration: A randomized controlled study. *J. Orthop. Sci. The Authors*; 2016;21:373–80.

Chapter 4

Evaluation of biocompatibility of scaffolds under static cell culture conditions

4.1 Introduction

All synthetic bone grafts or bone tissue scaffolds should undergo biocompatibility evaluation to understand them better. The indications used for the approval of quality of a material consist of *in vitro* tests also known as cell culture experiments; *in vivo* tests also known as animal experiments and clinical tests. Keeping this in mind; any proposed bone graft or scaffold undergoes extensive *in vitro* evaluation to rule out the bad outcomes. The advantages of *in vitro* tests are, being experimentally manageable, repeatable, fast and relatively low cost. Generally these tests are performed in a cell-culture dishes or plates, where the material comes into the contact with the cultured cells or cells are seeded on the materials. [1].

So any proposed bone scaffold / graft should undergo biocompatibility evaluation, cells must adhere, function normally, and migrate onto the surface and distribute through the inner layers. There are several studies in literature, where the scaffolds were subjected to two (2D) dimensional cell culture analyses to determine their potential as bone graft substitutes [2–5]. In chapter 3, the author discussed some of the bone graft substitutes like APACERAM, SUPERPORE, Apatite fiber scaffold, Hydroxyapatite/collagen sponge etc., All these substitutes showed good osteoconductivity, bioactivity, resorbability *in vitro* and *in vivo* [6–8].

So similarly, in this chapter, I evaluated the biocompatibility of the scaffolds under 2D cell culture with osteoblast like cell line MG-63 cells. In **chapter 3**, fabrication and characterization of scaffolds with collagen or gelatin as binders was discussed in detail and in this chapter their biocompatibility was characterised and discussed.

4.2 Materials and Methods

Chemicals used in this research were purchased from Wako Pure Chemical Ltd., Japan if without further notice.

4.2.1 Fabrication of scaffolds

The CP1Col, CP2Col and CP2Gel_GA, CP2Gel_GA scaffolds were fabricated in the dimension of 10 mm in diameter and 5 mm in height. A collagen and gelatin sponges as the same size as the scaffold was also fabricated. The fabrication mechanism was discussed in **Chapter 3**.

4.2.2 *In vitro* cell culture

The human osteoblast-like cell line, MG-63, derived from human osteosarcoma was used for the experiment. The MG-63 cells were subcultured in 75 cm² tissue culture flasks using a complete medium, Dulbecco's modified Eagle's medium (DMEM, Sigma Aldrich, USA) supplemented with 10 % (v/v) fetal bovine serum (Sigma Aldrich, USA) and 1 % (v/v) penicillin/streptomycin (Gibco[®], Life technologies, Japan) in an incubator (HERAcell 150i, Thermo Scientific, Japan) at 95 % relative humidity and 5 % CO₂.

All the scaffolds and sponges were sterilized by the ethylene oxide gas (EOG) method and conditioned with the complete medium at 37 °C for 3 h. After absorbing away the medium from the scaffolds using a sterilized filter paper (Advantec, 5C, 90mm), the scaffolds were placed in a tissue culture dish (100 × 20 mm, FALCON[®] USA), 8 × 10⁵ cells suspended

in 60 μ L of the complete medium was seeded onto CP1Col, CP2Col scaffolds; 1×10^5 cells suspended in 50 μ L of the complete medium was pipetted onto CP1Gel_GA, CP2Gel_GA scaffolds and incubated at 37 °C for 2 h. After the incubation, the cell-seeded scaffolds were transferred into each well of 6-well plates (Gibco[®], USA). Then, 6 mL of the complete medium was added to each well and cultured for 7 days in the incubator. The medium was refreshed every 2 days.

After 7-day culture, osteoblastic differentiation was induced by an osteogenic medium, the complete medium supplemented with 10 mM β -glycerolphosphate (Reagent Grade, Sigma Aldrich, USA) and 50 μ g/mL ascorbic acid. The osteogenic medium was refreshed every 2 days and cultured for 21 days. At various time intervals, the cell-scaffold constructs were harvested and used for the assays of cell adherence, DNA content, viability/cytotoxicity and osteoblast differentiation. The results of the CP1Col and CP2Col, CP1Gel_GA and CP2Gel_GA were the same for many assays; hence the results of the CP2Col, CP2Gel_GA are shown and discussed in this chapter as the representative if mentioned otherwise.

4.2.3 Cell adherence and Viability/cytotoxicity

The cell-scaffold constructs after 1, 7 and 21 day culture were fixed with 10 % neutral buffered formalin solution at room temperature for 2 days. After 2 days, the fixed constructs were removed, washed with distilled water thrice, dehydrated in graded series of ethanol and freeze-dried. The mid vertical cross section of the freeze-dried constructs was observed for cell adhesion and distribution using SEM.

Cell viability was evaluated by the live/dead cell staining assay using cell stain double staining kit (Dojindo Laboratories, Japan) according to the manufacturer's instruction. Briefly, the cell-scaffold constructs at 1, 7 and 21 day cultures were washed thrice with PBS

(Sigma Aldrich, USA) and incubated in 2 μ M calcein-AM and 4 μ M propidium iodide solution in the PBS for 15 min. After the incubation, the constructs were observed for live and dead cells using a fluorescence microscope (BX51Olympus Corp., Japan) immediately.

4.2.4 Cell proliferation and Alkaline phosphatase assay

The cell proliferation in the scaffolds was quantified by the DNA amount in the cell-scaffold constructs. After 1, 7, 14 and 21 day cultures, each construct was harvested, homogenized on ice in the glycine lysis buffer containing 0.1 M glycine (pH 10.4), 1 mM $MgCl_2$ and 0.2 % (v/v) TritonX-100 and incubated for 15 min in an ice box. Each sample was centrifuged at 12,000 rpm for 5 min, and the supernatant was transferred to a new centrifuge tube and stored at -80 °C until further analysis. The total DNA content was measured with a multiplate reader (GENius; TECAN, Männedorf, Switzerland) by the Hoechst 33258 method. Briefly, 100 μ L of diluted sample was mixed with 100 μ L of Hoechst dye 33258 (Dojindo Laboratories, Japan) in a 96-well microplate (FALCON[®], USA). Emissions at 458 nm excited by 360 nm light were measured, and the DNA content was calculated with a standard curve ($R^2=0.999$) prepared using a calf-thymus DNA (Sigma Aldrich, USA).

The osteoblastic differentiation was evaluated by the alkaline phosphatase (ALP) activity assay using p-nitrophenol phosphate (pNPP) as a substrate. The cell lysates at 7, 14 and 21 days of the culture were prepared as the same as the DNA quantification. Fifty microliter of the lysate was mixed with 50 μ L of pNPP in the 96-well microplate and incubated at 37 °C for 30 min. The reaction was stopped by adding 1 N NaOH and the amount of p-nitrophenol (pNP) was calculated from a light absorbance at 405 nm using a standard curve prepared from serial dilutions of pNP. The measurement was repeated five times in each sample. The ALP amount was normalized against the amount of the total DNA amount in each sample.

4.2.5 Statistical analysis

All data were expressed as mean \pm standard deviation (SD). One-way analysis of variance performed to reveal significant differences. Turkey's post hoc test was performed for pairwise comparison with a level of significance, p , at less than 0.05.

4.3 Results

4.3.1 Scaffolds with collagen as binder

The live/dead staining images of the cells over the scaffolds after day 1 and 7 days of culture are shown in Fig. 4.1. The results showed that most of the cells were viable and very few or negligible dead cells were found in both the scaffolds.

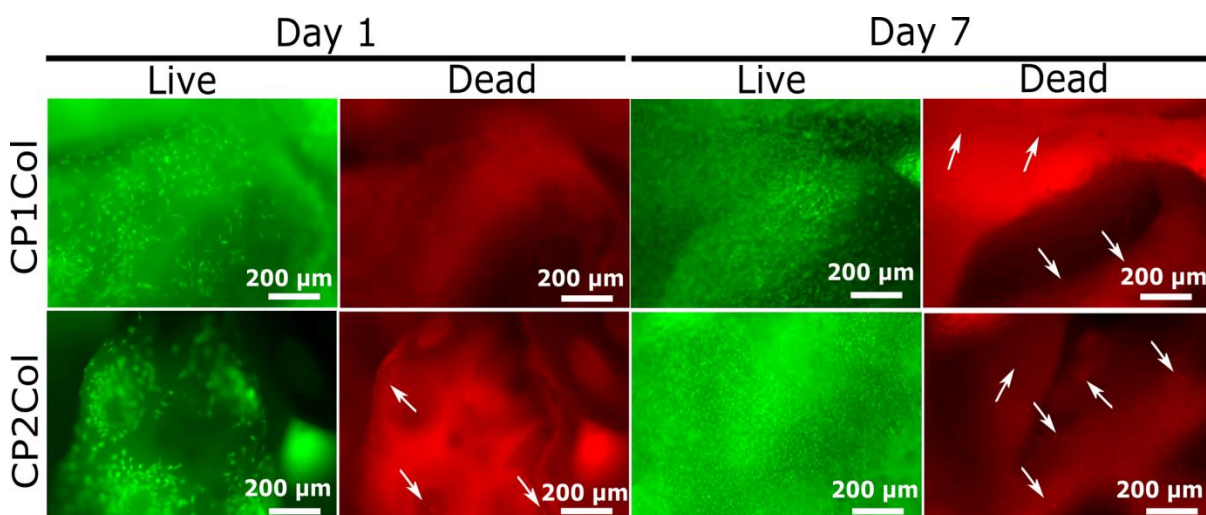


Figure 4.1 Viability fluorescence images of scaffolds. White arrows indicate the dead cells.

MG- 63 cells seeded on the scaffolds attached to the surface and continue to grow *in vitro*. The cells demonstrated good initial attachment to the surfaces of scaffolds after day 1 of cell seeding as shown in Figs. 4.2a-b. According to the SEM observations at day 7, cells showed good migration and proliferation into the pores of CP1/CP2 granules (Figs. 4.2 c-d)

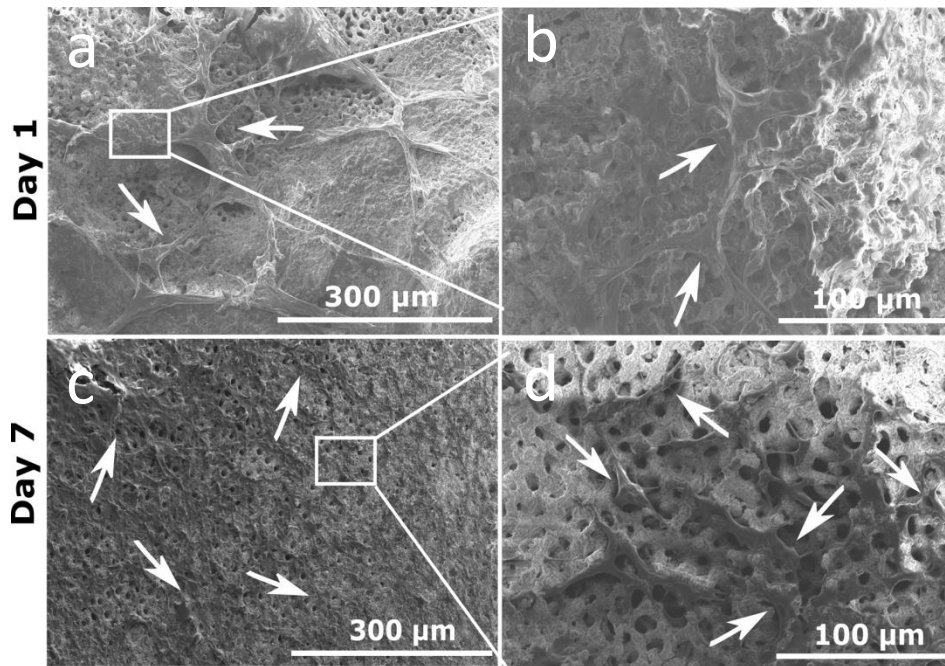


Figure 4.2 Vertical cross section SEM images of cells cultured on CP2Col scaffold after day

Cell proliferations, evaluated by time-dependent changes of DNA amounts in the cell/scaffold constructs, indicated that the MG-63 cells in the scaffolds (Fig. 4.3a) demonstrated significantly higher proliferation than that of the control, conventional collagen sponges, at day 7, 14 and 21. The ALP activity shown in Fig. 4.3b revealed that significantly high ALP activities were observed at day 14 and 21 for the test group in comparison to the control collagen sponge group, though no significant differences on day 7.

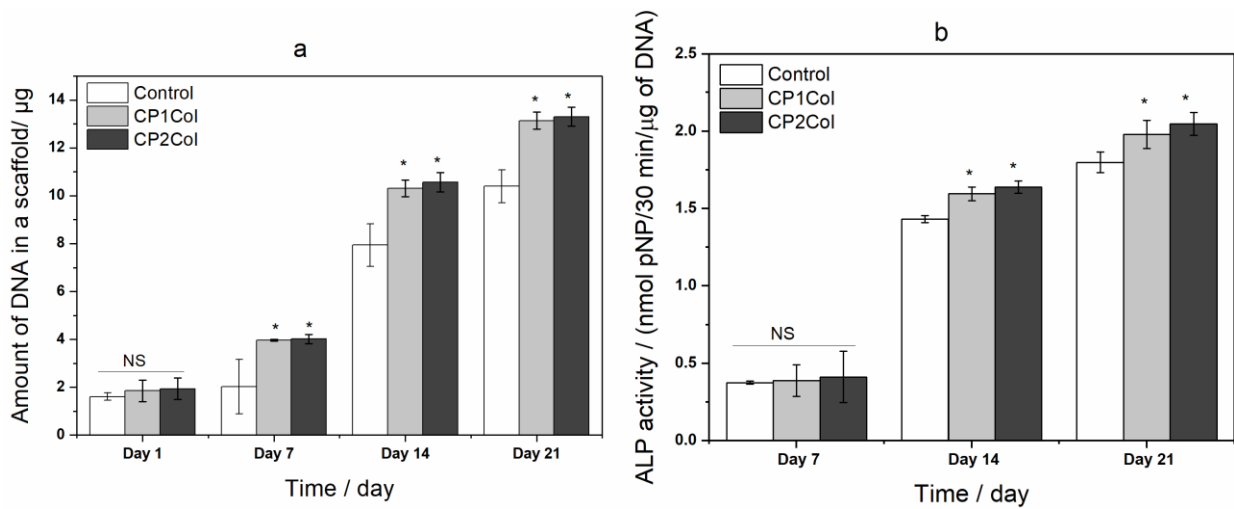


Figure 4.3 (a) Total DNA content assay of MG-63 cells cultured on scaffolds. **(b)** Alkaline phosphatase activity assay of MG-63 cells cultured on scaffolds. Data are represented as mean \pm SD for 5 samples. * Indicates significant differences ($p < 0.05$) when compared with control. NS means no significant difference.

4.3.2 Scaffolds with gelatin as binder

According to the SEM observation at day 1 (Fig. 4.4a), cells got adhered onto the wall of the scaffold CP2Gel_GA. From Fig. 4.4b it is clear that at day 21, cells migrated into the pores of the granules. Fig. 4.5 shows the comparison of the cell penetration between control gelatin and CP2Gel_GA scaffold. It is clear from Fig. 4.5a at day 21, that the cells did not penetrate into the gelatin sponge. All the cells were grown mostly on the surface of the sponge. Whereas, in CP2Gel_GA scaffold (Fig. 4.5b), cells got well distributed into the scaffold.

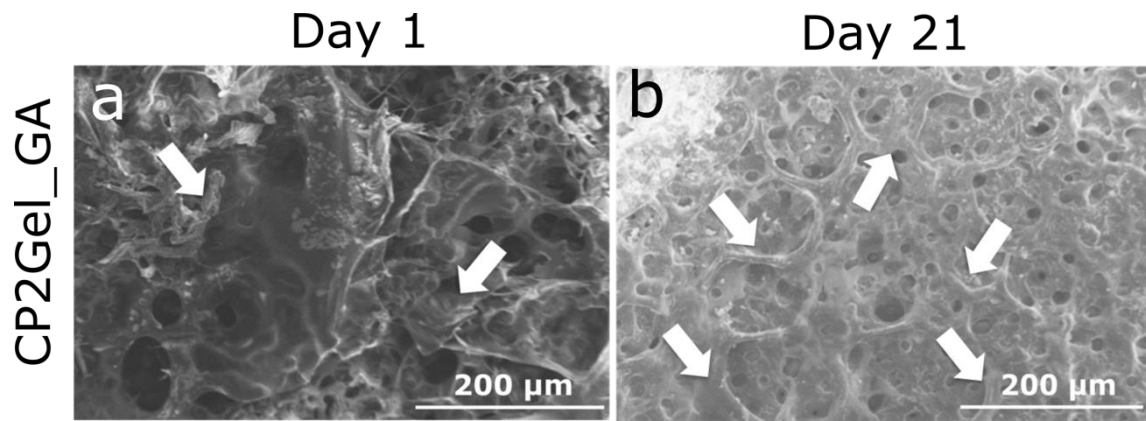


Figure 4.4 Vertical cross section SEM images of cells cultured on CP2Gel_GA scaffold
White arrows indicate the regions of adhered cells.

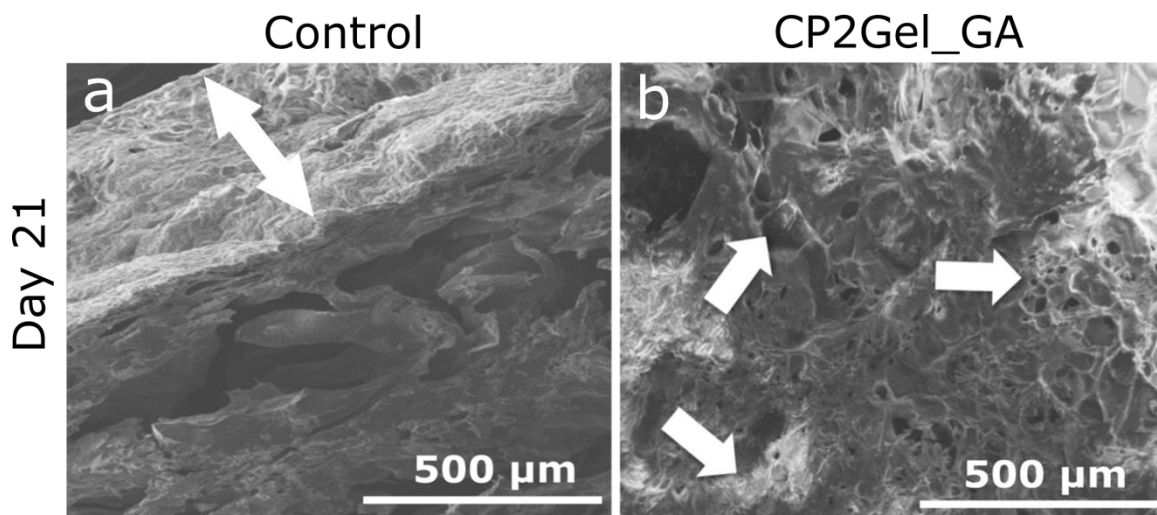


Figure 4.5 Vertical cross section SEM images of cells cultured on (a) Control and (b) CP2Gel_GA at day 21. White double headed arrow in (a) indicate the only region of adhered cells. White arrows in (b) indicate the several regions of adhered cells.

The live/dead staining images of the cells over the scaffolds after day 1 and 21 days of culture are shown in Fig. 4.6. The results showed that most of the cells were viable and very few or negligible dead cells were found in both the scaffolds. Fig. 4.7 shows the comparison between the scaffold CP2Gel_GA and control gelatin sponge. At day 21, no dead

cells were observed on CP2Gel_GA (Fig. 4.7d) but in control many dead cells were observed (Fig. 4.7b). The results show that scaffolds CP1Gel_GA/CP2Gel_GA was more viable compared to control gelatin sponge.

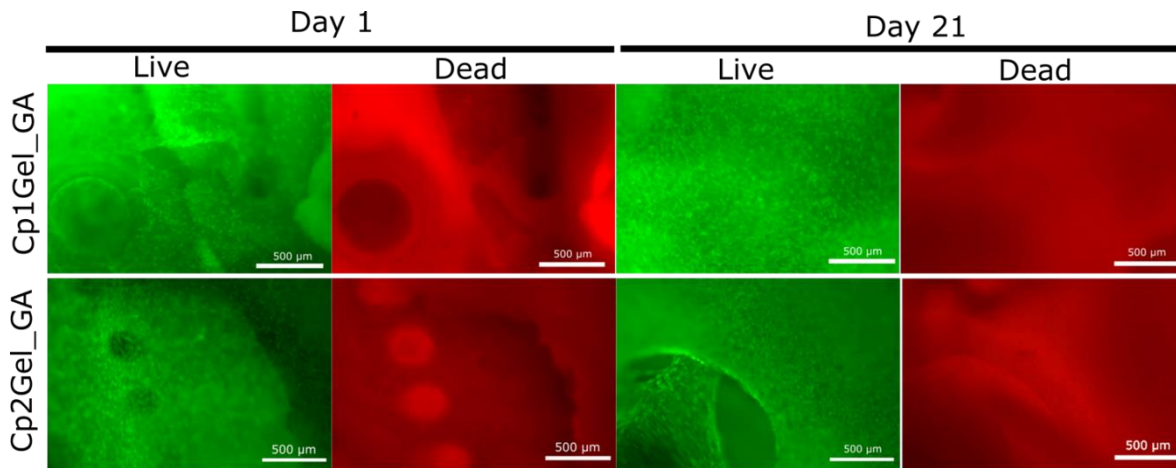


Figure 4.6 Viability fluorescence images of scaffolds. White arrows indicate the dead cells.

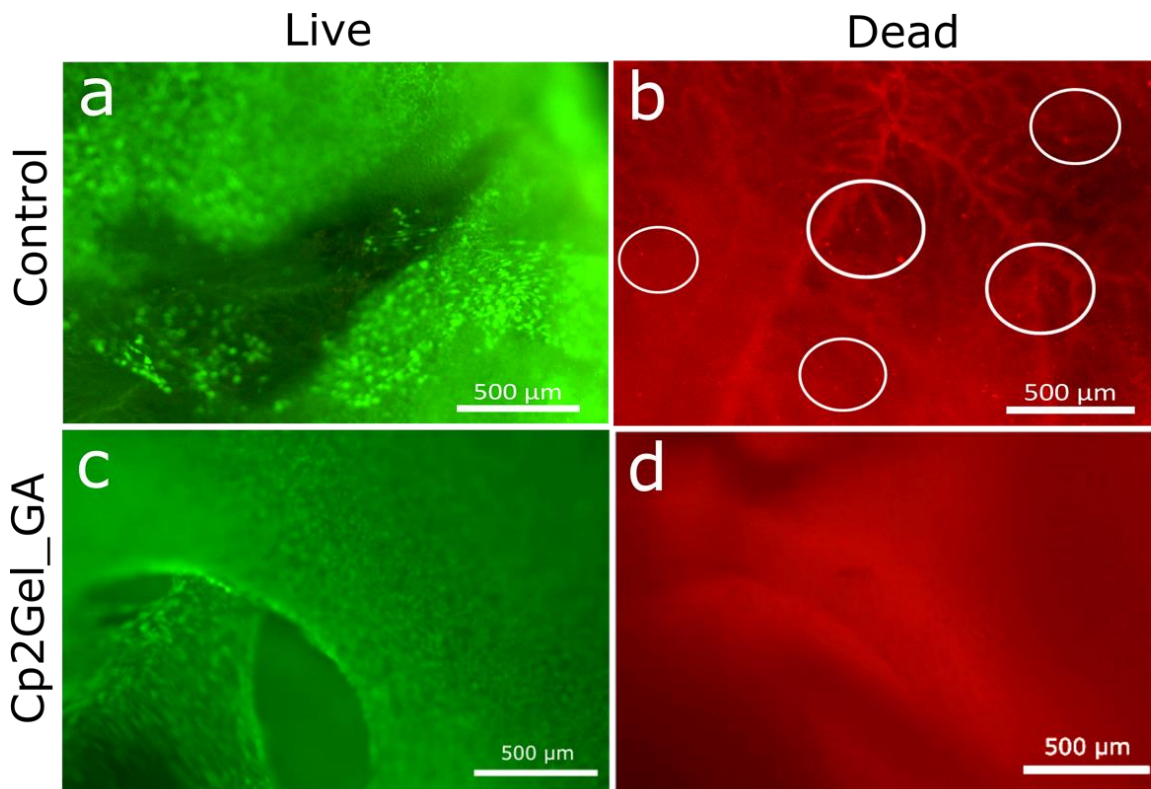


Figure 4.7 Viability fluorescence images of control (a,b) and CP2Gel_GA (c,d) at day 21. White circle regions in (b) indicate the dead cells.

Cell proliferations, evaluated by time-dependent changes of DNA amounts in the cell/scaffold constructs, indicated that the MG-63 cells in the scaffolds (Fig. 4.8a) demonstrated significantly higher proliferation than that of the control, conventional collagen sponges, at day 14 and 21. The ALP activity shown in Fig. 4.8b revealed that significantly high ALP activities were observed at day 14 and 21 for the test group in comparison to the control collagen sponge group, though no significant differences on day 7. This suggested that the presence of Mg containing BCP granules stimulated an early stage of osteoblastic differentiation.

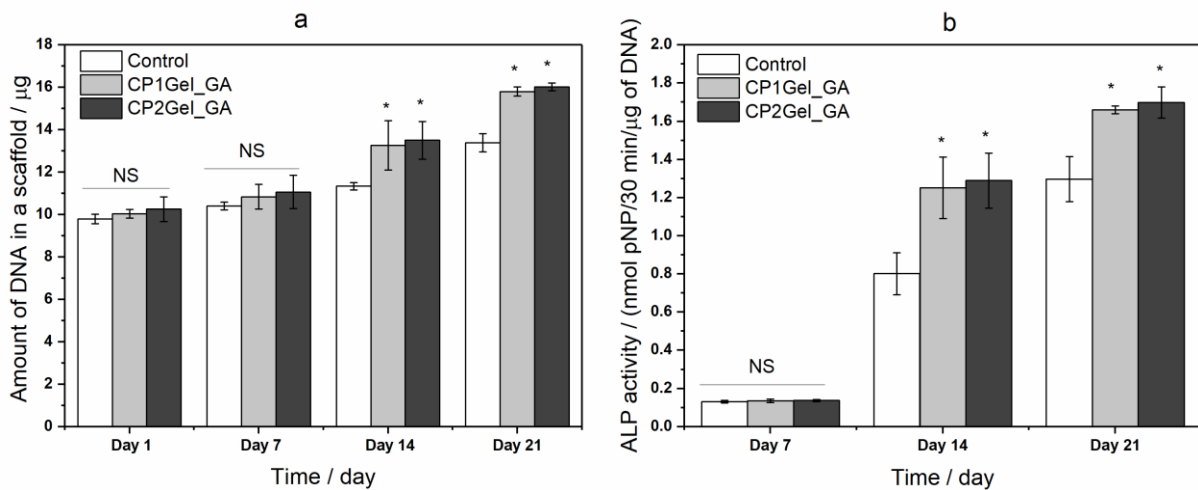


Figure 4.8 (a) Total DNA content assay of MG-63 cells cultured on scaffolds. (b) Alkaline phosphatase activity assay of MG-63 cells cultured on scaffolds. Data are represented as mean \pm SD for 5 samples. * Indicates significant differences ($p < 0.05$) when compared with control. NS means no significant difference.

4.4 Discussion

4.4.1 Scaffolds with collagen as binder

No significant cytotoxicity was observed in any scaffold. From mid vertical cross section images of SEM, cell adherence onto the granules and migration into their macropores were clearly observed. In addition, cell proliferation was highly enhanced in both the CP1Col

and CP2Col scaffolds after day 7, 14 and day 21 in comparison to the control collagen sponge. The ALP activity at day 7 showed no significant differences among all the groups, due to the formation of cell-cell interactions in its peripheral area.[9] The increase in the ALP activity for the cells in the present scaffolds was higher and showed significant difference with that of the control collagen sponge, because calcium phosphate granules in the presently fabricated scaffolds could enhance the early stage of osteoblastic differentiation. Matsuno *et al.*,[10] reported collagen disadvantages as a bone void filler, that the collagen sponge after implantation degraded completely in 4 weeks, although the collagen sponge was replaced by soft connective tissue and newly formed bone without showing the formation of the typical bone network. In fact, collagen is phagocytosed by macrophages instead of osteoclasts; thus, no signal transduction to osteoblasts occurs and no bone formation is promoted.

Biphasic calcium phosphate possesses several advantages over HAp and TCP due to their controlled bioactivity and balance between resorption/solubilization which guarantees the stability of the biomaterial while promoting bone ingrowth.[11] A report by Eun-Ung Lee *et al.*,[12] showed that BCP composite with collagen (BCPC) provided proper space maintaining capacity and osteoconductive property compared to collagen sponge and BCP block. This result suggests that BCPC can be efficiently utilized in various clinical applications.

4.4.2 Scaffolds with gelatin as binder

Gelatin is derived from collagen by hydrolysis and its chemical composition is very similar to collagen. It has been widely used in pharmaceutical, food and medical purposes due to its excellent biocompatibility and biodegradability [13,14]. Despite the advantages of gelatin, the hydrogel doesn't function as good scaffold for migration, proliferation, and differentiation of cells, due to its non-homogenous porous structure[15]. So in this study, I

prepared a composite by simple mixing of gelatin solution with BCP granules which resulted in the formation of homogeneous porous composite.

From mid-vertical cross section images of SEM, it is clear that cells adhered well and penetrated inside the scaffold whereas cells grew only on the surface in the control gelatin sponge. The CP1/CP2 granules in the scaffold provided the homogenous porous structure necessary for cell migration. From cytotoxicity evaluation it was evident that the scaffolds were non-cytotoxic in nature. More dead cells were observed in control gelatin sponge than the scaffolds. The chemical crosslinking did not affect the viability of the cells on the scaffolds. Cell proliferation and ALP activity was also significantly higher at day 14 and 21 compared to control gelatin sponge. The presence of Mg containing BCP granules could enhance early stage osteoblast differentiation [16,17].

The composite scaffolds CP1Gel_GA/CP2Gel_GA provided critical space for proliferation and differentiation of cells. In the present study, I used BCP granules that were homogeneously distributed within the sponge matrix of crosslinked gelatin. The composite had an open pore microstructure, which is necessary for the migration, proliferation and the Mg²⁺ containing BCP granules enhanced the differentiation of cells. The polymer gelatin acted as a binder for the scaffolds and the BCP granules provide space for the bone formation at the defect site.

4.5 Conclusion

The scaffolds fabricated with porous biphasic CP1/CP2 granules and collagen or gelatin provided essential porosity, bioactive surface for cell attachment and proliferation. Also, the scaffolds created a favorable environment for differentiation of cells, which can favor increased bone formation in comparison with control collagen/gelatin sponge. Furthermore, the *in vitro* biological evaluation showed that the scaffolds were non-cytotoxic.

The scaffolds proved to be biocompatible and have the potential to be utilized as artificial bone filler.

Acknowledgement

This **Chapter 4**, in part, was a reprint of the publications

1. Manchinasetty NVL, Oshima S, Kikuchi M. Preparation of flexible bone tissue scaffolds utilizing sea urchin test and collagen. *Journal of Materials Science: Materials in Medicine* 2017; 28(11):184-1- 184-12 with permission.

2. Manchinasetty NVL, Kikuchi M. Fabrication and characterization of porous scaffold utilizing the test of sea urchin and gelatin (manuscript under preparation).

4.6 References

1. Elshahawy W. Biocompatibility. In: Costas Sikalidis Bioceramics, Ceramics and Environment BT-A in C-E and MC, editor. Rijeka: InTech; 2011. p. Ch. 15.
2. Polo-Corrales L, Latorre-Esteves M, Ramirez-Vick JE. Scaffold Design for Bone Regeneration. *J. Nanosci. Nanotechnol.* 2014;14:15–56.
3. Karageorgiou V, Kaplan D. Porosity of 3D biomaterial scaffolds and osteogenesis. *Biomaterials.* 2005;26:5474–91.
4. Damien CJ, Parsons JR. Bone graft and bone graft substitutes: a review of current technology and applications. *J. Appl. Biomater.* UNITED STATES; 1991;2:187–208.
5. Amini AR, Laurencin CT, Nukavarapu SP. Bone tissue engineering: recent advances and challenges. *Crit. Rev. Biomed. Eng.* 2012;40:2.
6. Tanaka Y. Development of titanium fixation screw for hydroxyapatite osteosynthesis (APACERAM). *Surg. Neurol.* United States; 2008;70:545–9; discussion 549.
7. Suzuki K, Nagata K, Yokota T, Honda M, Aizawa M. Histological evaluations of apatite-fiber scaffold cultured with mesenchymal stem cells by implantation at rat subcutaneous tissue. *Biomed. Mater. Eng.* Netherlands; 2017;28:57–64.

8. Kikuchi M, Ikoma T, Itoh S, Matsumoto HN, Koyama Y, Takakuda K, et al. Biomimetic synthesis of bone-like nanocomposites using the self-organization mechanism of hydroxyapatite and collagen. *Compos. Sci. Technol.* 2004;64:819–25.
9. Yoshida T, Kikuchi M, Koyama Y, Takakuda K. Osteogenic activity of MG63 cells on bone-like hydroxyapatite/collagen nanocomposite sponges. *J. Mater. Sci. Mater. Med. United States*; 2010;21:1263–72.
10. Matsuno T, Nakamura T, Kuremoto K, Notazawa S, Nakahara T, Hashimoto Y, et al. Development of beta-tricalcium phosphate/collagen sponge composite for bone regeneration. *Dent. Mater. J. Japan*; 2006;25:138–44.
11. Lobo SE, Livingston Arinzeh T. Biphase Calcium Phosphate Ceramics for Bone Regeneration and Tissue Engineering Applications. *Mater.* . 2010.
12. Lee E-U, Kim D-J, Lim H-C, Lee J-S, Jung U-W, Choi S-H. Comparative evaluation of biphasic calcium phosphate and biphasic calcium phosphate collagen composite on osteoconductive potency in rabbit calvarial defect. *Biomater. Res.* 2015;19:1–7.
13. Davidenko N, Schuster CF, Bax D V, Raynal N, Farndale RW, Best SM, et al. Control of crosslinking for tailoring collagen-based scaffolds stability and mechanics. *Acta Biomater.* 2015;25:131–42.
14. Gámez Sazo RE, Maenaka K, Gu W, Wood PM, Bunge MB. Fabrication of growth factor- and extracellular matrix-loaded, gelatin-based scaffolds and their biocompatibility with Schwann cells and dorsal root ganglia. *Biomaterials.* 2012;33:8529–39.
15. Annabi N, Nichol JW, Zhong X, Ji C, Koshy S, Khademhosseini A, et al. Controlling the Porosity and Microarchitecture of Hydrogels for Tissue Engineering. *Tissue Eng. Part B. Rev.* 140 Huguenot Street, 3rd Floor New Rochelle, NY 10801USA: Mary Ann Liebert, Inc.; 2010;16:371–83.
16. Holzapfel BM, Reichert JC, Schantz J-T, Gbureck U, Rackwitz L, Nöth U, et al. How smart do biomaterials need to be? A translational science and clinical point of view. *Adv. Drug Deliv. Rev.* 2013;65:581–603.

17. Fellah BH, Gauthier O, Weiss P, Chappard D, Layrolle P. Osteogenicity of biphasic calcium phosphate ceramics and bone autograft in a goat model. *Biomaterials*. Netherlands; 2008;29:1177–88.

Chapter 5

Evaluation of biocompatibility of scaffolds under pressure/perfusion cell culture conditions

5.1 Introduction

When evaluating the biocompatibility of three dimensional scaffolds as potential substitutes in static 2D cell culture, circulation of medium is absent. The nutrient transport only occurs by diffusion and which may increase the concentration of metabolites and nutrients at the peripheral area and may hinder the distribution of cells to inner layers of the scaffold [1,2]. So the disadvantages of using static 2D cell culture system are inefficient nutrient transportation, decrease in waste removal which results in poor cell proliferation, and non-uniform cell distribution, limitation in the usage of dimensions of scaffolds [3]. Technically 2D culture system uses the principle of diffusion to provide nutrients and oxygen to cells and waste removal, but when using 3D scaffolds/samples for evaluation, diffusion is not sufficient [4]. Hence more complex bioreactor systems are required for culture media circulation and efficient transportation of nutrients to cells, which leads to uniformity. Bioreactor systems not only increase the mass transport inside the 3D scaffolds, they also reduce handling steps and contamination. They also help to control the environment, such as nutrient supply, temperature, pH, oxygen and carbon dioxide [5,6]. It is hypothesized that the cells lining in the lacunar and canalicular spaces in bone are influenced by the mechanostimulation provided by the interstitial fluid flow, which stimulates the proliferation or differentiation [7–9]. Thus this would be a clear advantage to use fluid flow in *in vitro* cell culture.

Based on the advantages of the 3D cell culture system, researchers used several types of 3D culture system such as rotating wall vessels [10,11], perfusion systems [12–14] and spinner flasks [15] in the evaluation of the biocompatibility of the scaffolds or sponges. Spinner flasks and rotating wall vessels use convection for well mixing of culture media around the samples, which leads to effective nutrient transport into porous structure [11]. On the other hand, perfusion systems perfuse fluid directly through the scaffold, ensuring good mass transport and this phenomenon have been also shown to increase the expression levels of osteoblastic markers [16,17]. Based on these advantages, Glowacki *et al.*, reported that viability and function of murine bone marrow [18] and osteosarcoma cells [19] cultured in three dimensional collagen sponges were maintained by a low rate (1.3mL/min) perfusion of culture medium. Based on the above results, Mizuno *et al.*, developed a novel pressure/perfusion culture system, where hydrostatic fluid pressure (HFP) and medium perfusion was applied to chondroblasts cultured in the sponge to maintain the chondrogenic activity of the cells [20]. This system also enhanced the activity and viability of the osteoblastic MG-63 cells in the center of the collagen sponges [21].

In **Chapter 4**, the biocompatibility of the scaffolds was evaluated under 2D cell culture system and concluded that the scaffolds CP1Col/CP2Col, and CP1Gel_GA/CP2Gel_GA, had higher ability in proliferation, adherence, distribution and ALP activity compared their respective control. In this chapter, the biological function of the scaffolds was evaluated under the conditions that mimic biological conditions of bone, *i.e.*, a pressure/perfusion 3D cell culture system with the application of HFP.

5.2 Materials and Methods

5.2.1 Chemicals

Chemicals used in this research were purchased from Wako Pure Chemical Ltd., Japan if without further notice. The supplies required for real-time reverse transcription polymerase chain reaction (Real time RT-PCR) was purchased from Invitrogen unless otherwise mentioned.

5.2.2 Samples

Fabrication of scaffolds with collagen or gelatin as binder was discussed in **Chapter 3**. In **Chapter 4**, the biocompatibility of the scaffolds we evaluated under static 2D cell culture conditions. No significant difference was found between CP1Col and CP2Col and same for CP1Gel_GA and CP2Gel_GA. So, for experiments based on scaffolds with collagen as binder, only CP2Col was used as sample and collagen sponge was used as control. And for experiments based on scaffolds with gelatin as binder, only CP2Gel_GA was used as sample and gelatin sponge was used as control. The dimension of the scaffolds used in this study was 8 mm in diameter and 10 mm in height.

5.2.3 Pressure/perfusion culture and cell seeding conditions

A pressure/perfusion culture system designed by Mizuno *et al.*, was used in this study[20,22], where the system applies HFP to the samples with constant perfusion of medium. The system consists of debubbler, perfusion pump, pressure gauge, glass column, back pressure regulator reservoir and tubing (Fig. 5.1). The flow rate was controlled by the perfusion pump and constant HFP was applied by the back pressure regulator. All the components except for the debubbler, perfusion pump and pressure gauge were maintained inside the incubator (5 % CO₂, 95 % relative humidity). The tubing in this apparatus was

made 15 m long, where the medium temperature is increased to 37 °C, to cover for the loss of the temperature in the medium that passed through the debubbler, perfusion pump and pressure gauge which are outside of the incubator.

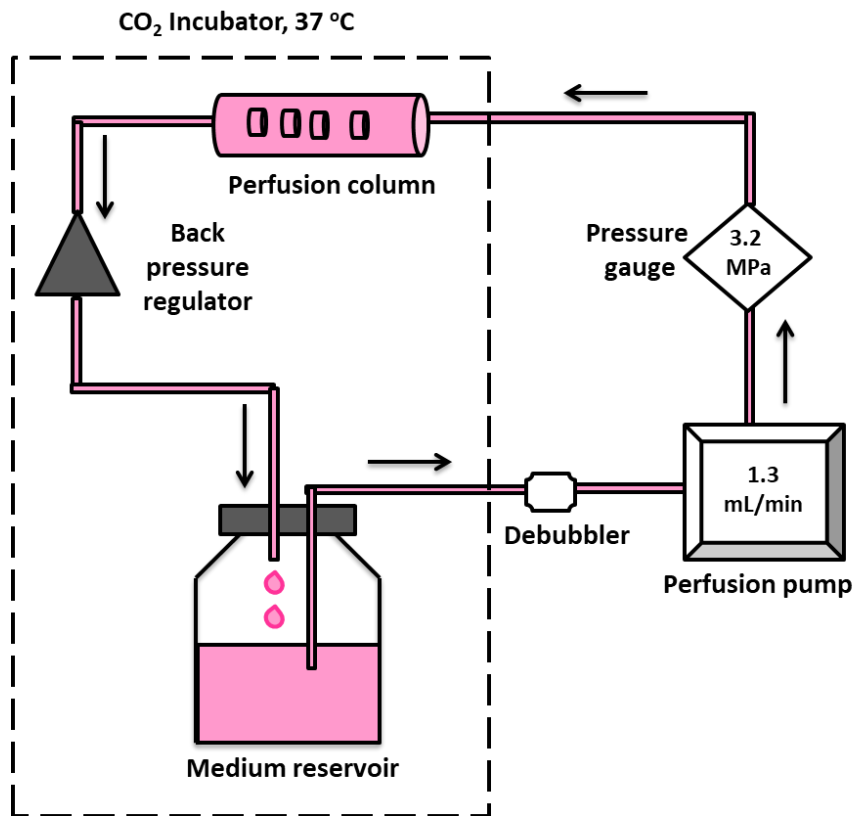


Figure 5.1 Pressure/perfusion cell culture system

The human osteoblast-like cell line, MG-63, derived from human osteosarcoma was used for the experiment. The MG-63 cells were sub-cultured in 75 cm² tissue culture flasks using a complete medium, Dulbecco's modified Eagle's medium (DMEM, Sigma Aldrich, USA) supplemented with 10 % (v/v) fetal bovine serum (Sigma Aldrich, USA) and 1 % (v/v) penicillin/streptomycin (Gibco[®], Life technologies, Japan) in an incubator (HERAcell 150i, Thermo Scientific, Japan) at 95 % relative humidity and 5 % CO₂. All the scaffolds and sponges were sterilized by the ethylene oxide gas (EOG) method and conditioned with the

complete medium at 37 °C for 3 h. After absorbing away the medium from the scaffolds using a sterilized filter paper (Advantec, 5C, 90mm), the scaffolds were placed in a tissue culture dish (100 × 20 mm, FALCON[®] USA), 1 × 10⁶ cells suspended in 50 µL of the complete medium was seeded onto each scaffold and incubated at 37 °C for 2 h. After the incubation, the cell-seeded scaffolds were transferred into each well of 24-well plates (Gibco[®], USA). Then, 2 mL of the complete medium was added to each well and cultured under static condition for 24 h to complete cell attachment on the sponge.

Only perfusion was applied at 1.3 mL/min to the columns to support cell proliferation for first 6 days. At Day 7, the medium was changed to osteogenic medium that is composed of growth medium supplemented with 50 µg/mL L-ascorbic acid and 10 mM β-glycerophosphate (Sigma-AldrichCo., USA), and pressure (3.2 MPa) was applied together with 1.3 mL/min perfusion. The medium was changed every 3 days (2.5 mL/sponge/day) and cultured for 21 days.

5.2.4 Cell proliferation

The cell proliferation in the scaffolds was quantified by the DNA amount in the cell-scaffold constructs. After 3-, 7-, 10-, 14- and 21-day cultures, each construct was harvested, homogenized on ice in the glycine lysis buffer containing 0.1 M glycine (pH 10.4), 1 mM MgCl₂ and 0.2 % (v/v) TritonX-100 and incubated for 15 min in an ice box. Each sample was centrifuged at 12,000 rpm for 5 min, and the supernatant was transferred to a new centrifuge tube and stored at -80 °C until further analysis. The total DNA content was measured with a multiplate reader (GENius; TECAN, Männedorf, Switzerland) by the Hoechst 33258 method. Briefly, 100 µL of diluted sample was mixed with 100 µL of Hoechst dye 33258 (Dojindo Laboratories, Japan) in a 96-well microplate (FALCON[®], USA)). Emissions at 458 nm

excited by 360 nm light were measured, and the DNA content was calculated with a standard curve ($R^2=0.999$) prepared using a calf-thymus DNA (Sigma Aldrich, USA).

5.2.5 Cell distribution in scaffolds

Cell-scaffold constructs cultured for 3 and 21 days were washed with PBS and fixed in 10% neutral buffered formalin for 2 days. The constructs were decalcified in 10 % ethylenediaminetetraacetic acid disodium salt dihydrate (EDTA 2Na, Sigma Aldrich, USA) solution for 7 days. The decalcified samples were dehydrated, embedded in paraffin and sectioned to get the vertical cross sections of constructs with 8 μm thickness. Cell nuclei in the sections were stained with 2 $\mu\text{g}/\text{mL}$ 4',6-diamidino-2-phenylindole, dihydrochloride (DAPI, Dojindo Molecular Technologies, Inc.) and observed under a fluorescence microscope (Olympus, Tokyo, Japan). The images of nuclei staining were imported into ImageJ software to analyze the integrated fluorescence intensities in the center zone. The integrated intensity of each ROI was divided by the area of ROI to obtain the average intensity. The average intensity of each ROI was subtracted from the average intensity of background [23].

5.2.6 Real time RT-PCR

The quantification of gene expressions of alkaline phosphatase (ALP) and osteocalcin (OCN) were measured as indicators of osteogenic activity using the similar process reported by Yoshida *et al.*, [22]. Glyceraldehyde-3-phosphate dehydrogenase (GAPDH) was chosen as an internal standard housekeeping gene. After 7, 14 and 21 days of culture, total cellular RNA was extracted using TRIZOL[®] according to the manufacturer's instructions. One microgram of RNA was converted to cDNA by reverse transcription. The reverse transcription was performed at 42 °C for 75 min in a reaction volume of 20 μL containing 5 X first strand buffer, 0.1 M DTT, 10 mM dNTPs, Oligo-dT 12-18, RNase

inhibitor, superscript II and RNA solution. The reverse transcriptase in the sample was inactivated by heating at 70 °C for 10 min. RT-PCR was performed to evaluate the relative quantification of gene expressions using Thermal cycler dice™ real time system II TP900/960 (TaKaRa Bio INC, Applied Biosystems). cDNA was added to a reaction volume of 25 µL with qPCR™ Master Mix (EUROGENTEC Bel, Belgium), sequence specific primers (10 µM) and Taqman® MGB probes. Table 5.1 shows the sequence of target specific primers and probes used in this study. Thermocycling conditions were 48 °C for 30 min (reverse transcription) and 95 °C for 10 min (initial denaturation) followed by 40 cycles at 95 °C for 15 sec (denaturation) and 60 °C for 45 sec (annealing and extension). Gene expression levels relative to GAPDH were calculated using a comparative Ct method.

Table 5.1 Sequences for primers and probes used in RT-PCR analysis

Gene	Forward primer	Reverse primer	Taqman® MGB probes
ALP	5'-atggggaaggtgaaggtcg-3'	5'-taaaagcagaaatggtgacc-3'	5'-FAM-cgccaatacaccacaaatccgttgac-MGB-3'
OCN	5'-caatccggactgtgacgagtt-3'	5'-ccgtagaagcgccgatagg-3'	5'-FAM-cacatcgctttcag-MGB-3'
GAPDH	5'-atggggaaggtgaaggtcg-3'	5'-taaaagcagaaatggtgacc-3'	5'-FAM-cgccaatacaccacaaatccgttgac-MGB-3'

5.2.7 Statistical analysis

Proliferation and gene expression experiments were performed in triplicate for each condition. All data were expressed as mean ± standard deviation (SD). Student t-test and one-way analysis of variance performed to reveal significant differences. *P* values less than 0.05 were considered significant.

5.3 Results

5.3.1 Biocompatibility of scaffolds with collagen as binder

A significant difference in the amount of DNA between control collagen sponge and CP2Col was seen at day 14 and 21 (Fig. 5.2). This indicates that scaffold CP2Col has higher cell proliferation ability in comparison to control collagen sponge.

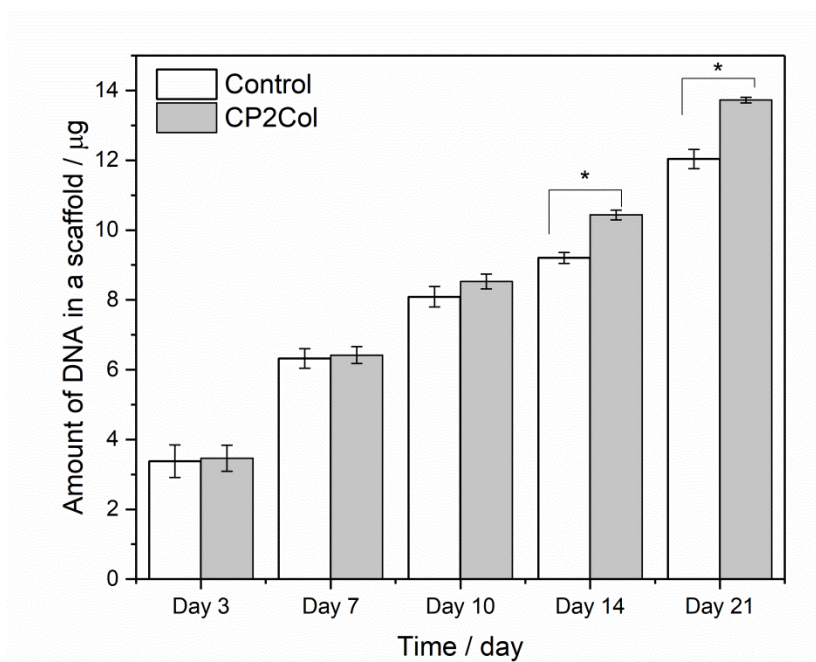


Figure 5.2 Total DNA content assay of MG-63 cells cultured on scaffolds. * Indicates significant differences ($p < 0.05$) when compared with control.

Qualitative and quantitative analysis of cell distribution in CP2Col and control collagen sponge at day 3 and 21 is shown in Fig. 5.3. From the Fig 5.3c & d it is clear that control collagen sponge shrunk in size while the scaffold CP2Col maintained its shape and integrity. At day 3, cells were seen only on the peripheral area in the control whereas in CP2Col cells got distributed. There is significant difference in the calculated average intensity at day 3 between control and CP2Col (Fig. 5.3e). At day 21, cells got evenly distributed in both control and CP2Col and no significant difference was found.

The Real time RT-PCR analysis results are shown in Fig. 5.4. At day 7, ALP expression was higher in control than CP2Col and later decreased at day 14 and 21, whereas there was an increasing trend for ALP expression in CP2Col (Fig. 5.4a). The expression levels of OCN showed an increasing trend in CP2Col and was significantly higher at day 21 compared to control (Fig. 5.4b).

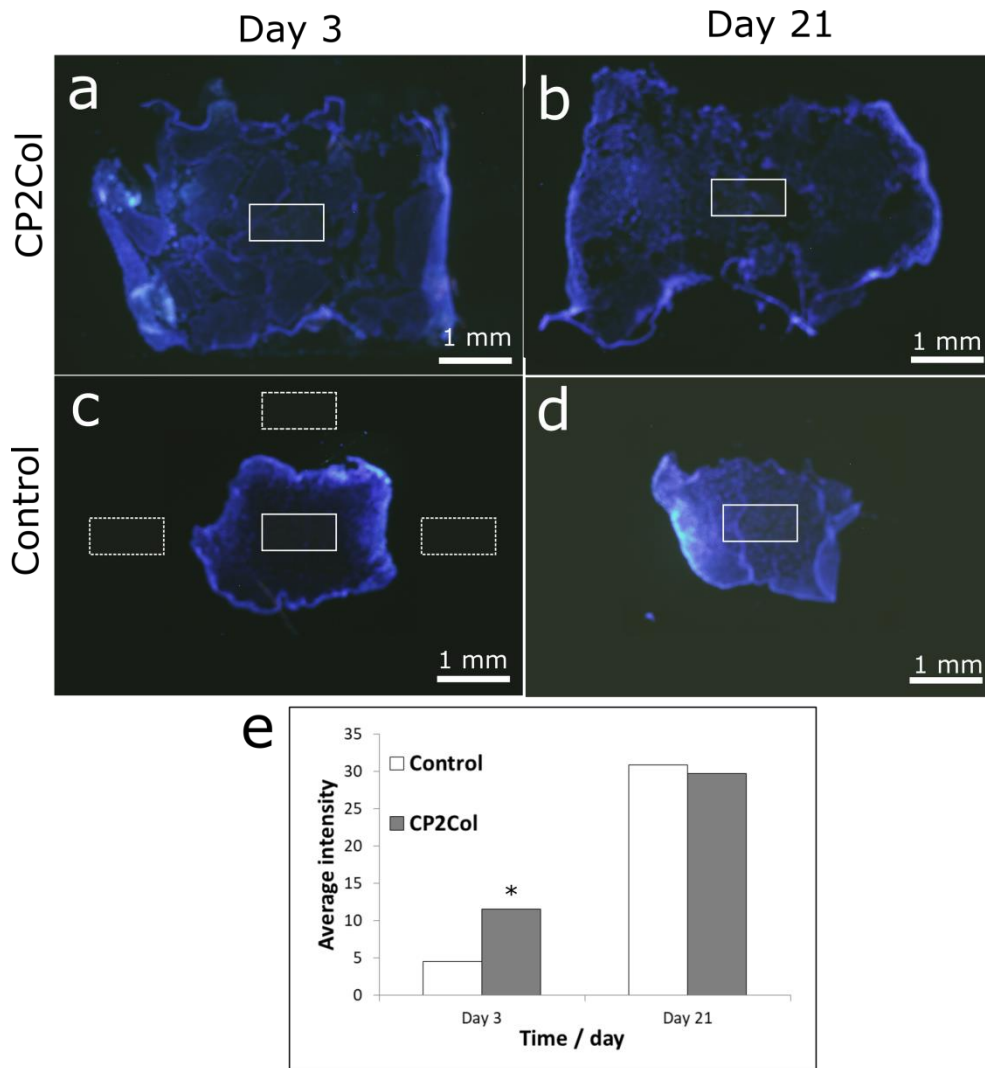


Figure 5.3 (a-d) Cell distributions in the scaffolds after 3 and 21 day culture. The integrated fluorescence intensities of nuclei staining in the ROI, the center zone of cross section ($500 \times 1000 \mu\text{m}$ solid rectangles) were quantified. The average intensity of each ROI was subtracted from the average intensity of background (dashed rectangles) (e) Calculated average intensity

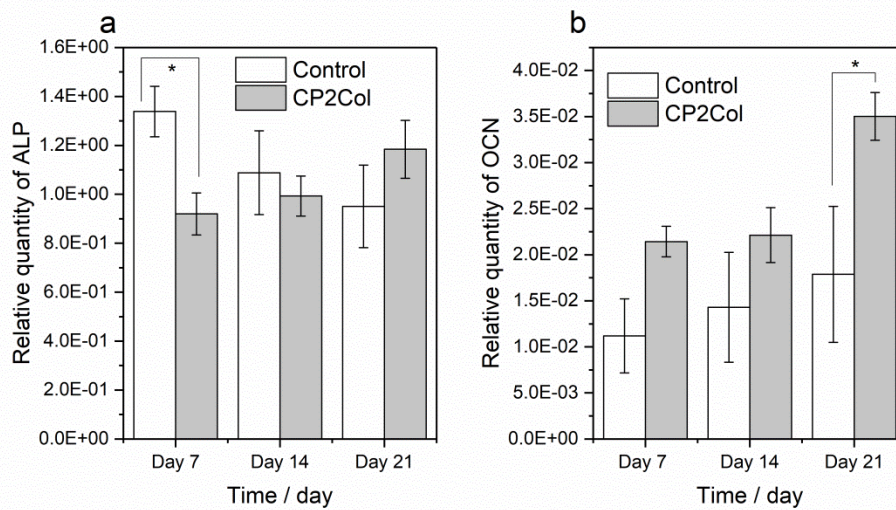


Figure 5.4 Real time RT-PCR analysis of (a) ALP and (b) OCN gene expressions. * Indicates significant differences ($p < 0.05$).

5.3.2 Biocompatibility of scaffolds with gelatin as binder

Cell proliferation by Total DNA quantification in control and scaffold CP2Gel_GA is shown in Fig. 5.5. A significant difference was found between CP2Gel_GA and control gelatin sponge was found at day 10, 14 and 21. This shows that CP2Gel_GA has higher ability in proliferation in 3D culture conditions.

Relative gene expression levels of ALP and OCN in control gelatin sponge and CP2Gel_GA are shown in Fig. 5.6. A significant difference was found between control and CP2Gel_GA at day 14 and 21 in the expression level of ALP, while the level of ALP was higher in Control at day 7 compared to CP2Gel_GA (Fig. 5.6a). The relative expression level of OCN was significantly higher in CP2Gel_GA at day 21 compared to control (Fig. 5.6b).

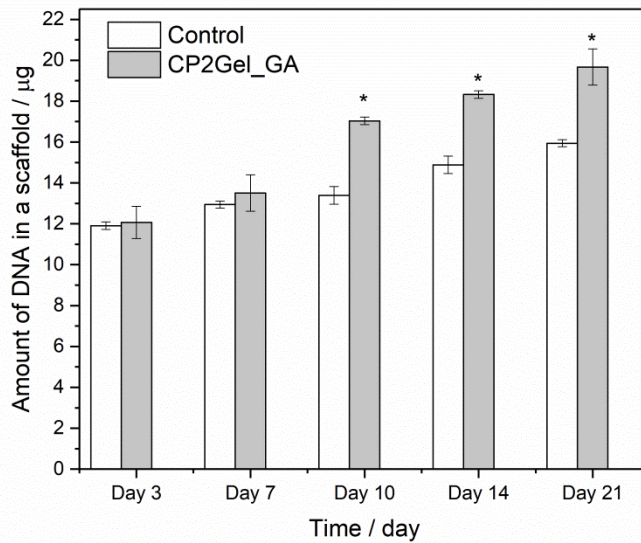


Figure 5.5 Total DNA content assay of MG-63 cells cultured on scaffolds. * Indicates significant differences ($p < 0.05$) when compared with control.

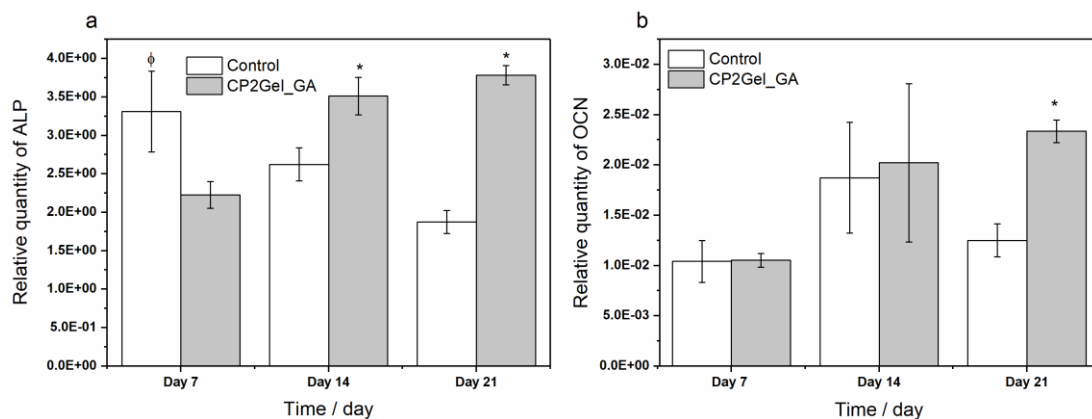


Figure 5.6 Real time RT-PCR analysis of (a) ALP and (b) OCN gene expressions. * Indicates significant differences ($p < 0.05$) compared with control. Φ Indicated significant difference ($p < 0.05$) compared with CP2Gel_GA.

5.4 Discussion

5.4.1 Scaffolds with collagen as binder

Cell proliferation ability in CP2Col was higher than control sponge at day 14 and 21 under pressure/perfusion culture conditions. Fig. 5.7a and b shows the comparison of cell proliferation under 3D and 2D conditions respectively. From Fig 5.7b, the cell proliferation

in CP2Col compared to control was higher at day 7, 14 and 21 under 2D condition but in 3D cell culture condition; in this case pressure/perfusion conditions improved the cell proliferation in control collagen sponge as well until day 10. Even though the cells continued to grow further, they were significantly higher in CP2Col at day 14 and 21 due to the space availability; the scaffold maintained its integrity throughout the culture whereas the control collagen shrunk in size leaving less area for the cells to grow.

Cell distribution in the center region of CP2Col (Fig. 5.3a) was higher than control at day 3; cells were observed only on the peripheral area of the control due to its poor interconnectivity in the porous structure and accordingly few or no cells migrated to the inner layer. Similar results were observed by Yoshida *et al.*, under similar cell culture conditions where few cells migrated to the inner layer of the collagen sponge, whereas the sample HAp/Col sponge showed good cell distribution [22].

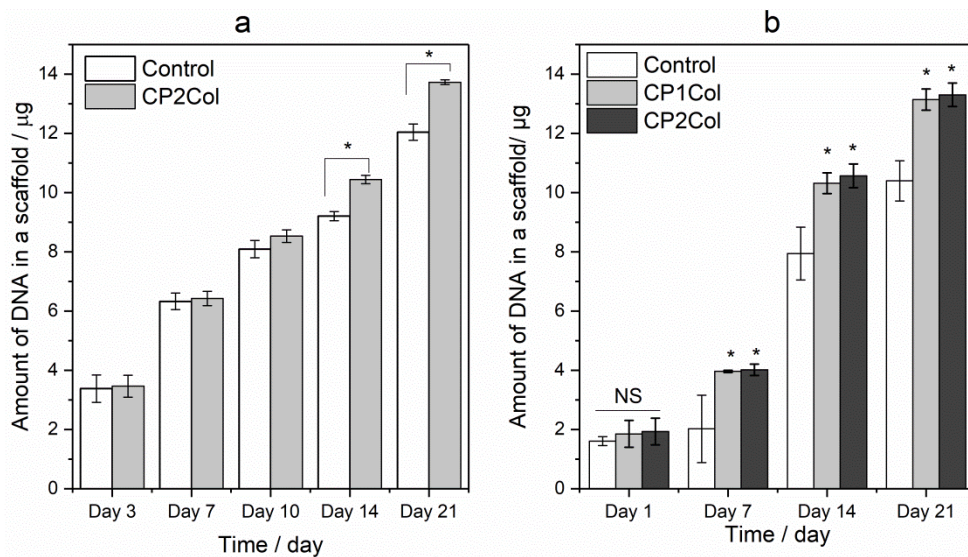


Figure 5.7 Total DNA content assay of MG-63 cells cultured on scaffolds with collagen as binder under (a) 3D condition and (b) 2D condition. * Indicates significant differences ($p < 0.05$) when compared with control. NS indicates no significant difference.

Gene expression level of ALP, an early stage marker of osteogenic activity, was higher in control collagen sponge than CP2Col, because of the cell-cell interactions required for the gene expression formed early in the collagen sponge. Like discussed above, cells in the collagen sponge didn't migrate to the inner layer in the early stages, most of the cells grew only on the surface, so the cells formed cell-cell interactions which is the requirement for ALP gene expression for osteoblast like cells. Cells in CP2Col migrated to the inner layer at early stages and enough cell density couldn't be achieved to form cell-cell interactions, hence the expression levels were low. But later, the trend of ALP expression increased in CP2Col but there wasn't any significant difference between collagen and CP2Col. Matsushima *et al.*, also reported cells cultured on Interpore[®] also required time to express ALP due to the high cell proliferation and distribution ability into the inner pores [24].

The latter stage marker for osteogenic activity, OCN, was higher in CP2Col and showed a significant difference at day 21 compared to collagen sponge. The level of OCN gene expression in collagen sponge was same throughout the culture. These results were also in agreement with Yoshida *et al.*, where similar trend was observed in the gene expression levels of ALP and OCN [22]. ALP expression was higher at day 7 in collagen sponge than the sample HAp/Col sponge and OCN expression showed an increasing trend. These results suggest that osteogenic activity is higher in CP2Col even without high ALP expression in comparison to control collagen sponge.

5.4.2 Scaffolds with gelatin as binder

Cell proliferation ability in CP2Col_GA was significantly higher than control collagen sponge under pressure/perfusion culture conditions. The comparison of cell proliferation in CP2Col_GA and control gelatin sponge under 3D and 2D conditions is shown in Fig. 5.8. Even under 3D culture conditions, cell proliferation was higher in CP2Gel_GA.

Like discussed in **Chapter 5**, gelatin sponge contains heterogeneous and less interconnected and pore structure. Non homogeneous and non-interconnected pores in scaffolds might hinder seeding and distribution of cells into the inner layers[25,26]. Void cores also accompany with poor mechanical property of the engineered final product[23,27,28]. From **Chapter 5**, Fig. 4.5 and 4.6, cells proliferated and got distributed to the inner layer of the scaffold CP2Gel_GA, whereas cells grew only on the peripheral area of the control gelatin sponge. The open pore and homogeneous structure of CP2Gel_GA scaffold facilitated even cell seeding and distribution of cells to the inner layers and thus facilitated higher cell proliferation.

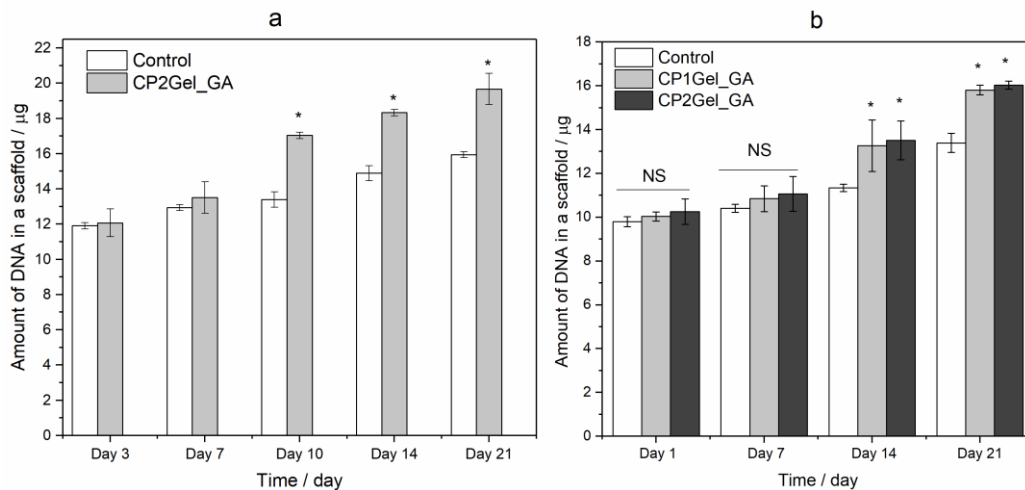


Figure 5.8 Total DNA content assay of MG-63 cells cultured on scaffolds with gelatin as binder under (a) 3D condition and (b) 2D condition. * Indicates significant differences ($p < 0.05$) when compared with control. NS indicates no significant difference.

Gene expression level of ALP was higher in gelatin sponge at day 7 may be due to the accumulation of cells which led to the formation of cell-cell junctions, a requisite for the expression of gene ALP. But at day 14 and 21, the level of ALP got decreased in control gelatin sponge and got significantly increased in CP2Gel_GA. Expression of OCN gene, the latter stage marker for osteogenic activity, was significantly higher in CP2Gel_GA at day 21. This suggests that the scaffold CP2Gel_GA with Mg^{2+} containing BCP granules enhanced the

osteogenic activity. These results also corroborate with study by Staiger MP *et al.*, where magnesium containing calcium phosphate was added to gelatin and observed increase in the level of proliferation, ALP and OCN compared to gelatin sponge [29].

The obtained results suggest that CP2Gel_GA provided good mechanical strength, interconnected porous structure which facilitated the cell proliferation to inner layers. The Mg²⁺ containing BCP granules provided the homogeneous structure for cell distribution and also contributed for the enhancement for osteogenic activity.

5.5 Conclusion

From *in vitro* biocompatibility evaluation of scaffolds prepared with collagen as binder, CP2Col and CP2Gel_GA with gelatin as binder under pressure/perfusion cell culture conditions showed higher cell proliferation and distribution ability compared to control. Higher osteogenic potential was seen in CP2Col and CP2Gel_GA compared to control collagen and gelatin sponge respectively. The homogeneous porous structure and Mg²⁺ containing BCP granules in the scaffolds facilitated good cell distribution and enhanced the osteogenic activity under 3D culture conditions. These results suggest that the scaffolds could be a potential candidate as artificial bone filler for non-load bearing defects.

Acknowledgement

This **Chapter 5**, in part, was a reprint of the manuscript under preparation

- 1) **Manchinasetty NVL**, Oshima S, Kikuchi M. Evaluation of the biocompatibility of scaffolds fabricated using test of sea urchin and collagen or gelatin as binder under pressure/perfusion culture conditions.

5.6 References

1. Sikavitsas VI, Bancroft GN, Mikos AG. Formation of three-dimensional cell/polymer constructs for bone tissue engineering in a spinner flask and a rotating wall vessel bioreactor. *J. Biomed. Mater. Res. United States*; 2002;62:136–48.
2. Fröhlich M, Grayson WL, Wan LQ, Marolt D, Drobnic M, Vunjak-Novakovic G. Tissue engineered bone grafts: biological requirements, tissue culture and clinical relevance. *Curr. Stem Cell Res. Ther.* 2008;
3. Stiehler M, Bunker C, Baatrup A, Lind M, Kassem M, Mygind T. Effect of dynamic 3-D culture on proliferation, distribution, and osteogenic differentiation of human mesenchymal stem cells. *J. Biomed. Mater. Res. A. United States*; 2009;89:96–107.
4. Sailon AM, Allori AC, Davidson EH, Reformat DD, Allen RJ, Warren SM. A Novel Flow-Perfusion Bioreactor Supports 3D Dynamic Cell Culture. *J. Biomed. Biotechnol.* Hindawi Publishing Corporation; 2009;2009:873816.
5. Yeatts AB, Fisher JP. Bone tissue engineering bioreactors: dynamic culture and the influence of shear stress. *Bone. United States*; 2011;48:171–81.
6. Carpentier B, Layrolle P, Legallais C. Bioreactors for bone tissue engineering. *Int. J. Artif. Organs.* 2011;34:259—270.
7. Sikavitsas VI, Bancroft GN, Holtorf HL, Jansen JA, Mikos AG. Mineralized matrix deposition by marrow stromal osteoblasts in 3D perfusion culture increases with increasing fluid shear forces. *Proc. Natl. Acad. Sci. U. S. A. National Academy of Sciences*; 2003;100:14683–8.
8. Kim HJ, Kim U-J, Leisk GG, Bayan C, Georgakoudi I, Kaplan DL. Bone regeneration on macroporous aqueous-derived silk 3-D scaffolds. *Macromol. Biosci. Germany*; 2007;7:643–55.
9. Sikavitsas VI, Temenoff JS, Mikos AG. Biomaterials and bone mechanotransduction. *Biomaterials. Netherlands*; 2001;22:2581–93.
10. Gao H, Ayyaswamy PS, Ducheyne P. Dynamics of a microcarrier particle in the simulated microgravity environment of a rotating-wall vessel. *Microgravity Sci. Technol. Germany*; 1997;10:154–65.

11. Goldstein AS, Juarez TM, Helmke CD, Gustin MC, Mikos AG. Effect of convection on osteoblastic cell growth and function in biodegradable polymer foam scaffolds. *Biomaterials*. Netherlands; 2001;22:1279–88.
12. Alvarez-Barreto JF, Linehan SM, Shambaugh RL, Sikavitsas VI. Flow perfusion improves seeding of tissue engineering scaffolds with different architectures. *Ann. Biomed. Eng.* United States; 2007;35:429–42.
13. Bancroft GN, Sikavitsas VI, Mikos AG. Design of a flow perfusion bioreactor system for bone tissue-engineering applications. *Tissue Eng.* United States; 2003;9:549–54.
14. Janssen FW, Oostra J, Oorschot A van, van Blitterswijk CA. A perfusion bioreactor system capable of producing clinically relevant volumes of tissue-engineered bone: in vivo bone formation showing proof of concept. *Biomaterials*. Netherlands; 2006;27:315–23.
15. Wang T-W, Wu H-C, Wang H-Y, Lin F-H, Sun J-S. Regulation of adult human mesenchymal stem cells into osteogenic and chondrogenic lineages by different bioreactor systems. *J. Biomed. Mater. Res. A*. United States; 2009;88:935–46.
16. Bjerre L, Bünger CE, Kassem M, Mygind T. Flow perfusion culture of human mesenchymal stem cells on silicate-substituted tricalcium phosphate scaffolds. *Biomaterials*. 2008;29:2616—2627.
17. Grayson WL, Bhumiratana S, Cannizzaro C, Chao P-HG, Lennon DP, Caplan AI, et al. Effects of initial seeding density and fluid perfusion rate on formation of tissue-engineered bone. *Tissue Eng. Part A*. United States; 2008;14:1809–20.
18. Glowacki J, Mizuno S, Greenberger JS. Perfusion enhances functions of bone marrow stromal cells in three-dimensional culture. *Cell Transplant*. United States; 1998;7:319–26.
19. Mueller SM, Mizuno S, Gerstenfeld LC, Glowacki J. Medium perfusion enhances osteogenesis by murine osteosarcoma cells in three-dimensional collagen sponges. *J. Bone Miner. Res.* United States; 1999;14:2118–26.
20. Mizuno S, Tateishi T, Ushida T, Glowacki J. Hydrostatic fluid pressure enhances matrix synthesis and accumulation by bovine chondrocytes in three-dimensional culture. *J. Cell. Physiol.* United States; 2002;193:319–27.
21. Kikuchi M, Kikuchi K, Johnson K GJ. Hydrostatic fluid pressure stimulated osteogenesis

by MG63 cells in porous collagen sponge. *J oromaxillo facial Biomech.* 2004. p. 10(1): 57-60.

22. Yoshida T, Kikuchi M, Koyama Y, Takakuda K. Osteogenic activity of MG63 cells on bone-like hydroxyapatite/collagen nanocomposite sponges. *J. Mater. Sci. Mater. Med. United States*; 2010;21:1263–72.

23. Chen S, Zhang Q, Nakamoto T, Kawazoe N, Chen G. Gelatin Scaffolds with Controlled Pore Structure and Mechanical Property for Cartilage Tissue Engineering. *Tissue Eng. Part C. Methods. United States*; 2016;22:189–98.

24. Matsushima A, Kotobuki N, Tadokoro M, Ohgushi H. Comparative Study of Ceramics Structure for Culturing Human Mesenchymal Stromal Cells. *Key Eng. Mater. Trans Tech Publications*; 2008;361–363:1067–70.

25. Chung C, Burdick JA. Engineering cartilage tissue. *Adv. Drug Deliv. Rev. Netherlands*; 2008;60:243–62.

26. Raghunath J, Salacinski HJ, Sales KM, Butler PE, Seifalian AM. Advancing cartilage tissue engineering: the application of stem cell technology. *Curr. Opin. Biotechnol.* 2005;16:503—509.

27. Wang Y, Kim U-J, Blasioli DJ, Kim H-J, Kaplan DL. In vitro cartilage tissue engineering with 3D porous aqueous-derived silk scaffolds and mesenchymal stem cells. *Biomaterials. Netherlands*; 2005;26:7082–94.

28. Zhang Y, Yang F, Liu K, Shen H, Zhu Y, Zhang W, et al. The impact of PLGA scaffold orientation on in vitro cartilage regeneration. *Biomaterials. Netherlands*; 2012;33:2926–35.

29. Staiger MP, Pietak AM, Huadmai J, Dias G. Magnesium and its alloys as orthopedic biomaterials: a review. *Biomaterials. Netherlands*; 2006;27:1728–34.

Chapter 6

Combined supplementation of calcium citrate and calcium carbonate on injectable and anti-washout hydroxyapatite/collagen bone paste utilizing sodium alginate

6.1 Introduction

Bioactive ceramics based artificial bone void fillers for some time have been replacing autologous bone grafts due to the problems presented by the latter such as chronic pain, deformity, donor site morbidity and scarring [1]. Recently, a rapid adoption of clinically injectable bone pastes is taking place. They provide an ease of fitting irregular-shaped defects thereby avoiding unexpected gaps between host and the fillers [2,3], and they require a minimally invasive surgery which reduces a patient's discomfort and healthcare costs. 'Apatite Cement', clinically a very successful paste, utilizes the hydration hardening reaction by conversion of comparatively unstable calcium phosphates to hydroxyapatite ($\text{Ca}_{10}(\text{PO}_4)_6(\text{OH})_2$, HAp) crystals [4]. Due to its very low biodegradability, HAp remains in the patient's body, where, its brittleness might cause a secondary fracture. Although high porosity in the sintered HAp might solve this problem in part, it is difficult to apply to apatite cement as sufficient porogen lowers its operability and fracture strength.

Application of biodegradable materials is the other solution for bone paste. Among the biodegradable bone void fillers such as porous β -tricalcium phosphate ($\beta\text{-Ca}_3(\text{PO}_4)_2$, β -TCP) and hydroxyapatite/collagen bone-like nanocomposite (HAp/Col), sintered β -TCP has been in clinical usage since 1970s. It has a high potential for dissolution by body fluid and resorption by osteoclasts, reactions necessary for new bone substitution. Fabrication of chelate setting α - and β -TCP pastes using inositol-6-phosphate as a chelating agent and their

potential in substitution with new bone has also been reported [5,6]. HAp/Col on the other hand, is prepared by the simultaneous titration method and is reported to have similar bone like nanostructure. It is incorporated into bone remodelling process to substitute with newly formed bone when implanted into bone defect [7,8]. Clinical trials on the porous HAp/Col proved to be a better material than porous β -TCP [9]. An injectable HAp/Col paste had been developed using sodium alginate [10,11], however, its anti-washout property was not sufficient for clinical use. To improve the anti-washout property, supplementation of various calcium compounds or organic acids were investigated [12] with supplementation of low soluble calcium compounds, calcium carbonate (CaCO_3) and calcium citrate (Ca-Cit), but only slight improvement was achieved.

Recently Sato *et al.* [13] reported influences of excess supplementation of low soluble CaCO_3 or Ca-Cit for the improvement of anti-washout property. The HAp/Col pastes showed a washout ratio at less than 10 % in mass by addition of Ca-Cit at 8 times or greater Ca^{2+} ion amounts than that for the equivalent reaction to Na-Alg with an observation of a slight decrease in the pH of the PBS after the anti-washout test. Further, a degradation of the paste prepared with supplementation of Ca-Cit at 20 times greater Ca^{2+} ion amounts than that for the equivalent reaction to Na-Alg was observed in Dulbecco's modified essential medium in 5 days. This result suggests that the formation of acid-induced alginate gel with high H^+ concentration inhibited eggbox structure formation. This phenomenon could be palliated by combined supplementation of acidic Ca-Cit and basic CaCO_3 .

In the present chapter, influences of combined supplementation of Ca-Cit and CaCO_3 on injectable HAp/Col paste were investigated.

6.2 Materials and Methods

6.2.1 Preparation of HAp/Col powder

The HAp/Col at a HAp and collagen mass ratio of 4:1 was prepared by a simultaneous titration of $\text{Ca}(\text{OH})_2$ (prepared from the alkaline analysis grade CaCO_3 , Wako pure chemicals Inc.) suspension and mixed solution of orthophosphoric acid (Reagent grade, Wako chemicals Inc.,) and type-1 porcine dermal collagen (Biomaterial grade, Nitta Gelatin Inc.,) with maintaining the water bath temperature at 40°C and pH of the reaction solution at 9 [8]. The HAp/Col obtained was compacted into disks by squeezing water using a uniaxial press at 20 MPa, freeze dried and crushed into 100-212 μm in size with a ball mill (FRITSCH, Pulverisette, Germany) *in vacuo* using zirconia ball of 15 mm Φ . The powder obtained was then dehydrothermally cross linked at 140°C for 12 h under a vacuum. In order to inhibit Ca^{2+} adsorption of the HAp/Col [14], the powder was treated with 20 mM CaCl_2 solution for 3 days, filtered, freeze dried and stored at 4°C .

6.2.2 Preparation of HAp/Col paste

The HAp/Col paste was prepared using the optimal conditions in Ref [12], where the powder to liquid (P/L) ratio is 0.60 and mass ratio of HAp/Col powder and sodium alginate (Na-Alg, low viscosity (80-120 cP)), Wako pure chemicals, Inc.) is 9:1. The calcium compound additives chosen were CaCO_3 and Ca-Cit (Wako pure chemicals, Inc.) The reaction equivalent amount of Ca^{2+} ion to Na-Alg used in the experiments was 1.67 mmol per 1g of Na-Alg reported in the Ref [12]. According to this, amounts of supplement were denoted as Nx, where N was multiplication number for the equivalent reaction amount of Ca^{2+} ion to Na-Alg. The HAp/Col paste was prepared by a mixing of the HAp/Col and Na-Alg aqueous solution with a combined supplementation of Ca-Cit and CaCO_3 under the conditions shown in **Table 6.1**, in which their abbreviations are also noted.

Table 6.1 Preparation conditions of the HAp/col paste with additives

HAp/Col (mg)	Na-Alg (mg)	H ₂ O (μ l)	Ca-Cit		CaCO ₃		Abbreviation	Final P/L ratio
			Times equivalent	Weight (mg)	Times equivalent	Weight (mg)		
170	18.9	264.4	8x	47.9	2x	6.30	8x-2x	0.79
			9x	53.9	1x	3.20	9x-1x	0.80
			10x	59.9	1x	3.20	10x-1x	0.82
			10x	59.9	2x	6.30	10x-2x	0.83
			12x	71.9	2x	6.30	12x-2x	0.87

x = Reaction equivalent amount of Ca²⁺ to Na-Alg (1.67 ± 0.07 mmol per 1 g of Na-Alg)

6.2.3 Characterization of HAp/Col paste

6.2.3.1 Viscosity test

Viscosity of the paste was measured using the method reported by Ishikawa *et al.*, [15] where 0.1 cm³ of the paste was mixed for 3 min and a 2-kg glass plate was placed on the paste for 10 min after start of mixing. The spread area at 10 min after placing the glass was measured using its digital photograph with the Image-J program (version 1.48, NIH, USA).

6.2.3.2 Washout property test

Washout property of the HAp/Col paste was measured according to the procedure in Japanese Industrial Standard “JIS T 0330-4 Bioceramics- Part 4.” The paste was prepared by mixing the raw materials for 3 min and was packed into a syringe of 4.8 mm in inner diameter and 16.5 mm in height. Within 5 minutes after mixing the paste was then squeezed onto a wire net with wire diameter of 0.5 mm and aperture of 2.0 mm. The paste was then soaked in 50 ml of phosphate buffered saline (PBS) and kept at 37 °C in an incubator up to

72 hours. A washout rate was calculated as the ratio of the paste on the wire net before and after soaking. The final pH of the solution was also measured.

6.2.3.3 Cytocompatibility test

All paste materials were sterilized using ethylene oxide gas (EOG). The paste raw materials were mixed, molded into the shape of a cylinder of 7 mm diameter and 5 mm in height and were aged for 24 hours in an incubator at 95 ± 5 % RH to harden. A blank and HAp/Col dense body were chosen as controls. HAp/Col dense bodies was prepared by compact dehydration of the HAp/Col as synthesized into 5 mm in height and punched out into 7 mm diameter. They were freeze dried, dehydrothermally crosslinked and sterilized using EOG respectively. Before cell culture experiment, the HAp/Col dense bodies were soaked in Dulbecco's Modified Eagle Medium (D-MEM) to adsorb Ca^{2+} ion and Mg^{2+} ions. MG-63 cells, derived from human osteosarcoma were used for the experiment. After a subculture of MG63 cells, 2×10^4 cells were seeded onto each well in a 6 well tissue culture treated polystyrene plate (TCPS). One day after seeding, the paste and control samples were placed in each well and cultured for 7 days. Medium was changed every 2 days. After desired time interval, the cells were detached by trypsin/EDTA and the cell numbers were calculated using hemocytometer. The used media was collected during the medium change to measure the Ca^{2+} and PO_4^{3-} ion concentrations using an inductively coupled plasma-atomic emission spectrometer (SPS7800, SII NanoTechnology, Japan; ICP-AES).

6.2.4 Statistical analysis

The results are shown as the mean \pm standard deviation. Statistical analysis was performed using one way analysis of variance with Turkey – HSD post hoc test. The statistical significance was set at $p < 0.05$.

6.3 Results

Spread area of the paste combination supplemented with Ca-Cit and CaCO₃ increased with Ca²⁺ amounts as shown in **Fig. 6.1**. Further, spread areas of the pastes supplemented with totally 10x Ca²⁺ ion, approximately 120-130 mm², was very similar to that of the paste solely supplemented with 10x Ca-Cit as reported by Sato *et al.*, [13]. These results suggested pastes supplemented with calcium compounds had higher influences on viscosity. Effects on initial viscosity with acid compounds as supplements were low in comparison to those of Ca²⁺ amounts. This could be caused by difference between strong eggbox gel and weak acid-induced gel.

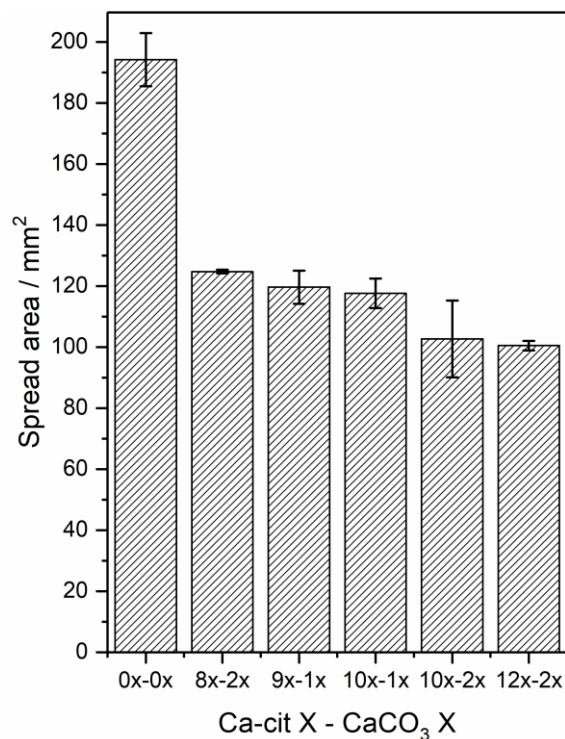


Figure 6.1 Spread area of the HAp/Col paste combination supplemented with CaCit and CaCO₃.

Data represent mean \pm standard deviation (SD) for n = 3.

Anti-washout property became better with increasing in total Ca^{2+} amounts up to 10x-2x and again worse at 12x-2x as shown in **Fig. 6.2**. The anti-washout ratios for the paste with combined supplementation demonstrated a smaller value at an amount of 10x-2x (2.42 ± 0.72 %) in comparison to the 10x of Ca-Cit solely supplemented pastes (5.91 ± 2.73 %). Further, the final pH of the solution was maintained as the original pH for the 10x-2x (7.34 ± 0.08) compared with the 10x of Ca-Cit supplemented paste (6.72 ± 0.06) [12]; though final pH of 10x-1x and 9x-1x increased.

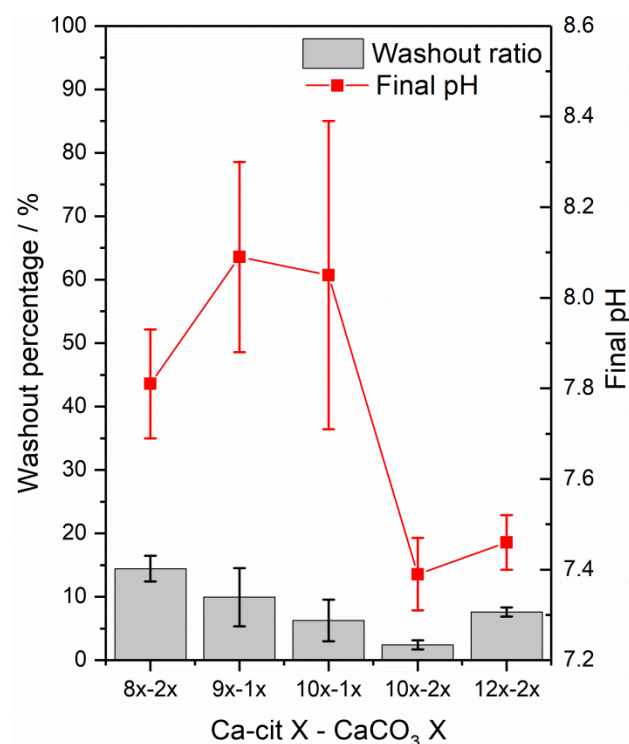


Figure 6.2 Washout behaviour and final pH of the medium after 72 h. Data represent mean \pm SD for n = 3.

Fig. 6.3 shows the cell proliferation curve for the MG-63 cells cultured with the HAp/Col pastes. The 9x-1x paste was not used for the cell culture test because the pH of the medium turned basic after 72 hours. Significant difference between the test groups and TCPS group were found for each measurement. All four combinations showed good proliferation activity without any significant difference compared to the HAp/Col dense bodies, which shows very good biocompatibility *in vivo* [7]. **Figure. 6.4a and 6.5b** show the changes in the

Ca²⁺ and PO₄³⁻ ion concentrations in the culture medium respectively. No significant changes in the suppression were observed from the changes in Ca²⁺ and reduction in PO₄³⁻ ion concentration.

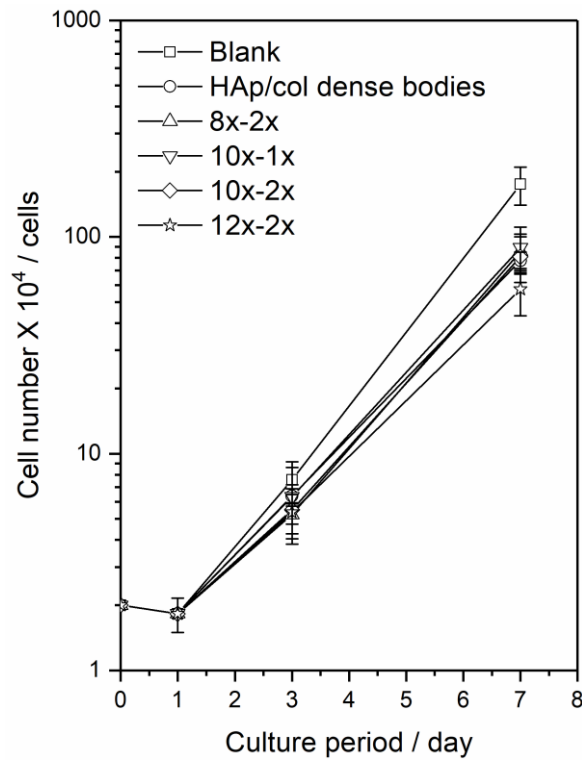


Figure 6.3 In vitro analysis of the combination of additives on HAp/Col paste. Data represent mean \pm SD for n = 5.

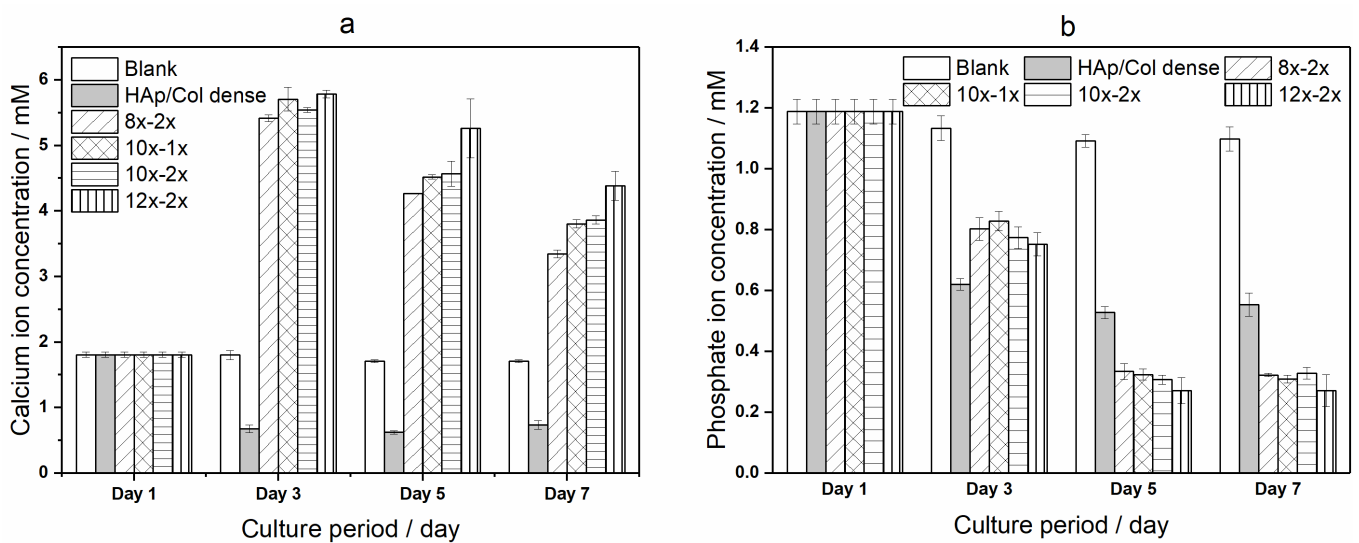


Figure 6.4 (a) Calcium ion and **(b)** Phosphate ion concentration of the culture medium after the cell culture test. Data represent mean \pm SD for n = 5.

6.4 Discussion

In the previous reports [12,13], to improve the anti-washout property of HAp/Col paste, the paste was supplemented with organic acid or calcium compounds, resulting in increase of viscosity and slight extension of washout time. The mechanisms for the increase in viscosity were different in each supplement; *i.e.*, acids increased viscosity of alginate by acidic environment and calcium compounds by crosslinkage of alginate via Ca^{2+} ions. The pastes prepared with high soluble calcium compound showed no improvements in anti-washout property, because high soluble calcium compounds discharge Ca^{2+} ions quickly to form short range gel near the calcium compounds, which increased in paste viscosity and inhibits the diffusion of Ca^{2+} ions to form long-range network to prevent the washout. Contrarily, the pastes prepared with low soluble calcium compound, CaCO_3 and Ca-Cit improved the anti-washout property. However, paste supplemented with 20x CaCO_3 decayed completely within 72 h and did not acquire sufficient wash out property. Large amounts of CaCO_3 allowed formation of eggbox gel to increase viscosity; however, the gel formation by low Ca^{2+} concentration due to low solubility of CaCO_3 , might be insufficient for the anti-washout in PBS by substitution of Ca^{2+} to Na^+ , which leads to the decomposition of alginate gel network. Contrarily, Ca-Cit supplementation showed anti-washout property because of alginate gelation by acidic pH. Acidic alginate gel might be stronger than the gel formed by small amounts of Ca^{2+} under PBS condition. In addition, Ca-Cit in the paste also formed the egg-box structure gradually by large amount of Ca^{2+} to reinforce the paste. However, the pH of the PBS after the anti-washout test became acidic, which can compromise the biocompatibility of the paste.

Similar reactions occurred in the paste with combined supplementation of Ca-Cit and CaCO_3 . First, Ca-Cit, comparatively higher solubility than CaCO_3 , dissolved in the paste and allowed to form weak acid-induced gel. Dissolution of CaCO_3 was followed by acid

environment and increased the pH, thus weakening the acid-induced gel. In the meantime, Ca^{2+} ions started to interact with gelation sites of alginate due to increase of free Ca^{2+} ions from chelation with citrates; this meant that the reason of small improvement in the wash out property by the solely supplementation of Ca-Cit [12] could not only be by inhibition of the eggbox formation by acid-induced gel but also by inhibition of interaction between Ca^{2+} ions and the eggbox sites. This is due to competitive reaction between the chelation by citrate and the eggbox formation.

Supply of Ca^{2+} ions from CaCO_3 less than or equal to 10 %, the amount of Ca^{2+} ions might not be sufficient for moving reaction equivalent to the eggbox structure formation; thus, the free Ca^{2+} ions leached from the paste and increased the pH. Contrarily, Ca^{2+} ions supplied from CaCO_3 more than 10 %, were used for the formation of eggbox structure as well as chelating with citrates; therefore, pHs were comparatively neutral than small Ca^{2+} ions supplied from CaCO_3 . Further, initial acid-induced gel formation was also important for anti-washout property; thus, the 10x-2x paste showed higher washout percentage than others. Increasing in the washout percentage for the 12x-2x paste could be due to the slight low CaCO_3 ratio than the 10x-2x paste. Summarizing the washout test, supplementation of CaCO_3 amount appropriately, *i.e.*, respective Ca-Cit and CaCO_3 amount of 10x and 2x; and 12x and 2x, improved the anti-washout property without impairing the pH of the PBS.

From **Fig. 6.4**, at day 3, the culture media of test groups contained 3 times higher Ca^{2+} ion concentration than control TCPS due to the gradual release of Ca^{2+} ions from CaCO_3 and Ca-Cit. But, the ratio compared to the control decreased as the culture period increased. In contrast, the Ca^{2+} ion concentration decreased in HAp/Col dense body, due to the adsorption of Ca^{2+} ions on HAp/Col as reported by Sotome *et al* [14]. From **Fig. 6.5**, the concentration of PO_4^{3-} ions continuously decreased with the culture period. The PO_4^{3-} ion concentration in the culture media of test groups and HAp/Col dense body was low compared to control TCPS.

Changes in Ca^{2+} and reduction in PO_4^{3-} ion concentration in the culture medium could affect the proliferation and differentiation of almost all cells; however, no quite suppression in the cell proliferation observed in the test and HAp/Col dense body group, which demonstrated that these ion concentration changes had no critical effects on cell viability and proliferation. The cytocompatibility of the pastes is as good as the HAp/Col, clinically used material in Japan.

These results suggest that the influence of the combined supplementation of Ca-Cit and CaCO_3 on the injectable HAp/Col paste improved the anti-washout property and pH control ability without critical influences on biocompatibility.

6.5 Conclusion

Combined supplementations of Ca-Cit and CaCO_3 improved the anti-washout property and pH controllability of the injectable HAp/Col paste. The improvements were caused by a competitive reaction occurred co-ordinately in the pastes. From *in vitro* cell culture studies, all combinations showed good cytocompatibility without any significant suppression of cell proliferations. Hence, the presently prepared HAp/Col pastes could be good candidates for injectable artificial bone, which has the potential for incorporation into bone remodelling process.

Acknowledgement

This **Chapter 6**, in part, was a reprint of the publication **Manchinasetty NVL**, Sato T, Aizawa M, Kikuchi M, et al. Influences of combined supplementation of calcium citrate and calcium carbonate on injectable and anti-washout hydroxyapatite/collagen bone paste utilizing sodium alginate. *Journal of Ceramic Society of Japan Ceram* 2017; 125: 579-583 with permission.

6.6 References

1. Damien CJ, Parsons JR. Bone graft and bone graft substitutes: a review of current technology and applications. *J. Appl. Biomater.* UNITED STATES; 1991;2:187–208.
2. Komath M, Varma HK, Sivakumar R. On the development of an apatitic calcium phosphate bone cement. *Bull. Mater. Sci.* 2000;23:135–40.
3. Nilsson M, Wielanek L, Wang J-S, Tanner KE, Lidgren L. Factors influencing the compressive strength of an injectable calcium sulfate-hydroxyapatite cement. *J. Mater. Sci. Mater. Med.* United States; 2003;14:399–404.
4. Fukase Y, Wada S, Uehara H, Terakado M, Sato H, Nishiyama M. Basic studies on hydroxy apatite cement: I. Setting reaction. *J. Oral Sci. Japan;* 1998;40:71–6.
5. Konishi T, Takahashi S, Zhuang Z, Nagata K, Mizumoto M, Honda M, et al. Biodegradable β -tricalcium phosphate cement with anti-washout property based on chelate-setting mechanism of inositol phosphate. *J. Mater. Sci. Mater. Med.* 2013;24:1383–94.
6. Konishi T, Mizumoto M, Honda M, Horiguchi Y, Oribe K, Morisue H, et al. Fabrication of novel biodegradable β -tricalcium phosphate cement set by chelating capability of inositol phosphate and its biocompatibility. *J. Nanomater.* 2013;2013.
7. Kikuchi M, Itoh S, Ichinose S, Shinomiya K, Tanaka J. Self-organization mechanism in a bone-like hydroxyapatite/collagen nanocomposite synthesized in vitro and its biological reaction in vivo. *Biomaterials.* 2001;22:1705–11.
8. Kikuchi M, Ikoma T, Itoh S, Matsumoto HN, Koyama Y, Takakuda K, et al. Biomimetic synthesis of bone-like nanocomposites using the self-organization mechanism of hydroxyapatite and collagen. *Compos. Sci. Technol.* 2004;64:819–25.
9. Shinomoya K, Ishizuki M, Morioka H, Matsumoto S, Nakamura T, Abe S, Beppy Y. A phase III randomized controlled trial of self organized hydroxyapatite/collagen composite versus beta tricalcium phosphate as bone substitute for treatment of osseous defect. *Seikei Geka.* 2012;63:921–6.
10. Kochi A, Kikuchi M, Shirotsaki Y, Hayakawa S, Osaka A. Preparation of Injectable Hydroxyapatite/Collagen Nanocomposite Artificial Bone. *Key Eng. Mater. Trans Tech*

Publications; 2012;493–494:689–92.

11. Lee KY, Mooney DJ. Alginate: Properties and biomedical applications. *Prog. Polym. Sci.* 2012;37:106–26.

12. Sato T, Kochi A, Shirotsaki Y, Hayakawa S. Preparation of injectable hydroxyapatite / collagen paste using sodium alginate and influence of additives. *J. Ceram. Soc. Japan.* 2013;775–81.

13. Sato T, Kikuchi M, Aizawa M. Preparation of hydroxyapatite/collagen injectable bone paste with an anti-washout property utilizing sodium alginate. Part 1: influences of excess supplementation of calcium compounds. *J. Mater. Sci. Mater. Med. United States;* 2017;28:49.

14. Sotome S, Uemura T, Kikuchi M, Itoh S, Tanaka M, Takahashi M, et al. In Vitro Evaluation of Highly Absorptive Ceramics Materials Needs Consideration of Calcium and Magnesium Ions Adsorbed to the Materials. *Key Eng. Mater. Trans Tech Publications;* 2001;218–220:153–6.

15. Ishikawa K, Miyamoto Y, Takechi M, Toh T, Kon M, Nagayama M, et al. Non-decay type fast-setting calcium phosphate cement: hydroxyapatite putty containing an increased amount of sodium alginate. *J. Biomed. Mater. Res.* 1997;36:393–9.

Chapter 7

Summary

With the aim of developing novel functional biomaterials with calcium phosphate and their composites, preparation and characterization of scaffolds utilizing test of sea urchin with biocompatible polymers or calcium phosphate polymer composites for artificial bone fillers were studied in this thesis. The summarized description for each other is now discussed.

In **Chapter 2**, skeletons of sea urchins namely *strongylocentrotus nudus* (SU1) and *strongylocentrotus intermedius* (SU2) were used to obtain calcium phosphate (CP1/CP2) by hydrothermal conversion in a phosphate containing solution. The composition of skeletons of sea urchin was found to be Mg containing calcite (Mg-CaCO_3) by XRD analysis and the skeletons were porous by nature with macropores in the range of 200-300 μm and micropores in the range of 20-50 μm by SEM analysis. The obtained calcium phosphate was found to be biphasic in nature consisting of magnesium containing tricalcium phosphate (Mg β -TCP, 82%) with small amount of hydroxyapatite (HAp, 18%) from XRD result, also corroborated by the FT-IR analysis results. The SEM evaluation revealed that the skeletons retained their original porous structure after conversion where the diameter of the macropores ranged from 200 to 250 μm and micropores 20 to 40 μm . From the calcination of the obtained calcium phosphate at 1000 $^\circ\text{C}$, and FT-IR analysis, the hydroxyapatite in the CP1/CP2 was found to be carbonate (CO_3^{2-}) containing Ca deficient hydroxyapatite. It was found that the presence of Mg^{2+} ion promoted the formation of β -TCP, and small amount of HAp due to the decrease in the Mg^{2+} ion concentration. The results suggested that the obtained biphasic calcium phosphate (BCP) from skeletons of sea urchin can be used in the fabrication of three dimensional (3D) scaffolds with the help of biocompatible binders.

In **Chapter 3**, the fabrication of shape controllable and flexible 3D scaffolds with the help of biocompatible polymers collagen or gelatin was described. The scaffolds were fabricated by simple mixing of the CP1/CP2 granules with collagen or gelatin in a desired shape and size, freeze-drying and crosslinking. The scaffolds with collagen as binder, CP1Col/CP2Col were crosslinked dehydrothermally and found to be stable at 37 °C in PBS solution from stability analysis. The scaffolds with gelatin as binder (CP1Gel_GA/CP2Gel_GA), were stable only with chemical crosslinking at 37 °C in PBS. From the cross-sectional images of scaffolds using SEM, it was found that macropores and micropores were well maintained even after some pores were blocked by the polymer coating. The granules in the scaffold helped in the formation of homogeneous and interconnected porous structure. They showed good open porosity for cell migration and fluid infiltration, and adequate mechanical strength for handling operations. Overall, the binder collagen or gelatin helped in maintaining the shape and integrity of the scaffolds, whereas the granules reserved the space for bone formation. The scaffolds could be a potential candidate for non-load bearing defects.

In **Chapter 4**, biocompatibility of the scaffolds under 2D cell culture with osteoblast cell line MG-63 cells was evaluated. The cytotoxicity/viability evaluation showed that the scaffolds were non-cytotoxic in nature when compared to control. In CP1Gel_GA/CP2Gel_GA, very few dead cells were found when compared to control, where many dead cells were found. From cell adherence/distribution analysis, the mid vertical cross-sectional images by SEM, showed that cells adhered well onto the surface and penetrated into the inner layer of the scaffold. In control gelatin sponge, cells were seen only on the peripheral area. From cell proliferation analysis, scaffolds proved to be significantly higher in the proliferation rate compared to their respective controls. The scaffolds fabricated with porous biphasic CP1/CP2 granules and collagen or gelatin provided essential porosity,

bioactive surface for cell attachment and proliferation. Also, the scaffolds created a favorable environment for differentiation of cells, which can favor increased bone formation in comparison with control collagen and gelatin sponge. The scaffolds proved to be biocompatible under 2D culture conditions and have the potential to be utilized as artificial bone filler.

In **Chapter 5**, biocompatibility of the scaffolds under 3D pressure/perfusion cell culture conditions, with MG-63 cells was evaluated. The scaffolds CP2Col showed higher proliferation ability evaluated by the total DNA quantification, high cell distribution to the inner layers of the scaffold evaluated by staining decalcified vertical cross-section by DAPI compared to control collagen sponge. The control collagen sponge, cell grew only on the outer layer during the initial stages and shrunk in size, whereas, CP2Col maintained its integrity and shape throughout the culture time. In the scaffold CP2Gel_GA higher cell proliferation and distribution ability was seen compared to control gelatin sponge. Higher osteogenic potential was seen in CP2Col and CP2Gel_GA compared to control collagen and gelatin sponge respectively. The homogeneous porous structure and Mg containing BCP granules in the scaffolds facilitated good cell distribution and enhanced the osteogenic activity under 3D culture conditions. These results suggest that the scaffolds could be a potential candidate as artificial bone filler.

In **Chapter 6**, an injectable and anti-washout paste of hydroxyapatite/collagen (HAp/Col) nanocomposite was prepared utilizing sodium alginate by supplementation of calcium carbonate (CaCO_3) and calcium citrate (Ca-Cit). Combined supplementations of Ca-Cit and CaCO_3 improved the anti-washout property and pH controllability of the injectable HAp/Col paste. The improvements were caused by a competitive reaction that occurred coordinately in the pastes. From *in vitro* cell culture studies, all combinations showed good cytocompatibility without any significant suppression of cell proliferations. Hence, the

presently prepared HAp/Col pastes could be good candidates for injectable artificial bone, which has the potential for incorporation into bone remodelling process.

In future work, biocompatibility of the scaffolds and the injectable should be evaluated with primary cell line and later under *in vivo* conditions for more accurate analysis, to be considered for non-load bearing defects.

Publications and Research record

Publications

Chapter 2, 3, 4, 5 is based on following publications

- 1) **Manchinasetty NVL**, Oshima S, Kikuchi M. Preparation of flexible bone tissue scaffolds utilizing sea urchin test and collagen. *Journal of Materials Science: Materials in Medicine* 2017; 28(11):184-1- 184-12.
- 2) **Manchinasetty NVL**, Kikuchi M. Fabrication and characterization of porous scaffold utilizing the test of sea urchin and gelatin (manuscript under preparation).
- 3) **Manchinasetty NVL**, Oshima S, Kikuchi M. Evaluation of the biocompatibility of scaffolds fabricated using test of sea urchin and collagen or gelatin as binder under pressure/perfusion culture conditions (manuscript under preparation).

Chapter 6 is based on following publication

- 4) **Manchinasetty NVL**, Sato T, Aizawa M, Kikuchi M, et al. Influences of combined supplementation of calcium citrate and calcium carbonate on injectable and anti-washout hydroxyapatite/collagen bone paste utilizing sodium alginate. *Journal of Ceramic Society of Japan* 2017; 125: 579-583.

Oral presentations

Domestic

- 1) **Naga Vijaya Lakshmi M**, Sho Oshima, Masanori Kikuchi; *In vitro* evaluation of scaffolds fabricated with calcium phosphate granules derived from sea urchin test and gelatin; 29th Fall meeting of Ceramic Society of Japan; Hiroshima University, Hiroshima, Japan; September 7-9, 2016.

- 2) **Naga Vijaya Lakshmi M**, Masanori Kikuchi; Fabrication of porous scaffolds using calcium phosphate granules derived from sea urchin tests with collagen or gelatin as binder; Annual meeting of Ceramic Society of Japan; Waseda University, Tokyo, Japan; March 14-16, 2016.
- 3) **Naga Vijaya Lakshmi M**, Suetsugu Yasushi, Masanori Kikuchi; Conversion of sea urchin tests to calcium phosphate for bone implants; 28th Fall meeting of Ceramic Society of Japan; Toyama University , Toyama, Japan; September 16-18, 2015.

International

- 1) **Naga Vijaya Lakshmi M**, Sho Oshima, Masanori Kikuchi; *In vitro* evaluation of scaffolds fabricated using calcium phosphate granules converted from sea urchin test and collagen under pressure/perfusion cell culture system; The 15th International conference on Advanced Materials (IUMRS-ICAM); Kyoto University; Kyoto; Japan; August 27-September 1, 2017.
- 2) **Naga Vijaya Lakshmi M**, Sho Oshima, Masanori Kikuchi; *In Vitro* evaluation of porous scaffolds fabricated using calcium phosphate granules derived from sea urchin test with collagen or gelatin as a binder; 55th symposium on Basic Science of Ceramics; Okayama convention center, Okayama, Japan; January 12-13, 2017.
- 3) **Naga Vijaya Lakshmi M**, Sho Oshima, Masanori Kikuchi, *In vitro* evaluation of scaffolds fabricated with calcium phosphate granules derived from sea urchin test and collagen; Bioceramics 28; University of North Carolina, Charlotte, United states of America; October 18-21, 2016.
- 4) **Naga Vijaya Lakshmi M**, Suetsugu Yasushi, Masanori Kikuchi; Fabrication of shape controlled scaffold using calcium phosphate granules derived from sea urchin test and gelatin; 15th Asian Bioceramics Symposium; Tokyo Medical and Dental University, Tokyo, Japan; December 9-11, 2015.

Acknowledgment

There are many people, whom I owe a lot and who have helped me constantly during the tenure of my Ph.D. studies. I thank all of them from the bottom of my heart. First I would like to thank my supervisor, Prof. Masanori Kikuchi for the opportunity, encouragement, financial support and research guidance. His friendly nature and good scientific attitude is noteworthy.

I would like to express my sincere gratitude to our group's former and current administrative assistant Ms. Etsuko Yamada and Ms. Yuri Ikenobe for their generous and caring nature. I want to thank my present and former lab members Mr. Sho Oshima, Mr. Taira Sato, Ms. Yuka Takemura, for their consistent help, support and keeping the morale during Ph.D. Special thanks to Mr. Sho Oshima, for helping a lot in the experimental setups and characterization during my Ph.D. I am also thankful to Ms. Shipra Chauhan, Mr. Ranjith Kumar Bakku, Ms. Jagriti Mishra, Ms. Halley M Menezes, Ms. Risa Suzuki for their supportive nature during my initial times in Japan.

Most importantly, I would like to express my deepest love and gratitude to my beloved parents, Mr. Satya Srinivasa Babu M, Ms. Uma Devi M and my elder brother Mr. Ram Vinayak M for believing in me. I love them so much and would not have made it this far without them. Their motivation, financial support and sincere prayers helped me overcome the hurdles in my pursuit. I also want to thank my boyfriend Mr. Yaswanth Kodavali for being so supportive throughout. Thanks for taking the time to proof read my drafts and for your constructive feedback.

Last but not the least, I would like to thank Prof. Sridharan Madanagurusamy, without him I wouldn't have landed this Ph.D. opportunity. The financial support from MEXT and JASSO, Japan during my Ph.D. is sincerely acknowledged.